IMPACTS OF CHANGES IN PRECURSOR EMISSIONS FROM THE SAN FRANCISCO BAY AREA ON OZONE IN THE NORTH CENTRAL COAST AND SAN JOAQUIN VALLEY AIR BASINS

Final Report
Contract No. A932-133

Prepared for:

Research Division
California Air Resources Board
1102 Q Street
P.O. Box 2815
Sacramento, CA 95812

Submitted by:

Systems Applications International
101 Lucas Valley Road
San Rafael, California 94903

Prepared by:

S.G. Douglas
T.E. Stoeckenius
B.S. Austin
J.R. Pehling
C.A. Emery
C.Daly

February 1991

Disclaimer

The statements and conclusions in this report are those of the contractor and not necessarily those of the California Air Resources Board. The mention of commercial products, their source or their use in connection with material reported herein is not to be construed as either an actual or implied endorsement of such products.

Contents

Abstract

This study examines the effect of emissions reductions in the San Francisco Bay Area (SFBA) on ozone levels in the North Central Coast (NCC) and San Joaquin Valley (SJV) air basins. It includes three tasks:

Emissions trends analysis for the SFBA, NCC, and SJV air basins;

Identification of possible transport days and analysis of ozone trends in both the source and receptor basins on transport and no-transport days; and

Application of flux-plane calculations using air quality modeling results from the San Joaquin Air Quality Study to quantify the impact of emissions changes on interbasin transport.

The emissions trends analysis examined trends in emissions of reactive organic gasses (ROG), and oxides of nitrogen (NO_X) between 1979 and 1987 in the SFBA, NCC, and SJV air basins and selected counties within these air basins. To account for the fact that not all ROGs contribute equally to the formation of ozone, reactivity-weighted ROG trends were also examined. The analysis indicates that the SFBA has achieved large decreases in ROG (42 percent) and NO_X (24 percent) emissions during the period 1979 - 1987. ROG decreases in the NCC and SJV air basins have also been significant (16 and 39 percent, respectively). NO_X emissions have decreased in the NCC (44 percent) but have remained virtually constant in the SJV. Numerous uncertainties in the emissions inventories must be considered when interpreting the apparent trends.

Historical ozone concentration data for the SFBA, NCC, and SJV air basins were examined for the period 1979 - 1988. The objective was to determine how ozone levels within the air basins have changed during this period and to relate these changes to changes in emissions within the source and receptor basins. High-ozone days in the NCC or SFBA and high-ozone days in the SJV or SFBA were identified and categorized as transport, no transport, or indeterminate. Ozone trends were then calculated for both the SFBA and the downwind air basins and for selected monitors within each basin. Separate trends were calculated for transport and no-transport days. No statistically significant linear trends over the 1979 - 1988 period were observed at the 95% confidence level. Furthermore, no systematic differences between trends on transport and no-transport or indeterminate days were observed. However, ozone concentrations at the downwind monitors were higher on transport days.

Flux-plane calculations were performed using the meteorological and air-quality modeling results from the San Joaquin Valley Air Quality Study (SJVAQS) to provide quantitative estimates of pollutant flux between the SFBA and the NCC and the SJV during the period 7 - 8 August 1984. To examine the effect of emissions changes on the transport of ozone and precursor pollutants, fluxes were calculated for two different emissions scenarios.

The air-quality simulations consist of a base case and a sensitivity test in which anthropogenic emissions in the SFBA were eliminated. The results indicate that elimination of SFBA emissions can significantly reduce ozone concentrations in the NCC and SJV during meteorological conditions conducive to transport. The flux-plane calculations for the simulations indicate that while reduced ozone concentrations in the SFBA under the no-SFBA-emissions scenario results in a reduction of the flux of ozone into the downwind air basins somewhat, lower ozone concentrations in the downwind air basins are due primarily to a reduction in the amount of precursor pollutants that are transported from the SFBA to the receptor basins.

Figures

Tables

1 INTRODUCTION

Interbasin transport of ozone and precursor pollutants from the San Francisco Bay Area air basin may cause or contribute to violations of the California state ozone standard in the North Central Coast and San Joaquin Valley air basins. Numerous observational, data analysis, and modeling studies have shown that transport does exist (Dabberdt et al., 1983; Roberts and Main, 1989; ARB, 1990). However, the quantitative effects of ozone and ozone precursor transport have not been determined.

The transport of ozone and ozone precursor pollutants is governed by the complex mesoscale airflow patterns that characterize the San Francisco Bay Area, North Central Coast , and San Joaquin Valley air basins. These airflow patterns develop in response to the land-water temperature differences and the effects of complex terrain. Thus, the rugged terrain and extensive coastal environment of California make determination of interbasin transport of ozone and precursor emissions a complex and challenging problem. Analysis of this complex problem is further limited by available meteorological and air-quality data.

The 1988 California Clean Air Act requires the Air Resources Board to assess the relative contribution of upwind emissions to downwind pollutant concentrations in areas where transported pollutants have been identified to cause or contribute to violations of the state ozone standard. The objective of this study is to examine the effect of emissions reductions in the San Francisco Bay Area on ozone levels in the North Central Coast and San Joaquin Valley air basins. It includes three tasks:

Historical emissions trends analysis for the San Francisco Bay Area, North Central Coast, and San Joaquin Valley air basins;

Identification of possible transport days and analysis of ozone trends in both the source and receptor basins on transport and nontransport days; and

Application of flux-plane calculations using air quality modeling results from the San Joaquin Valley Air Quality Study to quantifying the impact of emissions changes on interbasin transport.

Results from the emissions trends analysis are given in Section 2. The classification of ozone episodes and results of the ozone trends analysis are described in Section 3. The flux-plane calculation results are given in Section 4. The results from all three tasks are summarized and integrated in Section 5. Conclusions and recommendations for further analysis are also provided in this final section.

2 EMISSION TRENDS ANALYSIS

The first step in understanding the role of transported precursor emissions in downwind areas is to determine long-term emission levels and trends in upwind and downwind areas. The emission trends analysis examined trends in ROG and NO_x between 1979 and 1987 in the San Francisco Bay Area (SFBA), San Joaquin Valley (SJV), and North Central Coast (NCC) air basins and selected counties within these air basins. OH reactivity-weighted trends were also calculated to account for the fact that certain ROGs contribute more to ozone formation than others.

METHODOLOGY

Estimates of biannual anthropogenic emission trends provided by the California Air Resources Board (ARB) (ARB, 1990a, 1990b, and 1990c) were used in the analysis. Trends were estimated for 1979, 1981, 1983, 1985, and 1987 using 1985 as the base year. NO_x, ROG, and OH-reactivity weighted ROG trends were calculated for each air basin and for selected counties within each air basin, including Alameda, Contra Costa, and Santa Clara counties (SFBA); San Joaquin and Stanislaus counties (SJV); and San Benito County (NCC). Trends were calculated by performing a linear least squares regression on the trend data provided by the ARB. Least-squares regression was used to determine whether the trends are significantly different from zero. It is important to note that the ROG trends are based upon anthropogenic ROG emissions and do not include biogenic emissions. Uncertainties arising from the emissions inventory development process are described later in this section.

RESULTS

Tables 2-1 through 2-3 present predicted (from the regression equations) ROG, OH-reactivity weighted ROG, and NO_x emissions as well as the r^2 value of the regression and the p value of the regression slope. The r-squared value (the proportion of variation of emissions about their mean explained by the regression) is a measure of the degree to which year-to-year changes in emissions follow a linear trend. The p value of the slope is the probability--under the null hypothesis that the true slope is zero--that the magnitude of the slope of a linear trend line is greater than the computed slope. If this probability is less than 5 percent, for example, the computed slope is conventionally said to be significantly different from zero at the 5 percent level. In most areas, large anthropogenic ROG and NO_x reductions were achieved between 1979 and 1987. For example, the regression-predicted ROG reductions over this period for NCC, SFBA, and SJV air basins are 17, 390, and 382 tons per day, respectively. NO_x reductions are 55, 155, and 3 TPD for these air basins.

Emission trends for ROG, OH-reactivity-weighted ROG, and NO_x are presented in a series of plots for each of the three air basins and individual counties. There are four figures for each pollutant: the first presents total trends for all three air basins and the remaining three figures present individual county trends. Each figure contains the actual ARB data points, the fitted trend line (based on a linear least squares fit), the trend line equation, and the total percent change between the 1979 and 1987 values predicted by the trend line.

The figures described above were specifically designed to highlight pollutant **trends** as shown by the slopes of the trend lines. Therefore, the scales on the ROG and NO_x charts are not consistent, nor do they necessarily begin at zero. Scales on the ROG OH-reactivity-weighted charts are normalized to 1.0 (for the ARB trend data points) for 1979. While the trend line equation is printed on each chart, the number of significant digits printed is not sufficient to derive the exact trend line position.

TABLE 2-1. ROG regression predicted values, 1979-1987 (tons per day).

Air Basin/County	1979	1981	1983	1985	1987	r^2	p Value
North Central Coast Air Basin	107.80	103.54	99.27	95.00	90.73	0.2284	0.207
San Benito County	5.54	5.16	4.78	4.41	4.03	0.8225	0.012
San Francisco Bay Area Air Basin	921.86	824.35	726.83	629.32	531.80	0.9024	0.007
Santa Clara County	192.28	176.56	160.83	145.10	129.37	0.9958	0.0
Alameda County	200.98	181.59	162.20	142.82	123.43	0.3589	0.143
Contra Costa County	160.75	142.80	124.85	106.91	88.96	0.7269	0.033
San Joaquin Valley Air Basin	977.46	882.06	786.66	691.25	595.85	0.8892	0.008
San Joaquin County	89.84	84.02	78.19	72.36	66.54	0.7204	0.034
Stanislaus County	54.83	49.70	44.57	39.44	34.30	0.9431	0.003

TABLE 2-2. OH-reactivity-weighted ROG regression predicted values, 1979-1987 (tons per day). (Actual values were normalized to one for 1979.)

Air Basin/County	1979	1981	1983	1985	1987	r^2	p Value
North Central Coast Air Basin	0.941	0.918	0.895	0.871	0.848	0.0416	0.371
San Benito County	0.958	0.886	0.813	0.741	0.669	0.7960	0.022
San Francisco Bay Area Air Basin	1.160	1.028	0.895	0.763	0.631	0.6945	0.04
Santa Clara County	1.008	0.912	0.816	0.720	0.624	0.9904	0.00
Alameda County	1.013	0.891	0.768	0.645	0.523	0.9936	0.00
Contra Costa County	0.931	0.833	0.735	0.638	0.540	0.8860	0.008
San Joaquin Valley Air Basin	0.957	0.876	0.796	0.715	0.635	0.9034	0.006
San Joaquin County	0.949	0.892	0.834	0.777	0.719	0.8260	0.017
Stanislaus County	0.974	0.888	0.801	0.715	0.629	0.9704	0.001

TABLE 2-3. NO_x regression predicted values, 1979-1987 (tons per day).

Air Basin/County	1979	1981	1983	1985	1987	r^2	p Value
North Central Coast Air Basin	125.53	111.82	98.12	84.41	70.70	0.8126	0.018
San Benito County	4.52	4.42	4.33	4.24	4.15	0.7451	0.029
San Francisco Bay Area Air Basin	646.72	607.87	569.02	530.17	491.32	0.9292	0.004
Santa Clara County	121.60	118.70	115.80	112.90	110.01	0.7713	0.025
Alameda County	114.22	110.50	106.78	103.06	99.34	0.2568	0.192
Contra Costa County	178.32	164.47	150.63	136.78	122.93	0.7321	0.032
San Joaquin Valley Air Basin	559.85	559.09	558.33	557.57	556.82	0.0077	0.444
San Joaquin County	56.91	56.66	56.41	56.17	55.92	0.3246	0.158
Stanislaus County	36.40	35.17	33.93	32.69	31.46	0.9591	0.002

ROG Trends

The general trends in ROG emissions for the NCC, SFBA, and SJV air basins are shown in Figure 2-1. ROG levels dropped 16%, 42%, and 39% respectively between 1979 and 1987. The relative emission levels are quite different; NCC emissions are a maximum of 116 tons per day (TPD) while SF and SJV emissions are maximums of 876 and 1035 TPD, respectively.

North Central Coast Air Basin ROG Trends

ROG emissions in the NCC have decreased steadily each year except 1985; in 1979 there were 116 TPD; by 1987 there were only 84.5 TPD. In 1985 there were large ROG emissions from accidental fires in Monterey county, causing the emissions that year to deviate from the general trend shown in Figure 2-1. Most decreases in ROG over the trend period are due to drops in on-road motor vehicle emissions, to a steady decrease in pesticide application, and to a lesser degree, total fuel combustion, particularly in the category "Other manufacturing/industrial." The predicted trend line shows an overall decrease of 16% over the trend period; however, the r^2 value is only .22 and the p value of 0.21 indicates that the trend is not statistically significant at the 95% level.

ROG emissions in San Benito County are presented in Figure 2-2. They account for only 3.8% of the total air basin inventory. They drop from 5.7 TPD in 1979 to 4.3 TPD in 1987. This decrease is due largely to decreases in pesticide application and in accidental fires. The overall reduction over the regression line is 27%. The p value of 0.012 suggests this reduction is statistically significant at the 95% level.

San Francisco Bay Area Air Basin ROG Trends

ROG emissions in the SFBA dropped from 871 TPD to 531 TPD over the trend period. In 1979 and 1981, ROG emissions were relatively constant; between 1981 and 1987 there is a downward trend onward. This is in spite of a huge (2000%) increase in pesticide application in 1981 and 1983. However, this increase may be in error as it

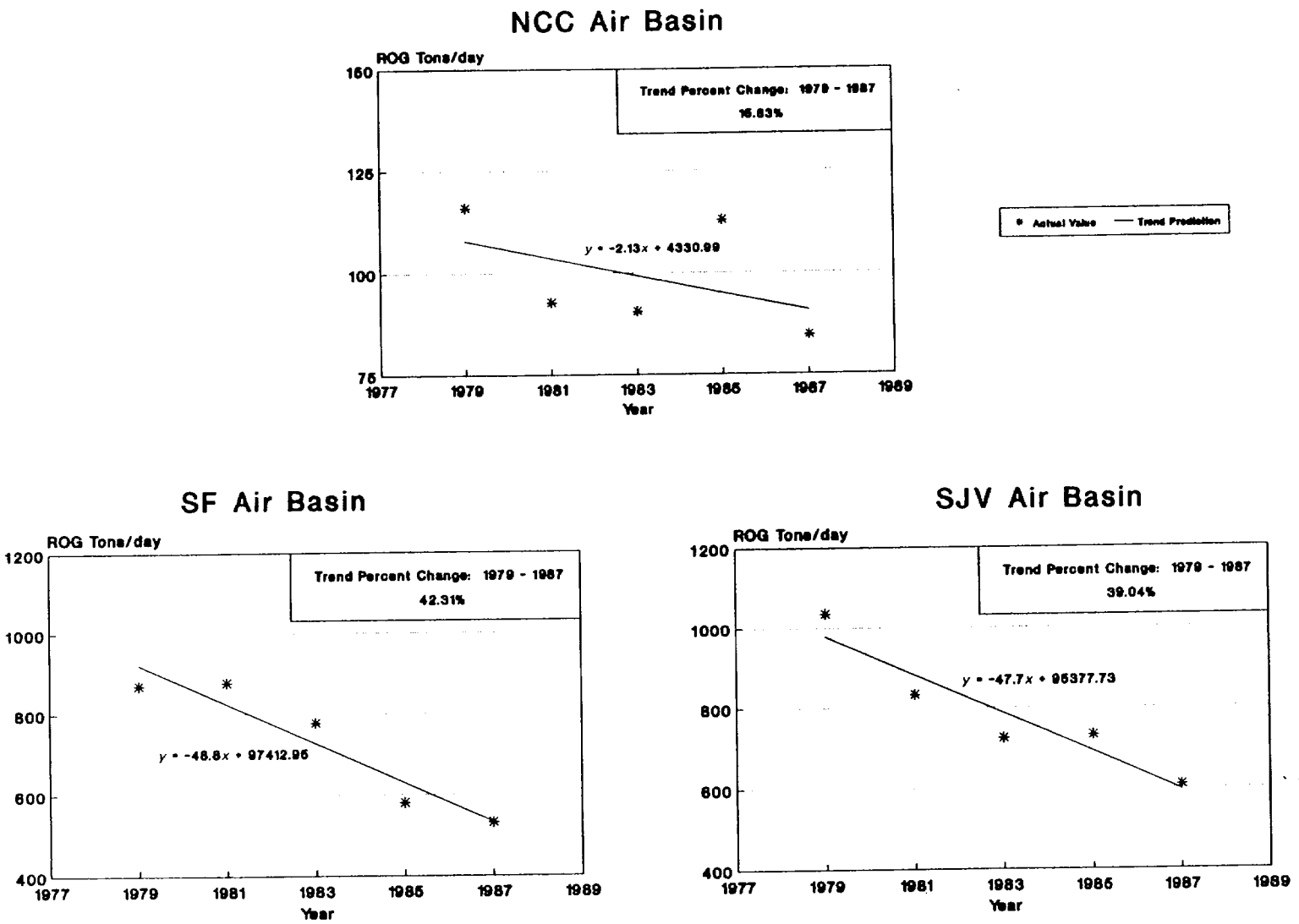

FIGURE 2-1. ROG emission trends in the NCC, SFBA, and SJV air basins (1979-1987).

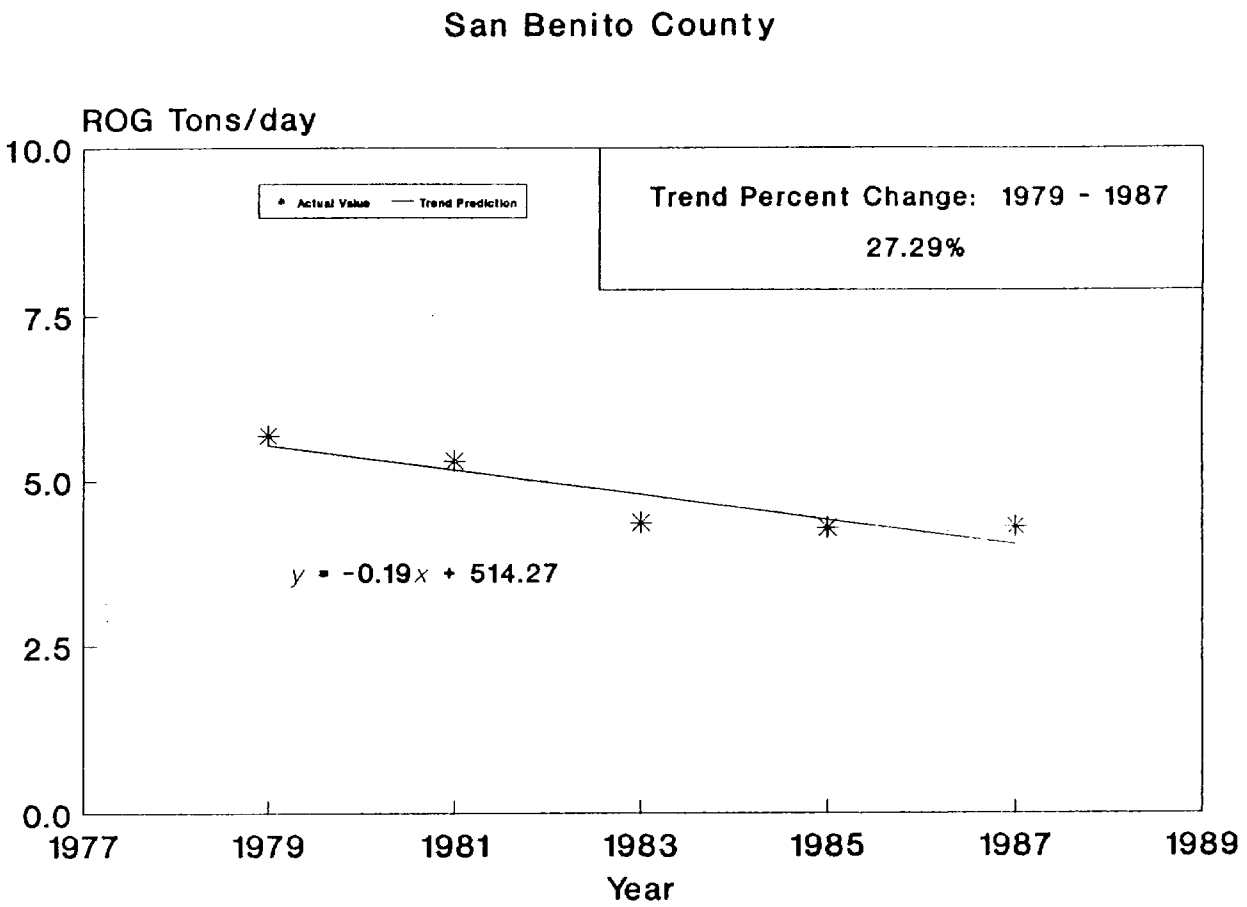

Figure 2-2. ROG Trends: North Central Coast Air Basin

is not consistent with published historical ARB inventories. In these two years pesticide application jumped from less than 1% of the total ROG inventory to approximately 16% of the inventory. Therefore, the actual decrease may be even larger than that shown in Figure 2-1. Major decreases in ROG emissions occurred in on-road motor vehicle emissions (a decrease of more than 200 TPD over the trend period) and solvent use (a 50 TPD decrease over the trend period, mostly from the categories "other surface coating" and "printing"). Oil and gas extraction and non-combustion petroleum refining emissions dropped 55 TPD and 21 TPD respectively. The r^2 value for the regression fit is high (0.90) and the p value of 0.007 strongly suggests that the overall trend is statistically significant.

ROG emission trends for the three selected SFBA air basin counties are shown in Figure 2-3. ROG emissions in Santa Clara County account for 24% of the total inventory for the air basin. Emissions dropped sharply over the trend period with most of the decrease due to mobile source reductions. Other significant decreases are similar to the air basin as a whole, occurring in petroleum marketing, surface coating and printing. The predicted regession line fits the data points closely and the r^2 value is equal to 0.996. The p value is 0.00, indicating a (near) zero probability that the slope of this line is not statistically significantly different from zero.

ROG emissions in Alameda County account for 21% of the total air basin inventory. They also dropped sharply over the trend period, except for 1983 when emissions from unplanned fires increased from less than 1 TPD to 94 TPD. The primary sources of emission decrease occurred in mobile sources, solvent use, and petroleum marketing. The sudden large increase in unplanned fires deviates from the general trend of the remaining data points. As a result, the r^2 value is low (0.36) and the p statistic is high (0.14). This suggests uncertainty over the signficance of the apparent overall downward trend.

ROG emissions in Contra Costa County account for 20% of the total inventory for the air basin. They also dropped significantly between 1979 and 1987. While the other counties had most significant decreases due to mobile sources, in Contra Costa County it was due to petroleum refining (53 TPD decrease). Decreases in other categories were steady but less dramatic. The regression fit is fairly good (r^2 = 0.73) and the p value is fairly low (0.03).

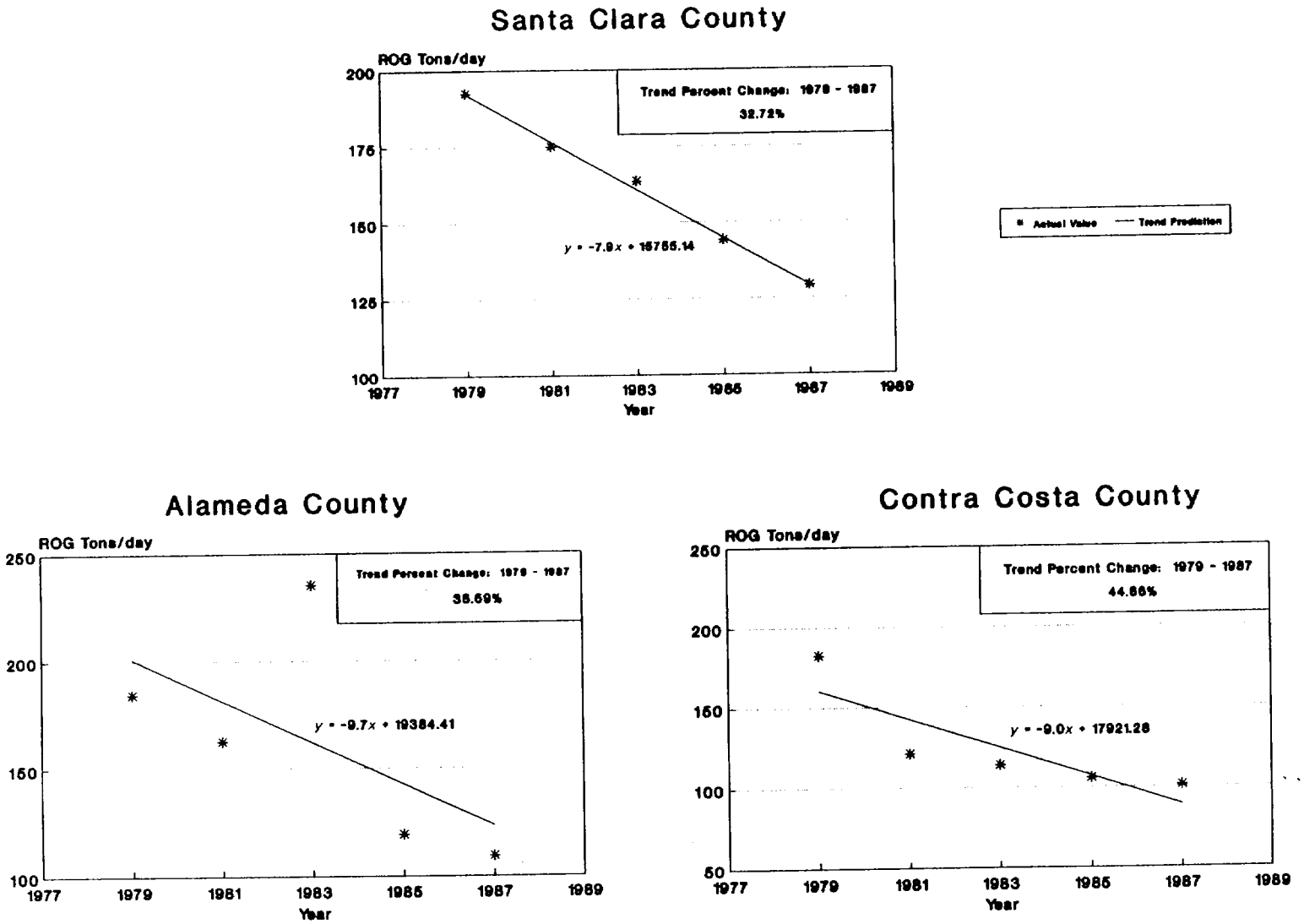

Figure 2-3. ROG Trends: San Francisco Air Basin

San Joaquin Valley Air Basin ROG Trends

ROG emissions in the SJV air basin decreased from 1035 TPD in 1979 to 609 TPD in 1987. The decreases are mostly due to on road motor vehicles (82 TPD reduction over the trend period) oil and gas extraction (262 TPD reduction over the trend period), and a steady decrease in pesticide application (a 60 TPD reduction over the trend period). There is little change in ROG emissions between 1983 and 1985 because small increases in oil and gas extraction, solvent use, waste burning, and unplanned fires offset the steady decrease in mobile sources. The regression line predicts a 39% reduction in ROG over the trend time period with a close fit (r^2 = 0.89). The p value is 0.008, suggesting that this trend is statistically significant at the 99% level.

ROG trends for San Joaquin and Stanislaus counties are shown in Figure 2-4. San Joaquin County is responsible for 11.6% of the total air basin ROG inventory. ROG emissions in this county decreased from 97 to 71 TPD over the trend period. On-road mobile sources dropped by 23 TPD, accounting for nearly all of the decrease. The regression fit is fairly close (r^2 = 0.72) and the p value is fairly low.

Stanislaus County represents 6% of the total air basin ROG inventory. Over the trend period, ROG dropped from 57 to 36 TPD. This 21 TPD decrease was mostly due to on-road mobile sources (10 TPD), pesticide application (6.5 TPD) and surface coating (3 TPD). The r^2 value (0.94) is quite high and the p statistic quite low (0.003).

OH Reactivity-Weighted ROG Trends

The trends discussed above represent unspeciated ROG. While the trends represent total emissions of all reactive organic gases, not all these gases contribute equally to the formation of ozone. In fact, certain reactive organic gases contribute significantly more to the formation of ozone than others. For example, formaldehyde has a large effect on ozone formation, while compounds such as toluene and paraffins have the least effect.

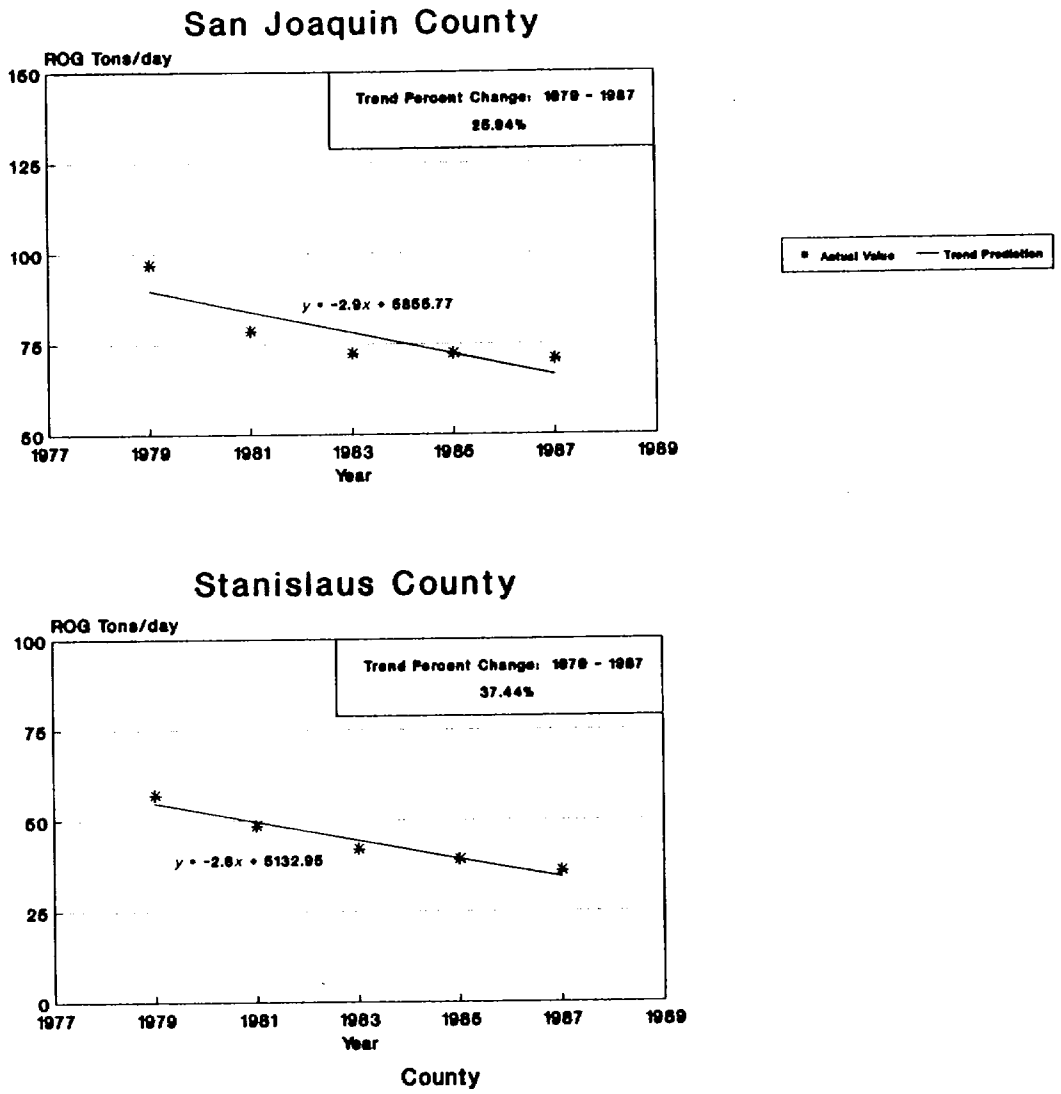

Figure 2-4. ROG Trends: San Joaquin Valley Air Basin

OH-reactivity weighted trends were derived from known speciation profiles of each source category (EPA, 1988) and from engineering judgement. The profiles were converted to reactivity factors that express the ozone-forming potential (as measured by OH reactivity) of the source category. The categories "mobile sources" and "solvent use" have the highest relative reactivities. Emissions for each source category were multiplied by these reactivity factors to derive reactivity-weighted emissions. These emissions were normalized to 1.0 in 1979 and plotted in Figures 2-5 through 2-8.

In the SFBA air basin the reactivity-weighted emissions fall at a slightly greater rate than unweighted ROG emissions, and the predicted trend lines for Alameda and Contra Costa counties fit the data more accurately than the unweighted ROG trends. Further, in the SFBA air basin the p values for OH-weighted ROG are lower than for unweighted ROG emissions. The SJV reactivity-weighted trends decrease at a marginally slower rate than unweighted trends, but have lower p values and higher r^2 values. NCC OH-weighted ROG emissions also decrease somewhat more slowly than unweighted ROG emissions but the r^2 values are lower and the p values higher.

NO_x Trends

In general, NO_x has been decreasing significantly in the NCC and SFBA air basins and increasing by a very small amount in the SJV air basin (Figure 2-9).

North Central Coast NO_x Trends

NO_x emissions in the NCC air basin decreased from 126 to 76 TPD between 1979 and 1987. This 50 TPD decrease was dominated by a 40 TPD drop in electric utilities emissions and decreases in on-road motor vehicles (5 TPD) and oil and gas production (4 TPD). San Benito County represents approximately 5% of the total air basin NO_x

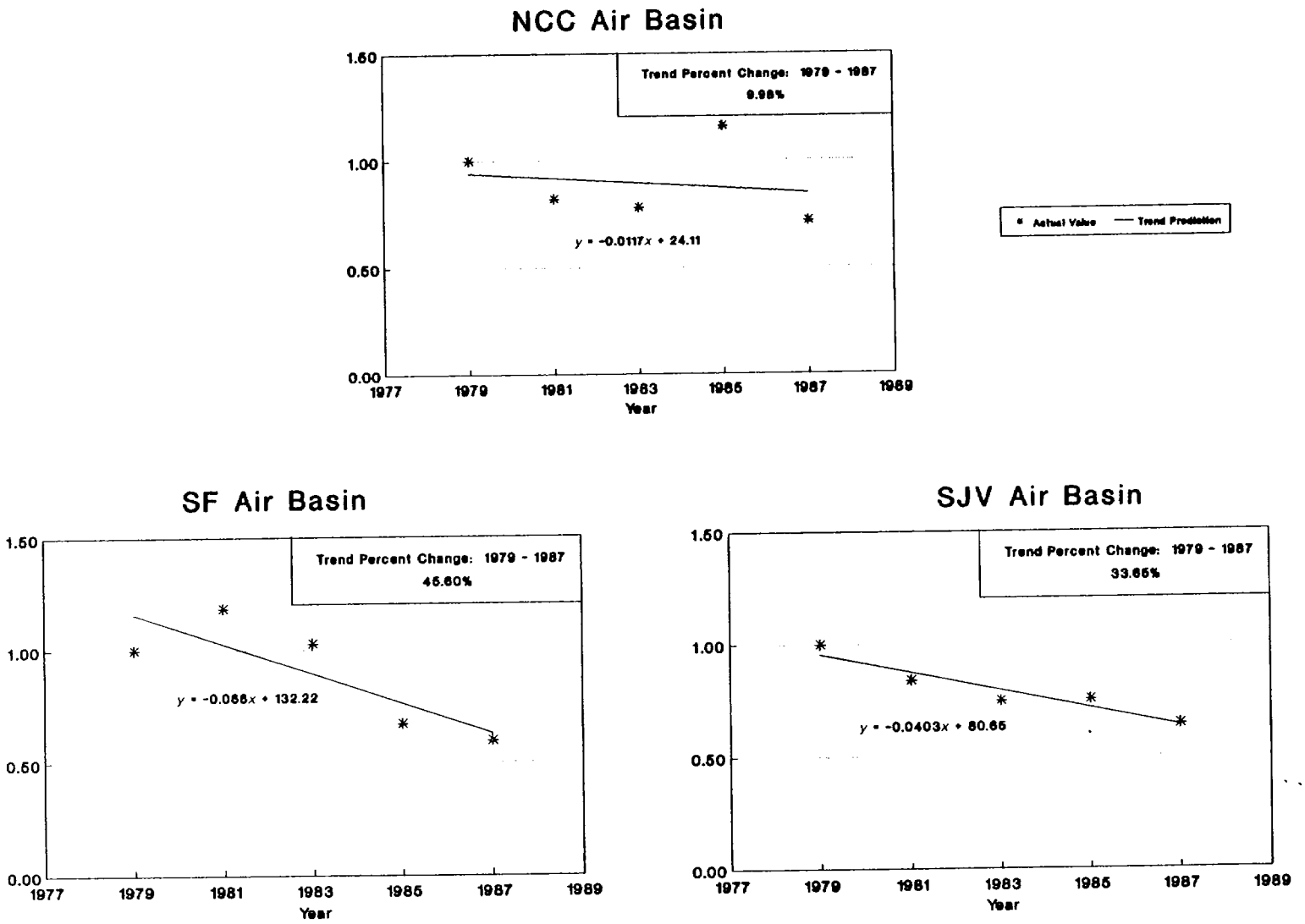

Figure 2-5. OH Reactive ROG Trends

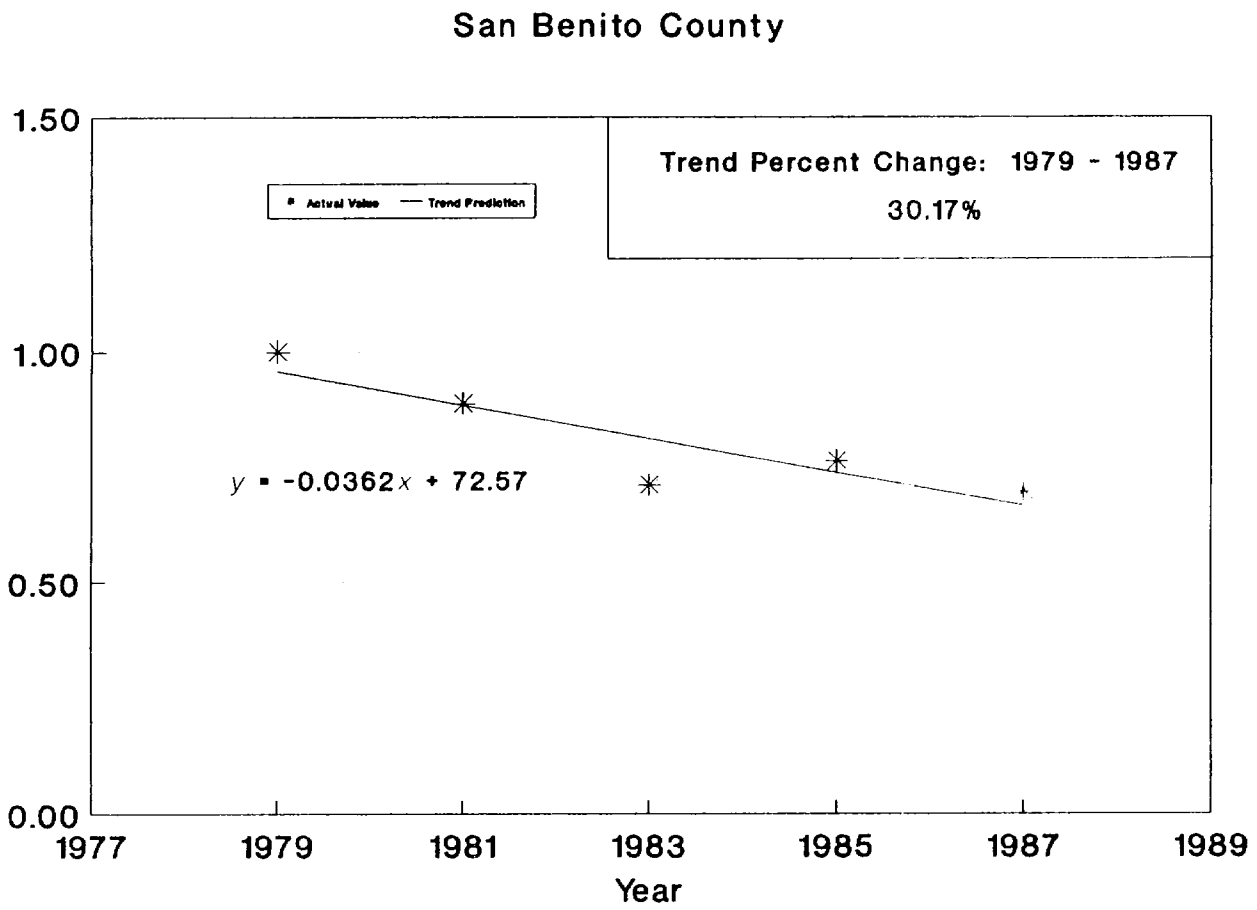

Figure 2-6. OH Reactive ROG: North Central Coast Air Basin

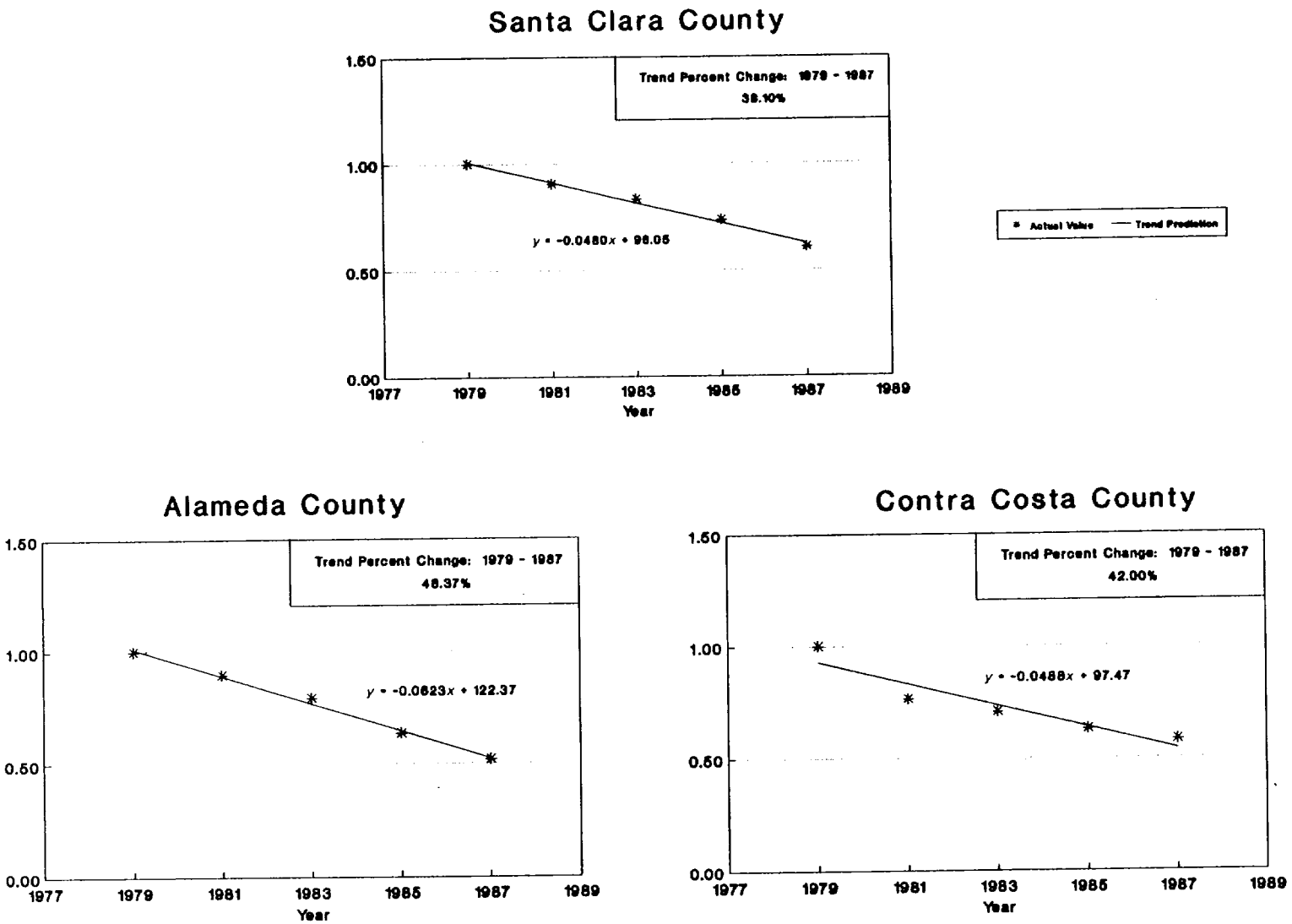

Figure 2-7. OH Reactive ROG Trends: San Francisco Air Basin

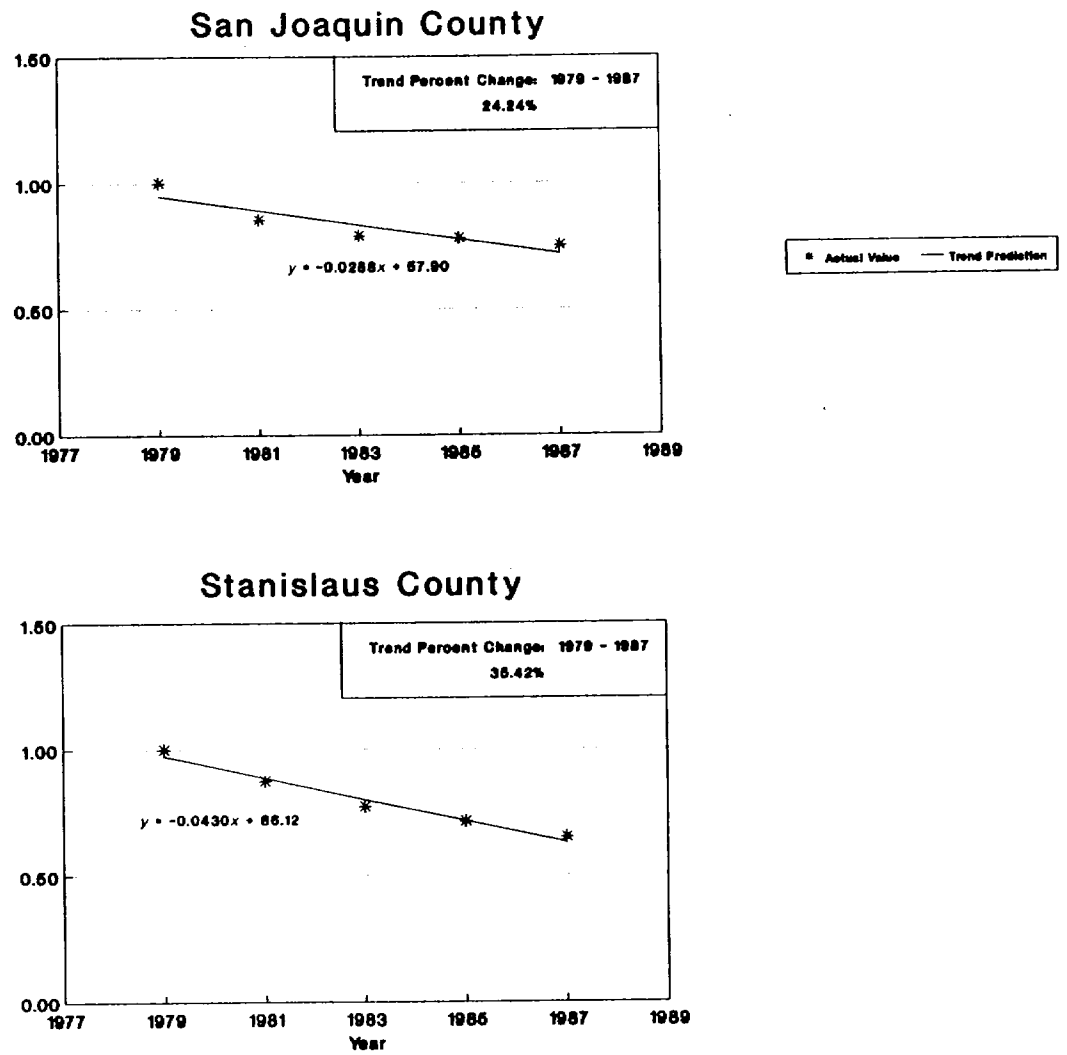

Figure 2-8. OH Reactive ROG Trends: San Joaquin Valley Air Basin

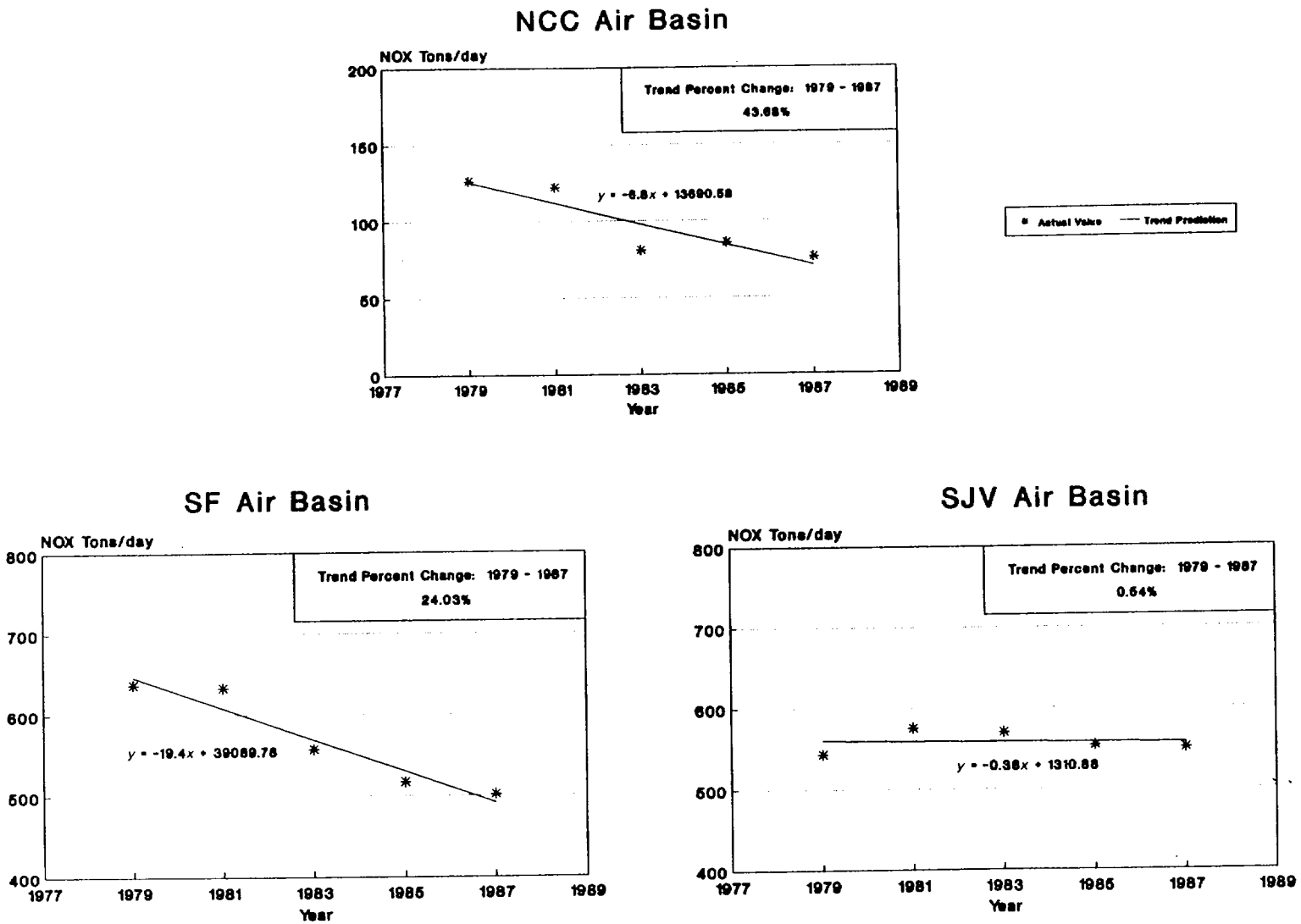

FIGURE 2-9. NO_x emission trends in the NCC, SFBA, and SJV air basins (1979-1987).

inventory (Figure 2-10). The r^2 value of .81 suggests a good fit to the data points and the p value of 0.018 indicates that the overall trend predicted by the regression is significant at the 98% level.

San Francisco Bay Area Air Basin NO_x Trends

The SFBA air basin had a 136 TPD NO_x decrease over the period 1979 (637 TPD) to 1987 (501 TPD). The decrease was dominated by mobile sources (71 TPD decrease) and by electric utility emissions (60 TPD decrease). There was also a significant decrease in petroleum refining emissions. In 1981 and 1983 there were significant increases in accidental fire emissions (rising from 1.75 TPD in 1979 to 36 TPD in 1981 and 27 TPD in 1983). In subsequent years these emissions returned to approximately the same levels as in 1979. The r^2 value is .93, strongly suggesting the regession equation produced a good fit to the data points. The p value of .004 also suggests the NO_x reductions constitute a statistically significant trend.

Santa Clara, which represents 22% of the air basin NO_x inventory, showed a 9.5% decrease over the trend period (Figure 2-11). A large decrease in light- and medium-duty cars and trucks was offset slightly by small but steady inceases in fuel combustion and NO_x emissions from heavy-duty diesel trucks.

NO_x emissions in Alameda County, which represent 19% of the air basin inventory, decreased by 13% over the trend period (Figure 2-11). The anthropogenic portion of the inventory decreased more than that; NO_x emissions in 1983 exceed those in 1979 and 1981 because of accidental fires. Most of the decrease is due to on-road motor vehicles. Small but steady increases were observed in the electric utility, other manufacturing, and fuel consumption categories.

Contra Costa accounts for 27% of the total air basin inventory (Figure 2-11). It shows the largest percent decrease over the trend period, decreasing from 189 to 135 TPD. Most of the decrease is due to electric utilities (43 TPD) and on-road motor vhicles (7 TPD).

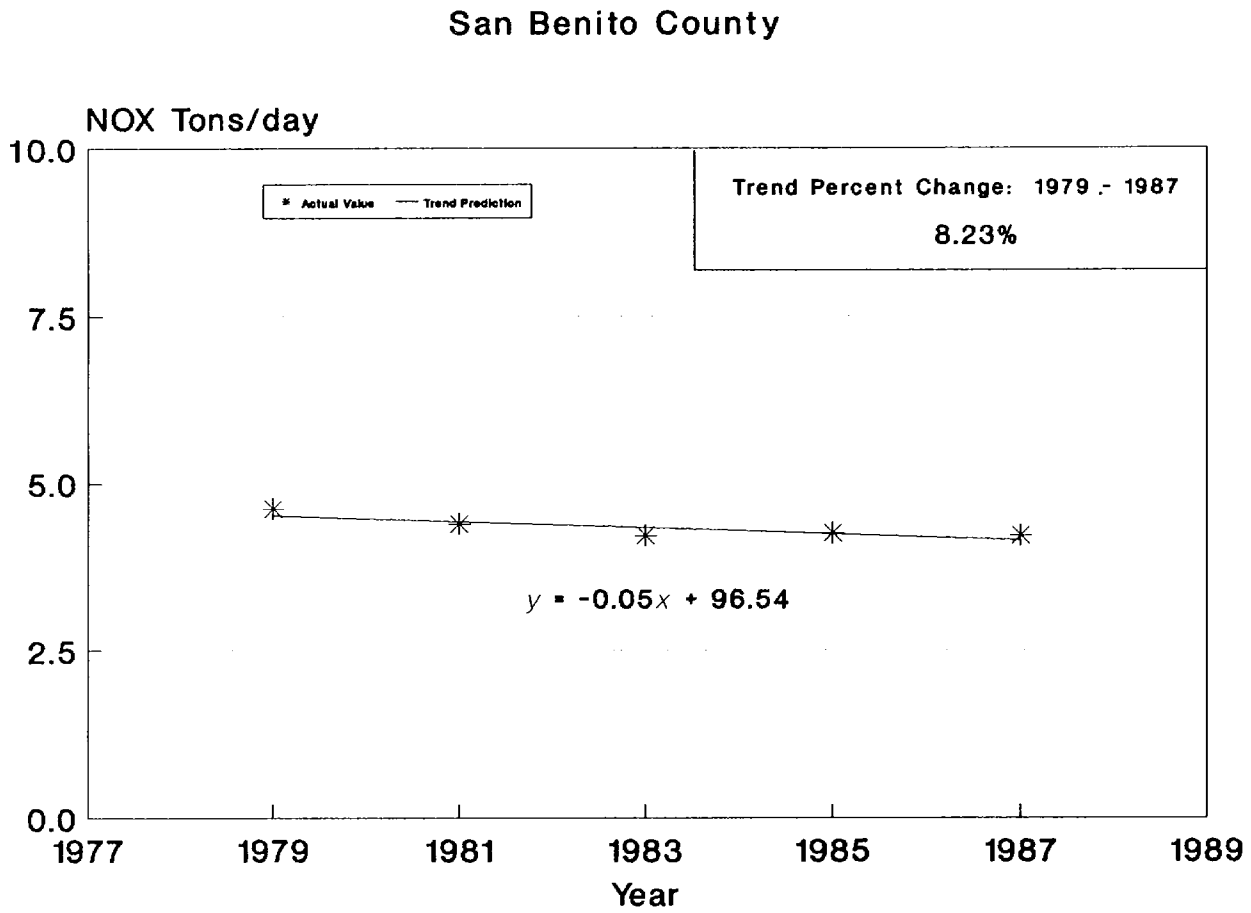

Figure 2-10. NOX Trends: North Central Coast Air Basin

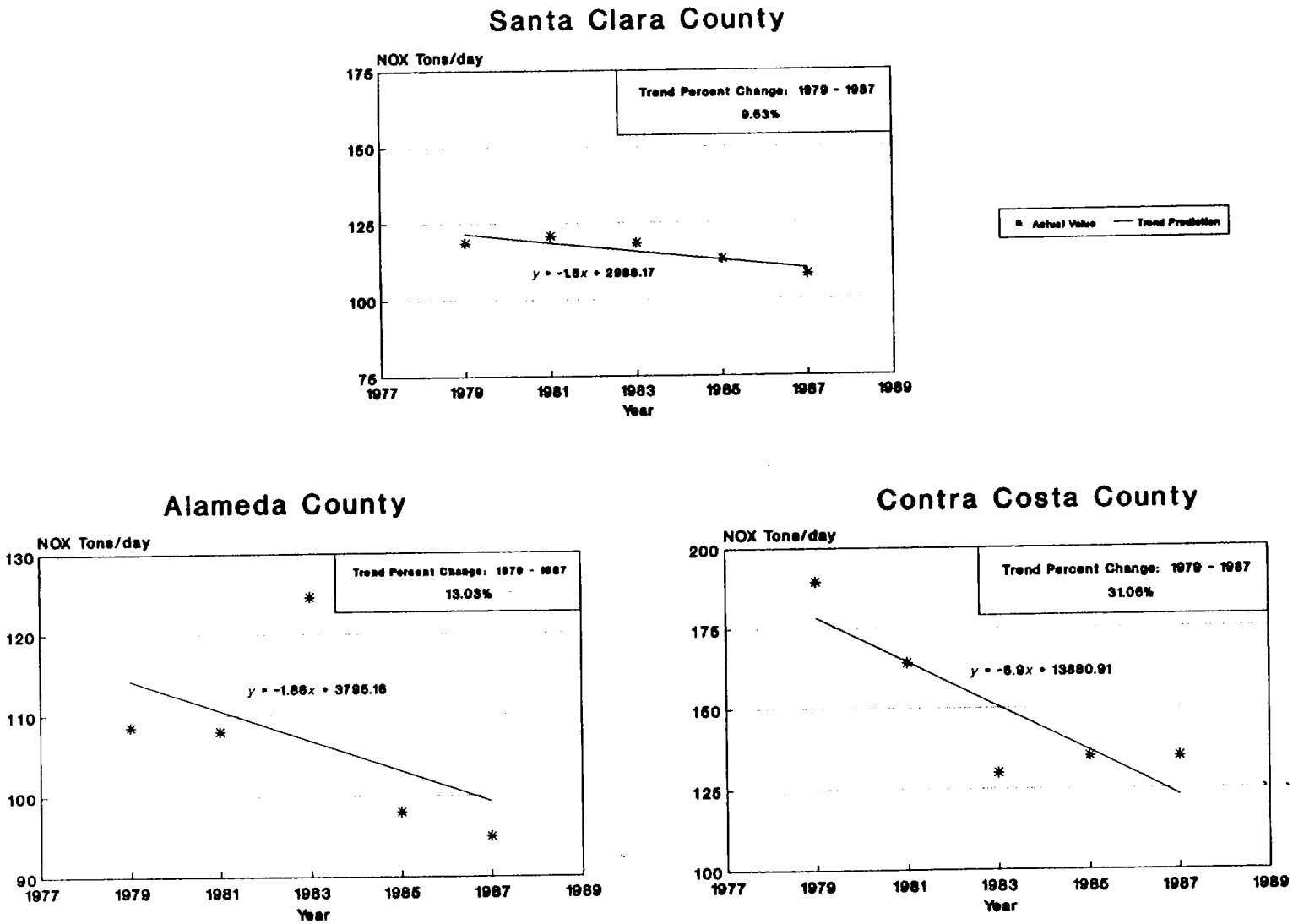

Figure 2-11. NOX Trends: San Francisco Air Basin

San Joaquin Valley Air Basin NO_x Trends

There is no observable NO_x trend in the SJV air basin; emissions remain almost completely flat over the entire trend period. The low r^2 value and high p value also imply there is little downward trend. Oil and gas production increases by 27 TPD while mobile source emissions decrease by 30 TPD. Figure 2-12 presents trends for San Joaquin and Stanislaus counties, which look similar to trends for the air basin in general. San Joaquin county represents 10% of the total NO_x inventory in the air basin and has the same pattern of increasing oil and gas production and decreasing mobile source emissions. Stanislaus county, representing 6% of the air basin NO_x inventory, has a slight downward trend in NO_x, caused by a 6 TPD decrease in motor vehicle emissions.

CONCLUSIONS

The emission trends for the SFBA show large regression-predicted decreases in ROG emissions (42%) and large regression-predicted decreases in NO_x emissions (24%). These decreases are statistically significant at 99.3% and a 99.5% confidence levels, respectively. In the two downwind air basins ROG decreases have also been significant (16% in the NCC and 39% in SJV), and NO_x has decreased in the NCC (44%) but does not appear to have decreased in the SJV. These decreases are discussed in connection with ozone air quality trends in Section 5. Numerous uncertainties in the emission inventories should be noted prior to interpretation of the apparent trends.

First, as noted in the introduction to this chapter, biogenic emissions, although they constitute a significant or even predominant portion of the ROG inventories in most California counties, are not currently included in the ROG estimates. As a result, actual ROG trends may be quite different than predicted with current methodology. Further, there are also a number of other under- or univentoried sources not included in the ROG and NO_x estimates used in this study.

In addition, the quality assurance of the trend estimates used in this study does not appear to have been thorough. For example, the 2000% increase is pesticide application in the SFBA in 1981 and 1983 is not consistent with published inventories (ARB, 1986).

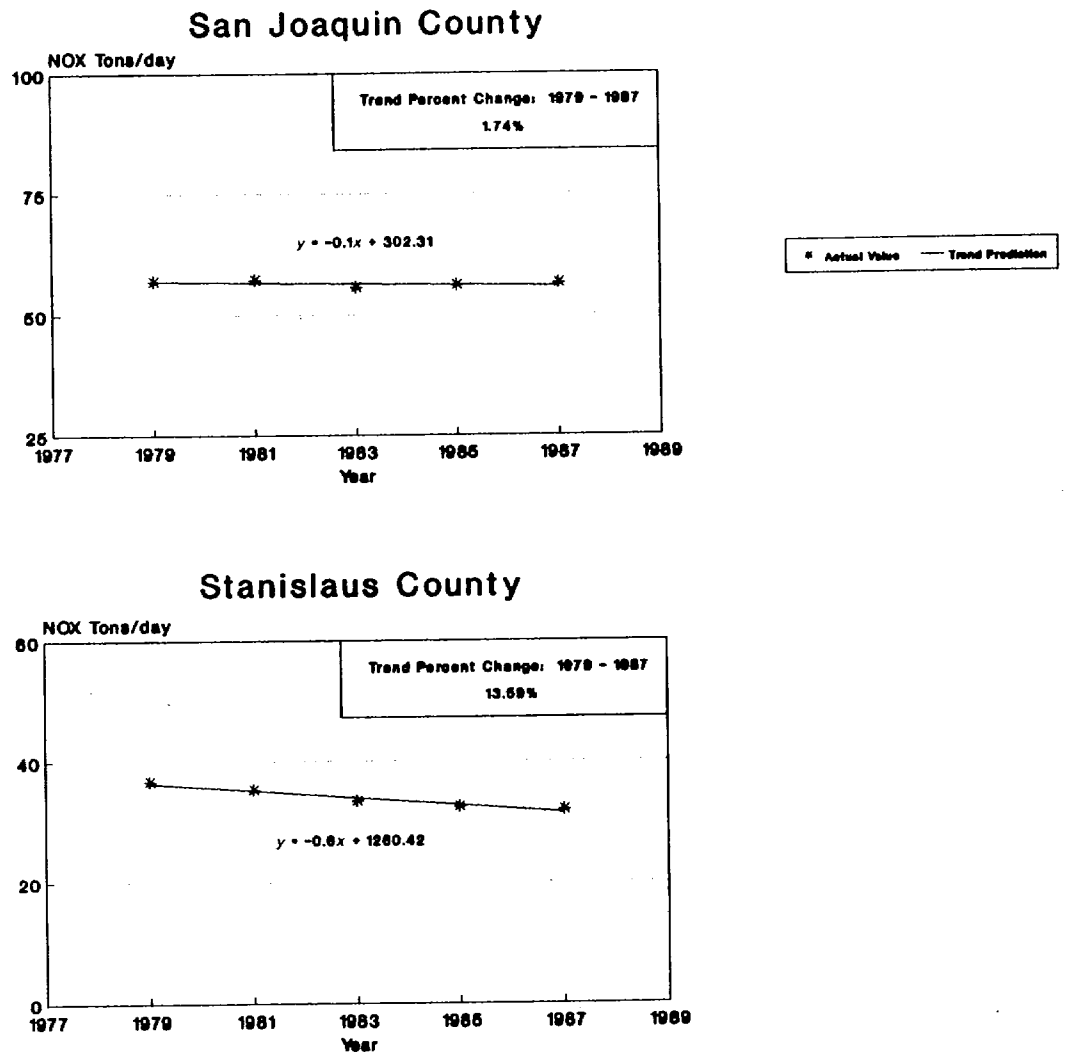

Figure 2-12. NOX Trends: San Joaquin Valley Air Basin

Finally, there are numerous uncertainties in many of the emission factors used in the emission inventory generation. The most significant example may be uncertainties in mobile source emission factors. For example, recent results of an automobile testing program sponsored by UNOCAL show that many older vehicles have emission rates far above the maximum expected and currently assumed by the California emission factor model EMFAC7E. In this program 20% of the vehicles tested had emissions larger than the emission testing system was able to measure. As another example, recent work by the ARB (Lawson et al., 1990) showed that far more vehicles become high emitters shortly after passing smog tests than is currently assumed in EMFAC7E. The tunnel study (Ingalls et al., 1989) further highlights these uncertainties. There are also concerns over (1) the representativeness of emission test procedures used for actual driving patterns (limited data available from the ARB Mobile Source Division indicate that actual driving patterns may produce far higher emissions than test cycle data), and (2) the contribution of unregistered vehicles (not currently estimated). Current ARB test programs and planned studies over the next two fiscal years as well as other ongoing studies are intended to address these issues and produce recommendations for improved and more accurate methodologies. In the interim, however, these uncertainties should be kept in mind when interpreting emissions and air quality trends.

3 ANALYSIS OF HISTORICAL OZONE CONCENTRATION DATA

In our analysis of historical ozone concentration data we examined ozone concentration data for the NCC, SJV, and SFBA air basins during the period 1979-1988 to determine how ozone levels within the air basins have changed during this period and to relate these changes to changes in emissions within the source and receptor basins. The first step in the analyis was to develop criteria for determining whether transport conditions exist in each of the receptor air basins. High-ozone days in the NCC or SFBA and high-ozone days in SJV or SFBA were identified and categorized as transport, no transport, or indeterminate. Ozone trends were calculated for both the source and receptor basins and for selected monitors within each basin. Separate trends were calculated for transport and no-transport days.

DATA

The following data were used in the identification and classification of ozone episodes: (1) hourly ozone data for all reporting stations within the SFBA, NCC and SJV air basins for the period April through October, 1979-1988; and (2) ARB numbered airflow patterns for the SFBA and SJV (Hayes et al., 1984), three to four times per day, for the period April through October, 1979-1988. The ARB airflow patterns for the SFBA are given in Figure 3-1. The airflow patterns for the SJV are given in Figure 3-2.

DEVELOPMENT OF TRANSPORT CRITERIA

Methodology

Hourly ozone and airflow pattern data for the period April through October, 1983-1985 were used to develop the transport criteria. All days within this period were

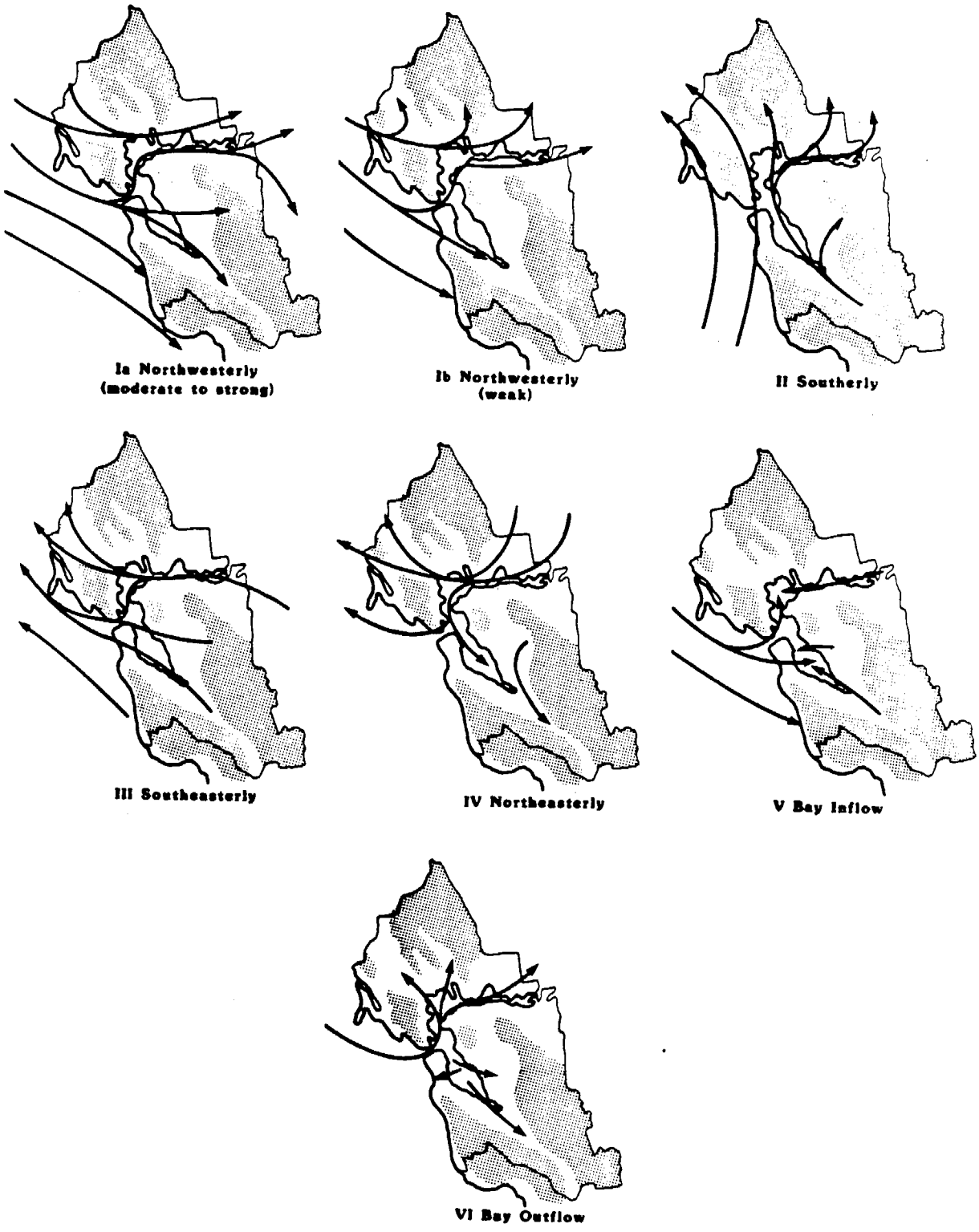

FIGURE 3-1. San Francisco Bay Area airflow pattern types. (Source: Hayes et al., 1984).

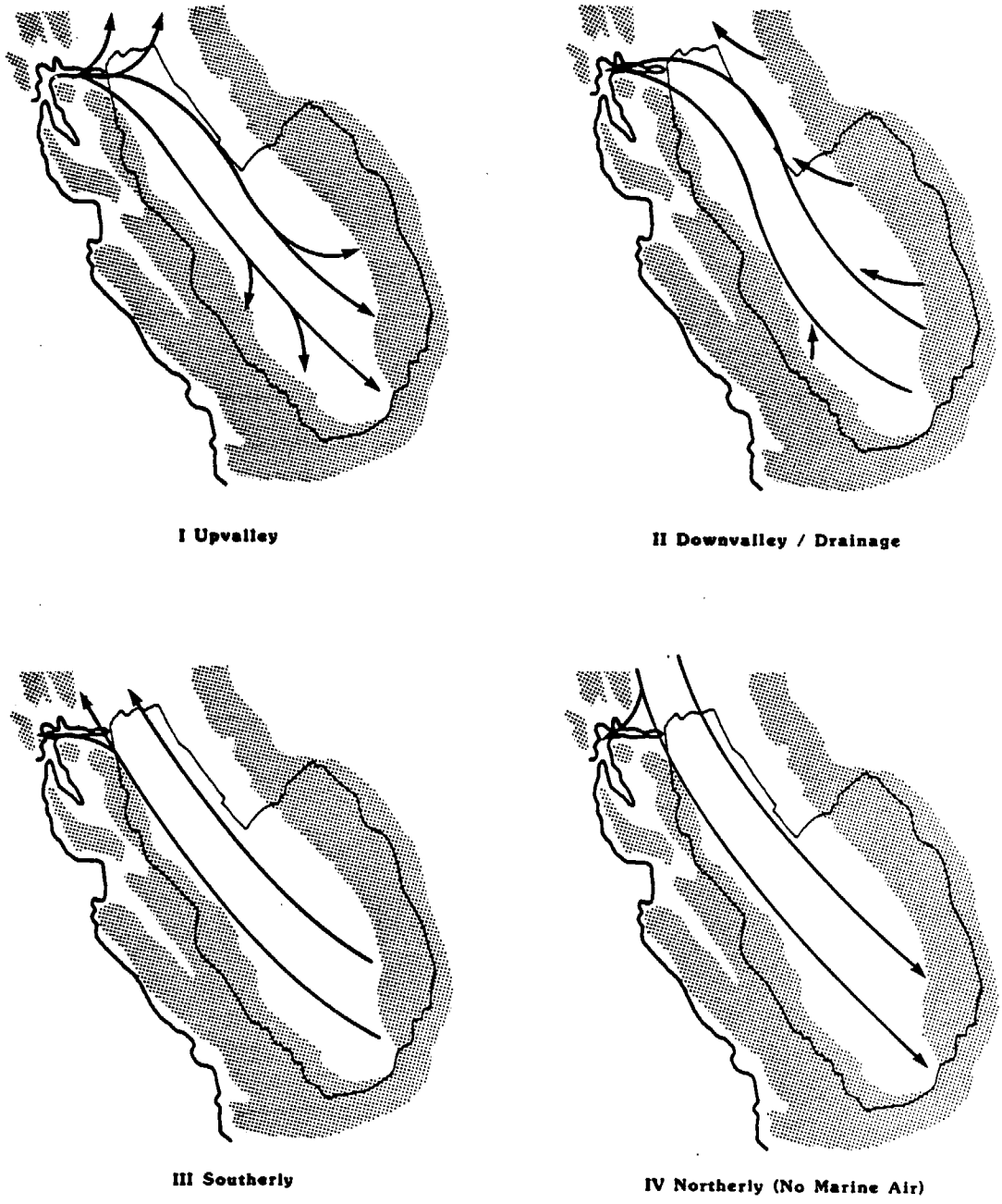

FIGURE 3-2. San Joaquin Valley airflow pattern types. (Source: Hayes et al., 1984)

first classified as transport, no transport, or indeterminate based on analysis of the ozone concentration data. Specifically, the basinwide ozone peak was examined. For the SJV, the peak ozone from the three northernmost counties (San Joaquin, Stanislaus, and Merced) was used. The decision to focus our analysis on the northern part of the SJV (NSJV) was based primarily on our inability to distinguish between transport and local production when the basinwide ozone peak occurred in the southern part of the SJV. This narrowed the focus of the analysis to same-day transport and thus eliminated the difficulties involved in determining multi-day transport events. Focus on the northern part of the SJV is consistent with the transport assessment performed by the ARB (1990d).

For the classification of days into the transport, no-transport, and indeterminate categories it was assumed that: (1) high ozone in the SFBA and low ozone in the downwind air basin (NCC or NSJV) is consistent with no transport, (2) high ozone in the SFBA and high ozone in the downwind air basin indicates possible transport, (3) low ozone in the SFBA and high ozone in the downwind air basin may indicate transport if ozone concentrations in the SFBA were high on the previous day, and (4) low ozone in the SFBA and low ozone in the downwind air basin are unimportant to this study. The California state ozone standard, 9 pphm (not to be exceeded), was used as the threshold for determining whether the basinwide peak ozone concentration was high or low. However, since ozone concentrations do not exceed 9 pphm very often in the NCC, this threshold was lowered to 8 pphm for this air basin in order to obtain a large enough sample of high ozone days in the NCC. The classification criteria based on basinwide peak ozone concentrations are summarized here:

	Peak Ozone (pphm)			Likelihood of
	SFBA	NCC	NSJV	Transport
1	>13	<=8	<=9	Lowest
2	>11	<=8	<=9	Low
3	>9	<=8	<=9	Low
4	>9	>8	>9	Moderate
5	<=9	>8	>9	High

Following the classification of the 1983-1985 days into the five transport categories listed above, the airflow patterns for each day within each category were then examined in a effort to find a relationship between airflow pattern and likelihood of transport.

Finally, the hourly ozone concentrations at several "gateway" monitors within each basin for each of the days within the transport categories listed above were examined. The "gateway" monitors included San Jose, Los Gatos, Gilroy, and Hollister for SFBA/NCC transport, and Pittsburg, Livermore, Bethel Island, Stockton, and Turlock for SFBA/NSJV transport.

The analysis evolved differently for the two transport couples (relationsnips between airflow patterns and ozone concentrations were found to be useful in determining SFBA/NSJV transport but not useful for determining SFBA/NCC transport). Results of the analysis were used to develop the transport criteria.

SFBA/NCC

No relationship was found between the SFBA airflow patterns and the liklihood of transport from the SFBA to the NCC as indicated by the basinwide peak ozone concentrations. This appears to be due to the fact that the SFBA flow pattern categories cannot be related to any particular flow regime in the NCC, at least none that have any bearing on transport. For example, using the SFBA patterns alone, it is not possible to differentiate between a northwesterly flow day in the SFBA on which a convergence zone between Gilroy and Hollister exists (no transport) and one on which it does not exist (transport).

Given this result, using relative ozone concentrations at gateway stations appeared to be the best way to differentiate between transport and no-transport days. The percentage of days on which the daily maximum ozone concentration at Gilroy ranked in the top three in the SFBA (Table 3-1) and the percentage of days on which the daily maximum ozone concentration at Hollister ranked as the highest peak ozone concentration within the NCC (Table 3-2) increases substantially between no-transport and transport days. Thus a high basinwide ozone peak in the NCC with

TABLE 3-1. Percent of high-ozone days in the NCC or SFBA on which Gilroy ranked in top three for peak O_3 in SFBA.

		NCC Peak O_3 (pphm)			
		≤6	≤7	≤8	>8
SFBA	>13	0%	0%	0%	25%
Peak	>11	5%	8%	7%	33%
O_3	>9	24%	29%	29%	46%
(pphm)	≤9	-	-	-	67%

TABLE 3-2. Percent of high-ozone days in the NCC or SFBA on which Hollister ranked highest for peak O_3 in NCC (1983-1985).

		NCC Peak O_3 (pphm)			
		≤6	≤7	≤8	>8
SFBA	>13	-	-	60%	-
Peak	>11	-	-	63%	-
O_3	>9	-	-	66%	69%
(pphm)	≤9	-	-	-	92%

relatively low peak ozone concentrations at Gilroy and Hollister indicates a no-transport day.

Determining no-transport was easier than determining transport. Ozone concentrations in the NCC were never excessively high. When coupled with moderate ozone levels in the SFBA it was not possible to differentiate between local, shared, or transport days. Further analysis of the timing of peak ozone concentrations and wind observations at Gilroy and Hollister might facilitate the identification of transport days.

Thus, our analysis for the SFBA/NCC transport couple resulted in only two transport categories: no-transport and indeterminate. The following transport criteria were developed: If the ratio of the peak daily ozone concentration at Gilroy to the basinwide average daily maximum ozone in the SFBA was less than 1.15 and the peak daily ozone concentration at Hollister was not the highest in the NCC then the day was classified as a no-transport day. To avoid difficulties posed by missing data, we used the ratio of the daily maximum ozone concentration at Gilroy to the basinwide average daily maximum ozone concentration in the SFBA rather than the ranking. Analysis of the average ratio within each of the five likelihood of transport categories showed that an average ratio of 1.15 best separated likely transport from unlikely transport days. All other days were categorized as indeterminate.

This categorization accounts only for transport from the SFBA to the NCC along the Santa Clara Valley. Overwater transport from the SFBA to the NCC has also been documented (Dabberdt et al., 1982). The principal zone monitoring station in the NCC that might be affected by overwater pollutant transport is Carmel Valley. Back trajectories calculated by the ARB for days when Carmel Valley exceeded the state standard in 1989 suggest that transport occurs from offshore into Monterey Bay and Carmel Valley. Thus, emissions from both the SFBA and the Monterey area could contribute to high ozone concentrations at Carmel Valley. Unfortunately, Carmel Valley could not be used in formulating criteria because a complete set of data for this monitor was lacking.

SFBA/NSJV

Analysis of the SFBA and SJV flow patterns within each of the likelihood of transport categories proved fruitful. The frequency of occurrence of the upvalley flow pattern at 1000 PST in the SJV (which would promote transport from the SFBA) increased from 10 percent on no-transport days to 78 percent on days consistent with transport (overall frequency is 61 percent). Conversely, the frequency of occurrence of the northerly flow pattern at 1000 PST in the SJV (which does not allow transport from the SFBA) decreased from 70 percent on no-transport days to 5 percent on transport days (overall frequency is 17 percent). In the SFBA, the frequency of occurrence of the bay outflow pattern at 1000 PST decreased from 40 percent on no-transport days to 5 percent on transport days (overall frequency is 11 percent). Since the bay outflow pattern is associated with weak winds/stagnation, this pattern is consistent with no transport. In summary, SFBA bay outflow and SJV northerly patterns were most likely to occur on days consistent with no transport, while the SJV upvalley pattern was most likely to occur on days consistent with transport (Table 3-3).

Combinations of transport patterns were examined to see if combined SFBA/SJV flow patterns would determine transport/no transport better than using the individual patterns. No better predictors were found.

Analysis of the ozone concentration data at the "gateway" sites indicated that Bethel Island is the key ozone monitor for determining transport from the SFBA to the NSJV. Bethel Island was ranked in the top three for deak daily ozone concentration zero percent of the time on no-transport days and 38 percent of the time on days consistent with transport.

Based on the analysis of of airflow patterns and ozone data, the criteria for transport are: If the SJV flow pattern at 1000 PST is upvalley and the ratio of the Bethel Island maximum ozone concentration to the basinwide daily maximum ozone concentration in the SFBA is greater than 1.15 then transport is likely. (Analysis of the average ratio within each of the likelihood of transport categories showed that an average ratio of 1.15 best separated likely transport days from unlikely transport days). If at least one of the two criteria for transport is not met and the the SJV flow pattern at 1000 PST is northerly or the SFBA flow pattern at 1000 PST is bay outflow then

TABLE 3-3. Frequency of flow patterns in NSJV and SFBA.

Peak O_3	(SFBA >11, NSJV ≤9)	(SFBA >9, NSJV ≤9)	(SFBA >9, NSJV >9)	(SFBA ≤9, NSJV >9)	Average
NSJV (1000 PST)					
Up Valley	10%	28%	48%	78%	61%
Northerly	70%	49%	17%	3%	17%
SFBA (1000 PST)					
Bay Outflow	40%	31%	23%	5%	11%

transport is not likely. Our analysis of combinations of flow patterns showed that using either the northerly SJV flow pattern or the bay outflow SFBA flow pattern is better than using both of these flow patterns together. All other days were categorized as indeterminate.

CATEGORIZATION OF OZONE EPISODES

Based on the above discussion of transport criteria, we developed a data base containing daily maximum ozone concentrations at all reporting SFBA, NCC, and NSJV monitoring stations for the months April - October for the years 1979 - 1988. Valid daily maxima readings were recorded only for days with nine or more hourly averages between 0900 and 2100 LST. All other days are listed with missing daily maxima. The data base also contains the 10:00 am SJV and SFBA ARB flow patterns (1000 LST) for each day. This comprises all of the information needed to apply the transport/no-transport criteria described above to each day.

Our first step was to create two subsets of the data base described above. One contains all days on which either the daily maximum ozone concentration at any SFBA monitor exceeded 9 pphm or the daily maximum ozone concentration at any NSJV monitor exceeded 9 pphm. The other contains all days on which either the daily maximum concentration at any SFBA monitor exceeded 9 pphm or the daily maximum concentration at any NCC monitor exceeded 8 pphm. The first set of days are hereafter referred to as the NSJV data set, while the second is referred to as the NCC data set.

The procedure used to categorize transport conditions between the SFBA and the NCC for days in the NCC data set is depicted in Figure 3-3. As discussed in the previous section, it was not possible to clearly identify transport conditions between SFBA and NCC, while no-transport days could be identified with a reasonable degree of confidence. We classified as no-transport those days on which the daily maximum concentration at Gilroy was not appreciably higher than the basinwide average daily maximum in the SFBA (ratio of Gilroy daily maximum ozone concentrations to SFBA average maximum ozone concentration less than 1.15) and the daily maximum con-

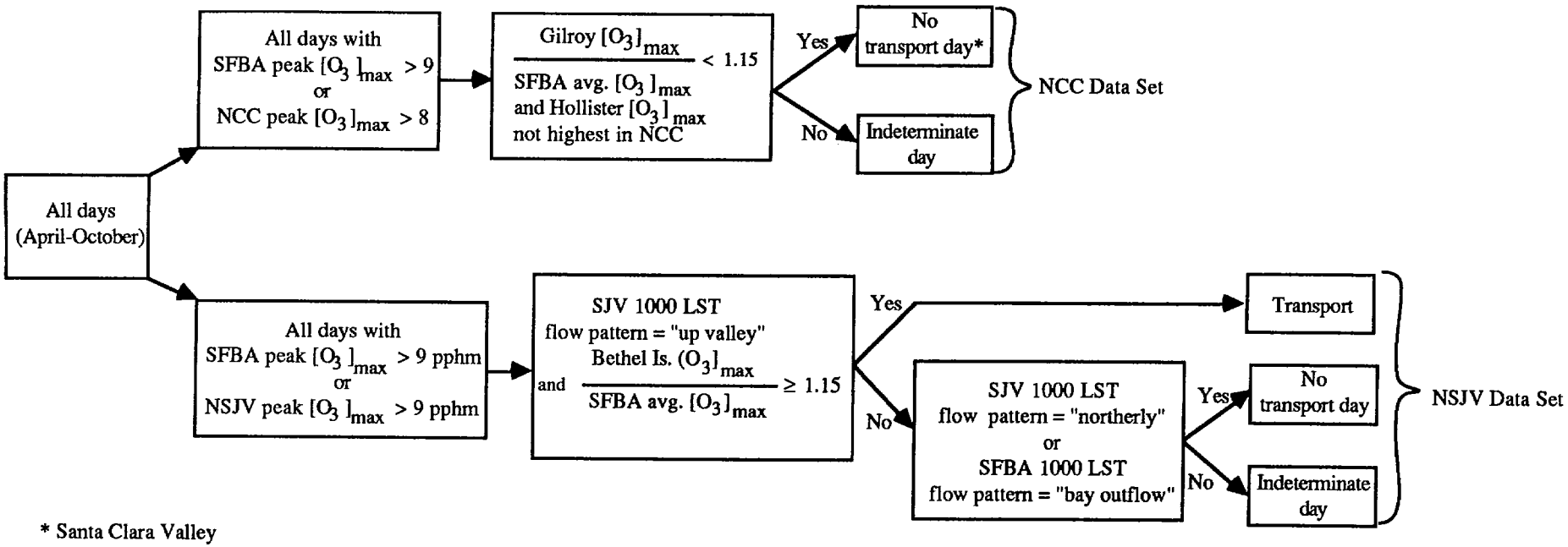

FIGURE 3-3. Classification criteria used to identify transport, no-transport, and indeterminate days for San Francisco Bay Area (SFBA) to North Central Coast (NCC) transport (NCC data set) and SFBA to Northern San Joaquin Valley (NSJV) transport (NSJV data set). $[O_3]_{max}$ = daily maximum hourly average ozone concentration.

centration in the NCC did not occur at Hollister. All other days were classified as indeterminate.

Transport conditions between the SFBA and the NSJV were determined through a combination of relative ozone concentrations and 1000 LST flow patterns as shown in Figure 3-3. Days in the NSJV data set were categorized as transport days if the 1000 LST flow pattern in the SJV was "up valley" and the daily maximum ozone at Bethel Island was relatively high (i.e., the ratio of Bethel Island daily maximum ozone concentration to the SFBA average maximum ozone concentration is greater than or equal to 1.15). Days not meeting the transport criteria were classified as no transport if the 1000 PST flow pattern in the SJV was "northerly" or the 1000 LST flow pattern in SFBA was "bay outflow". Any other days are classified as indeterminate. Since transport conditions on these days are not well defined, we did not perform separate trend analyses for them. However, the indeterminate days are included in the "all-day" trends as described below.

Because of missing data, not all days in the NCC and NSJV data sets could be categorized according to the procedure outlined in Figure 3-3. In particular, no days during 1979 in the NCC data set could be categorized since data for Gilroy were unavailable. Similarly, days during 1979 and 1980 in the NSJV data set could not be categorized because of the absence of data at Bethel Island. Table 3-4 shows the breakdown of days in the NCC and NSJV data sets into the various transport categories by year. With the exception of 1979 and 1986 in the NCC data set and 1979 and 1980 in the NSJV data set, only a small percentage of days could not be classified due to missing data. For the NCC data set, only 15% of all days were classified as no-transport. Given the prevalence of conditions favoring transport between SFBA and the NCC and NSJV, ozone trends calculated for no-transport days are based on a very small number of days in each ozone season. As a result, these trends are relatively uncertain, as discussed in the following section. For the NSJV data set, transport days outnumber no-transport days by about three to one. Roughly one quarter of all days were classified as indeterminate.

OZONE TRENDS

Trends in the seasonal average daily maximum ozone concentration were calculated for each transport category at selected monitoring sites in each air basin. Sites in the SFBA were chosen to represent air quality at the "gateways" into the NCC and NSJV basins. Gilroy was selected as the NCC gateway site and Bethel Island and Livermore were selected as the NSJV gateway sites. Monitors in the NCC and NSJV basins were selected based on the locations that are most likely to show responses to changes in SFBA emissions. Hollister was selected as the NCC site. The average daily maximum concentration over a group of five monitors in Stockton, Turlock and Modesto was selected for the NSJV. These monitors are: Hazelton St. in Stockton, Monte Vista in Turlock (W. Monte Vista in 1979) and 814 14th St. in Modesto (J St. prior to 1981).

For each air basin we also calculated trends in the seasonal mean value of the daily basin-wide peak ozone concentration for days in each transport category. These trends provide an indication of the effects of changes in emissions on ozone concentrations in the highest impact area within each basin. In keeping with the limited scope of this study, no attempt was made to account for the effects of missing data on any of the seasonal ozone summary statistics.

To provide an indication of the significance of year-to-year changes in ozone levels, we calculated 95% confidence intervals for each seasonal mean concentration based on the assumption that the daily maximum concentrations used to calculate the seasonal means in each transport category represent a random sample drawn from a normally distributed population. Although the distributions of daily maximum ozone concentrations can be expected to be approximately normal, ozone concentrations are known to exhibit some autocorrelation (i.e, they do not represent a true random sample). Therefore, the confidence interval widths we calculated can be expected to be somewhat understated. However, since days in the indeterminate and, especially, the no-transport categories are not in one continuous sequence, the autocorrelation will be minimized, which in turn will minimize the understatement of the confidence interval width. Unfortunately, the same cannot be said for the confidence intervals for "all days". Confidence intervals calculated in the manner described above reflect the effects of measurement error and day-to-day variations in meteorological

TABLE 3-4. Number of days in each ozone transport category by year.

TRANSPORT CATEGORY — YR(Year)

Frequency / Percent	1979	1980	1981	1982	1983	1984	1985	1986	1987	1988	Total
Missing Categorization Data	56 11.62	8 1.66	0 0.00	0 0.00	0 0.00	4 0.83	4 0.83	14 2.90	6 1.24	0 0.00	92 19.09
Indeterminate	0 0.00	36 7.47	44 9.13	26 5.39	47 9.75	36 7.47	40 8.30	18 3.73	35 7.26	36 7.47	318 65.98
No Transport	0 0.00	4 0.83	9 1.87	11 2.28	9 1.87	16 3.32	7 1.45	7 1.45	5 1.04	4 0.83	72 14.94
Total	56 11.62	48 9.96	53 11.00	37 7.68	56 11.62	56 11.62	51 10.58	39 8.09	46 9.54	40 8.30	482 100.00

NCC

TRANSPORT CATEGORY — YR(Year)

Frequency / Percent	1979	1980	1981	1982	1983	1984	1985	1986	1987	1988	Total
Missing Categorization Data	75 9.40	57 7.14	1 0.13	10 1.25	23 2.88	17 2.13	14 1.75	6 0.75	3 0.38	1 0.13	207 25.94
Indeterminate	0 0.00	0 0.00	28 3.51	18 2.26	20 2.51	16 2.01	32 4.01	24 3.01	23 2.88	24 3.01	185 23.18
No Transport	0 0.00	0 0.00	12 1.50	10 1.25	20 2.51	17 2.13	5 0.63	7 0.88	18 2.26	16 2.01	105 13.16
Transport	0 0.00	0 0.00	41 5.14	38 4.76	25 3.13	25 3.13	32 4.01	66 8.27	44 5.51	30 3.76	301 37.72
Total	75 9.40	57 7.14	82 10.28	76 9.52	88 11.03	75 9.40	83 10.40	103 12.91	88 11.03	71 8.90	798 100.00

NSJV

conditions (other than those conditions affecting transport) on the seasonal mean concentrations. They do not, however, account for the effects of day-to-day changes in the number of stations with valid daily maximum concentrations on the basin peak seasonal mean summary statistics.

NCC Data Set Trends

Trends for each selected monitoring site (or group of sites) for no-transport days, indeterminate days, and all days in the NCC data set are shown in Figures 3-4 to 3-7. Confidence intervals shown in the figures were calculated in the manner described above. To test the significance of these trends, a simple linear least squares regression analysis was performed for each case. Results of this analysis are shown in Table 3-5. None of the trends are significant at the 95% confidence limit, although the slight downward trend in the NCC seasonal mean basin-wide peak concentration is significant at the 92 percent level. In general, the no-transport day trends exhibit sharper year-to-year variations and have larger confidence intervals than the indeterminate day trends. This is a result of the relatively small number of days in each year classified as no-transport (see Table 3-4). No consistent differences between no-transport day and indeterminate day trends are evident.

A comparison of the all days trend for Hollister (Figure 3-4c) with the NCC basin-wide peak trend (Figure 3-5c) reveals that the two trends are nearly identical (with the exception of 1979), thus confirming that Hollister is the most common location of the NCC maximum concentration. The Hollister monitor was moved between the 1979 and 1980 ozone seasons, thus explaining the exception noted above. Trends for indeterminate days are also nearly identical, suggesting that Hollister was the site of the NCC peak on most of these days. A comparison of the no-transport day trends for Hollister with the NCC basin-wide peak shows that, while year-to-year changes are very similar, the seasonal basinwide mean peak values are noticeably higher in most years than the values at Hollister, thus suggesting that Hollister is the site of the NCC peak value less often on no-transport days than on other days. This is in keeping with our intuitive notion that NCC local ozone production is more likely to impact the Carmel Valley monitor than the Hollister monitor.

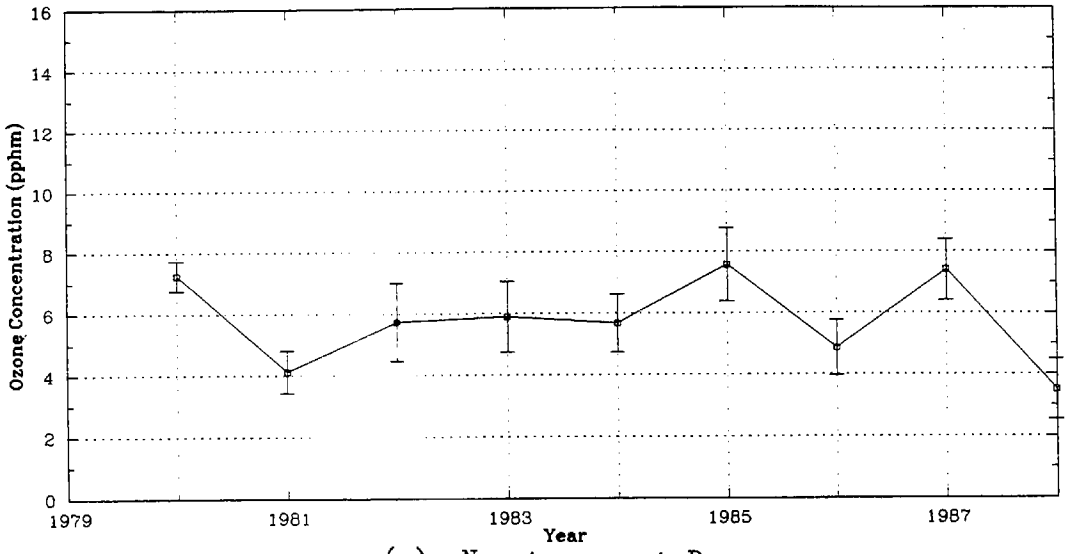

(a) Non-transport Days

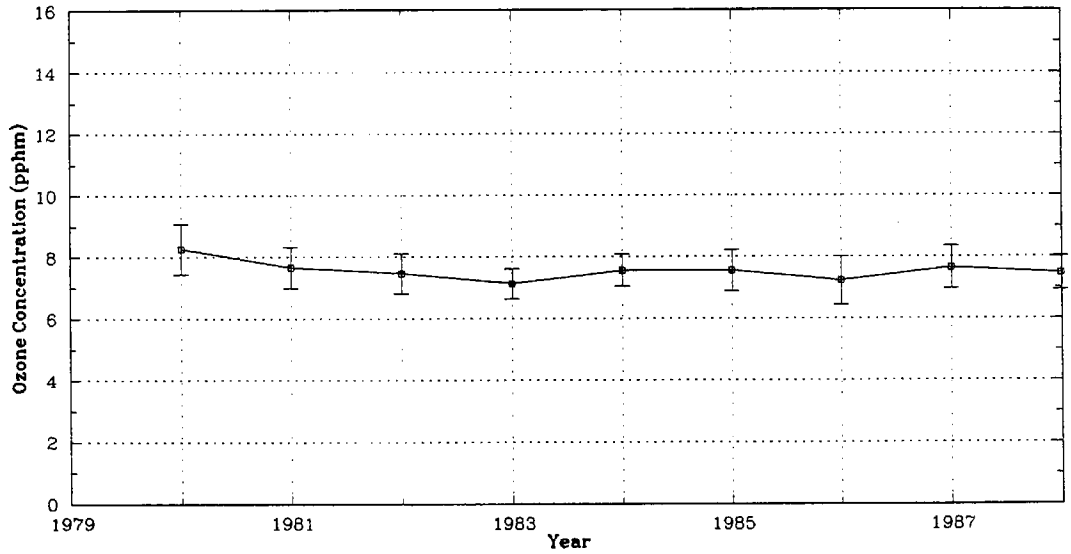

(b) Indeterminate Days

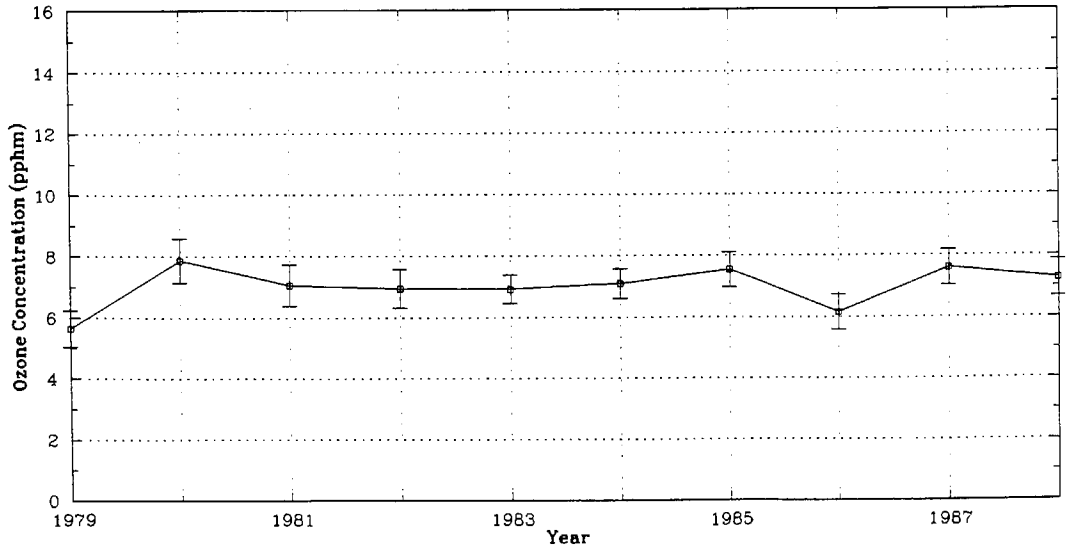

(c) All Days

Note: Error bars represent 95 percent confidence intervals.

FIGURE 3-4. Seasonal average daily maximum ozone trends for Hollister.

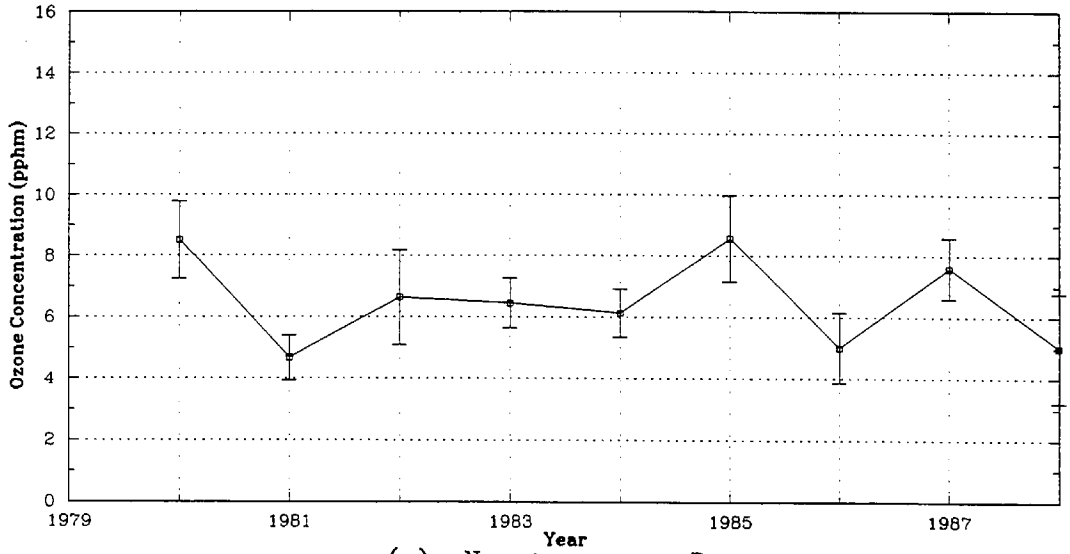

(a) Non-transport Days

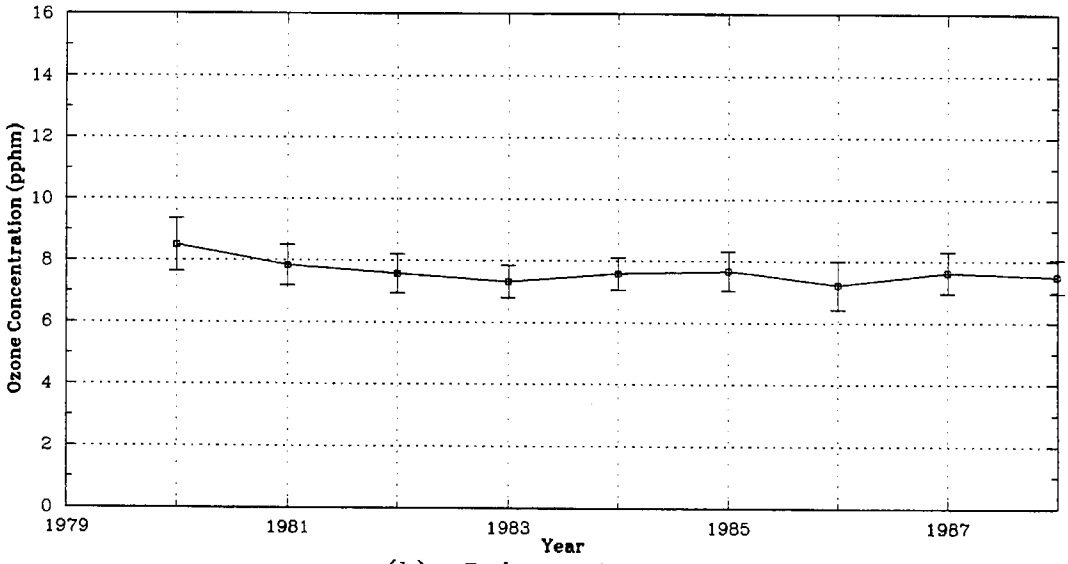

(b) Indeterminate Days

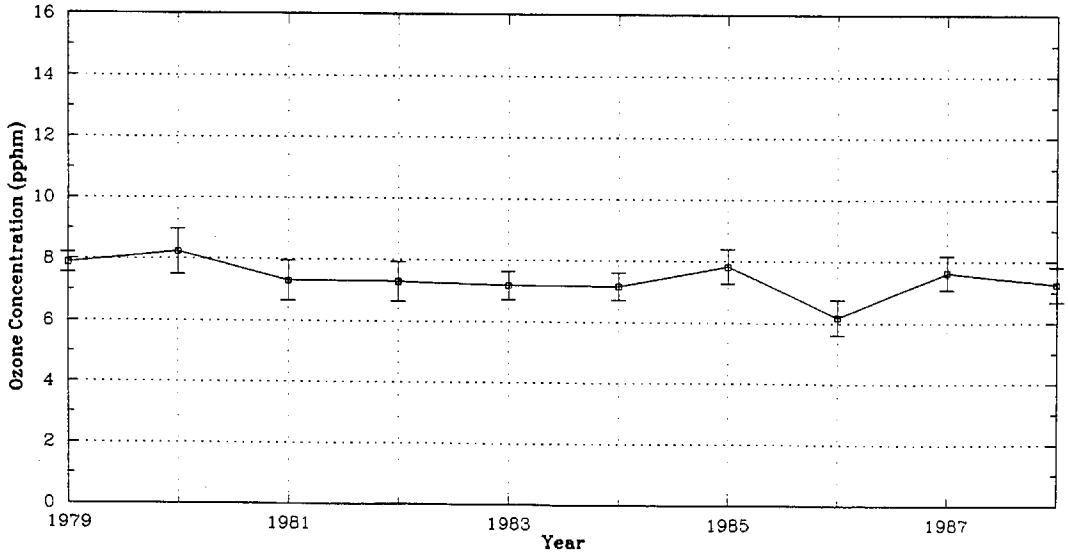

(c) All Days

Note: Error bars represent 95 percent confidence intervals.

FIGURE 3-5. Seasonal average basin peak daily maximum ozone trends for the NCC.

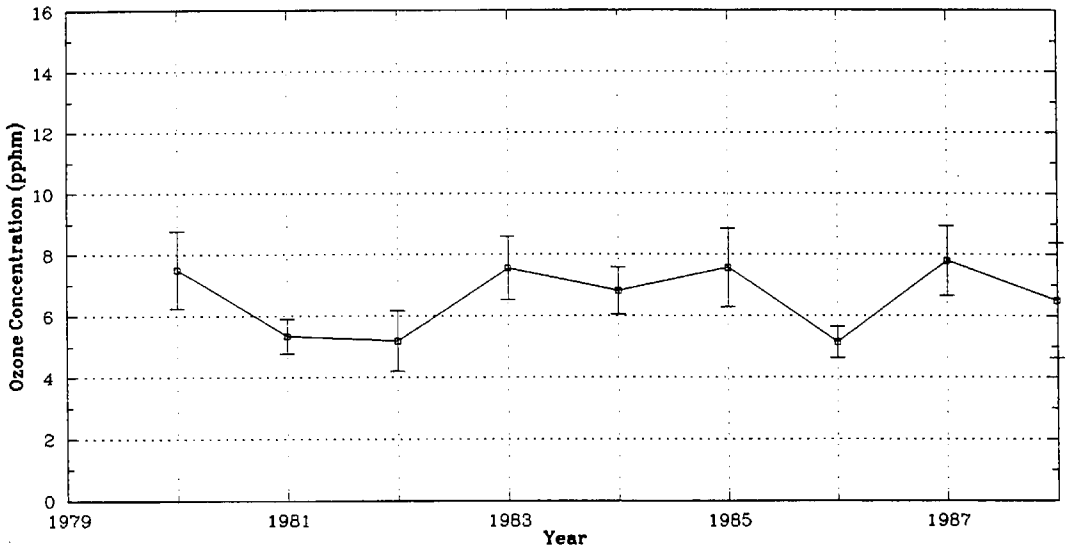

(a) Non-transport Days

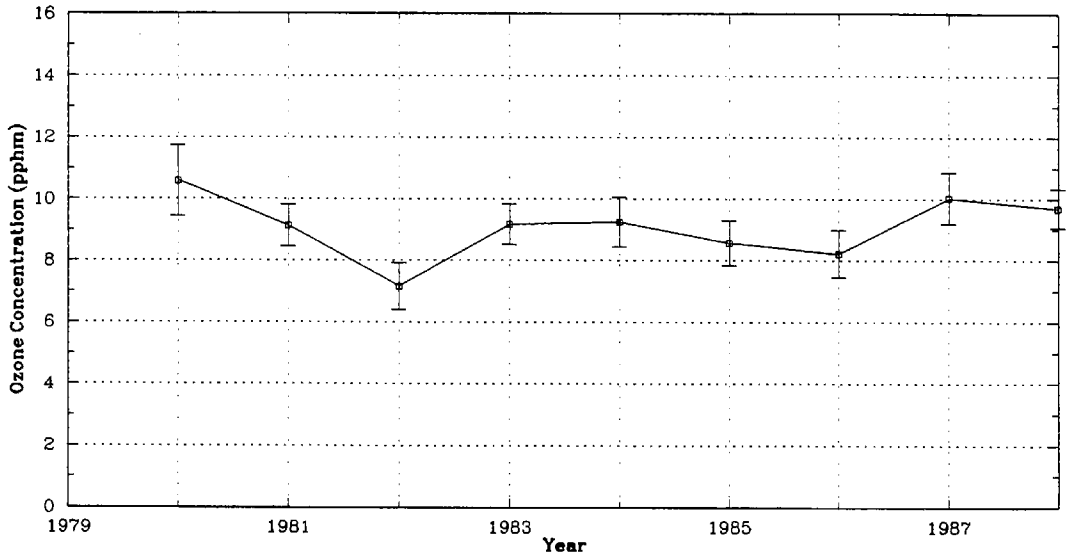

(b) Indeterminate Days

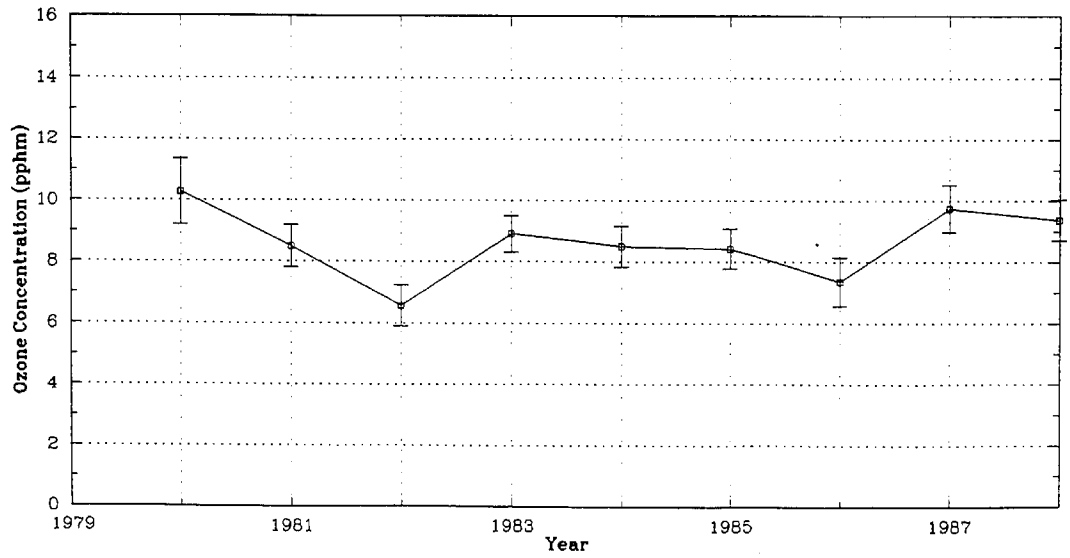

(c) All Days

Note: Error bars represent 95 percent confidence intervals.

FIGURE 3-6. Seasonal average daily maximum ozone trends for Gilroy.

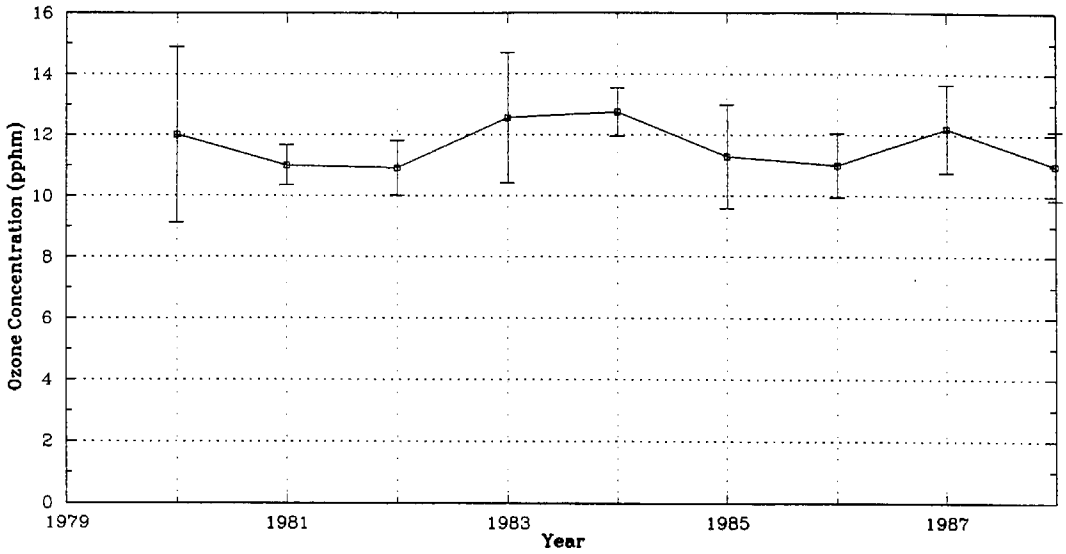

(a) Non-transport Days

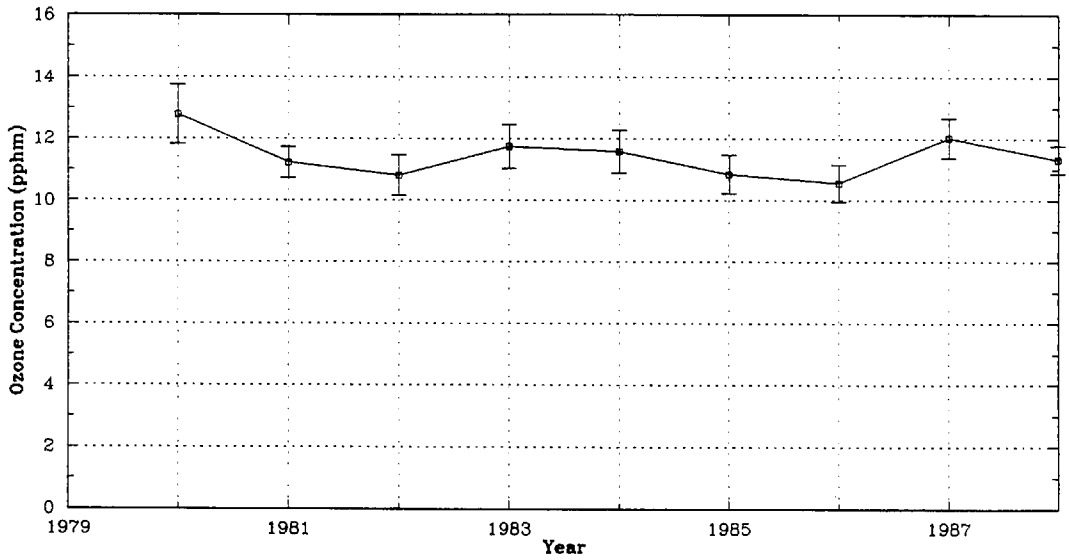

(b) Indeterminate Days

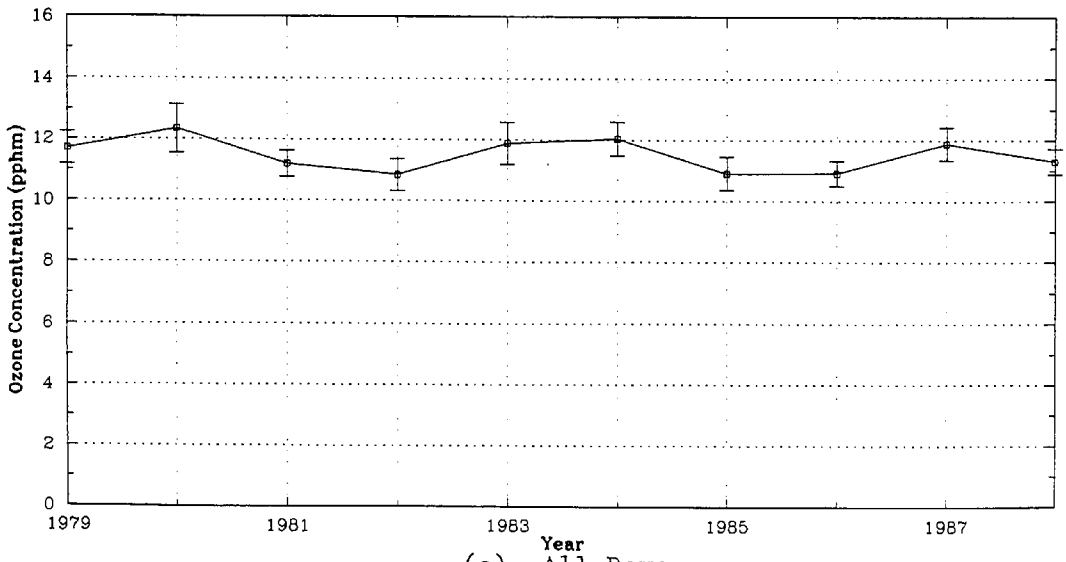

(c) All Days

Note: Errors bars represent 95 percent confidence intervals.

FIGURE 3-7. Seasonal average basin peak daily maximum ozone trends for the SFBA (NCC data set).

TABLE 3-5. Results of linear regression analysis, NCC data set.

Monitor(s)	Category	Trend (pphm/year)	Probability Trend ≠ 0	Trend Significant at 95 % Level
SFBA Basin Peak	All days	-0.05	0.53	No
	Indeterminate	-0.08	0.59	No
	No-transport	-0.02	0.19	No
NCC Basin Peak	All days	-0.08	0.82	No
	Indeterminate	-0.08	0.92	No
	No-transport	-0.11	0.39	No
Gilroy	All days	0.02	0.10	No
	Indeterminate	0.01	0.06	No
	No-transport	0.06	0.27	No
Hollister	All days	0.06	0.56	No
	Indeterminate	-0.05	0.79	No
	No-transport	-0.09	0.33	No

Seasonal mean daily maximum ozone concentrations at Gilroy on no-transport days (Figure 3-6a) are lower than those on indeterminate days (Figure 3-6b), as we would expect. However, the directions (up or down) of the changes from one year to the next are mostly the same for both transport categories. On indeterminate days, the trends at Gilroy are similar to those at Hollister with the notable exception of 1982. Higher concentrations prevail at Gilroy, which also experiences sharper year-to-year variations. The sharp drop in concentrations observed at Gilroy on indeterminate days in 1982 is not seen on any of the other trend plots. We know of no obvious explanation for this decrease.

NSJV Data Set Trends

Trends for each selected monitoring site (or group of sites) for no-transport and transport days as well as all days in the NSJV data set are shown in Figures 3-8 to 3-12. Confidence intervals shown in the figures were calculated in the same manner as for the NCC data set. The significance of trends was evaluated through least squares regression; none of the trends are significant at the 95 percent level (Table 3-6). As in the case of the NCC data set, because of the relatively small number of days falling in the no-transport category in most years, no-transport days have larger year-to-year variations and larger confidence intervals than do transport days (see Table 3-4). No consistent differences between transport and no-transport day trends are evident, although in most years the concentrations at the Stockton/Turlock/Modesto area monitors and the NSJV basinwide peak monitor are slightly higher on transport days than on no-transport days.

A comparison of the all-days SFBA basinwide peak trend based on the NSJV data set (Figure 3-12c) with the same trend based on the NCC data set (Figure 3-7c) reveals roughly the same year-to-year changes but with lower values obtained from the NSJV data set. These lower values are a result of the larger number of SFBA low-ozone days included in the NSJV data set (generally speaking, there are more high-ozone days in the NSJV than in the NCC; see Table 3-4).

It is instructive to compare the SFBA trends in Figures 3-7 and 3-12 with trends calculated for a number of seasonal summary statistics by Rosenbaum (1989).

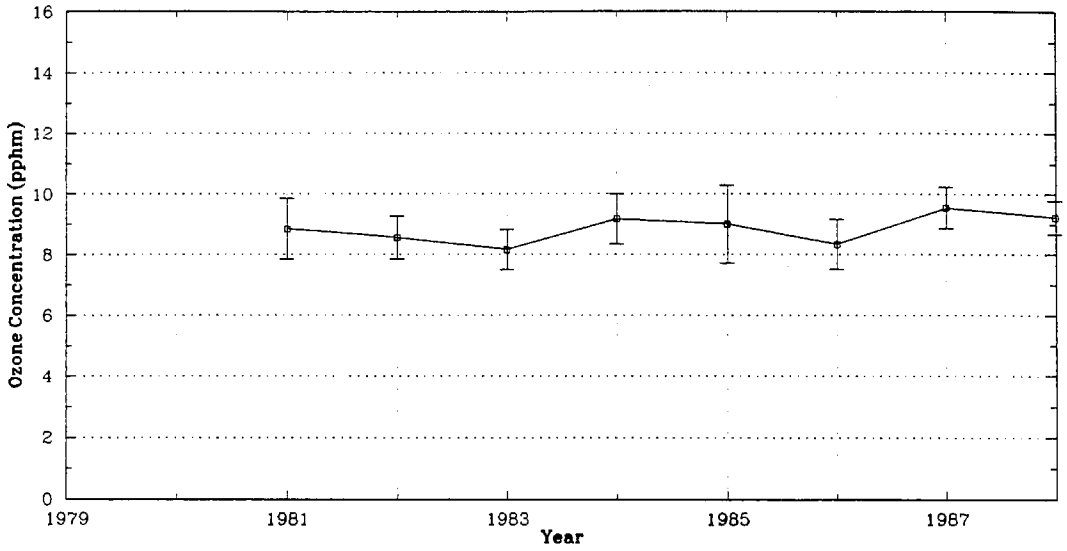

(a) Non-transport Days

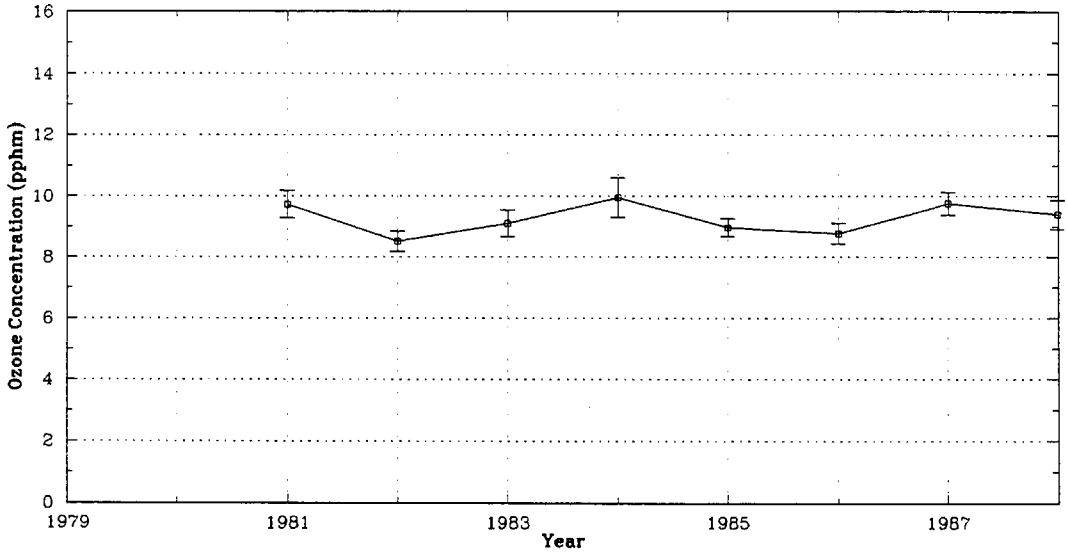

(b) Transport Days

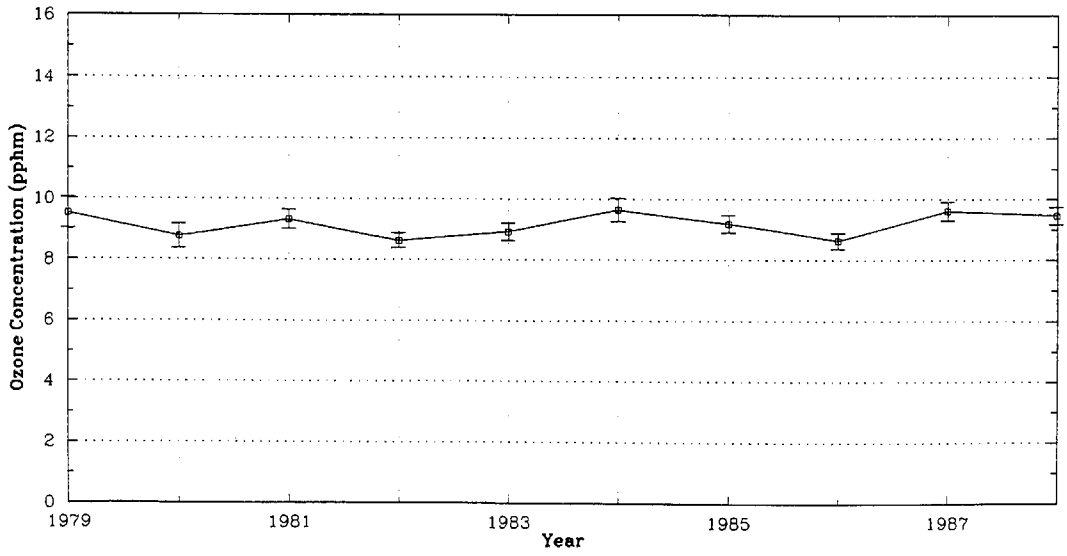

(c) All Days

Note: Error bars represent 95 percent confidence intervals.

FIGURE 3-8. Seasonal average daily maximum ozone trends for Stockton/Turlock/Modesto.

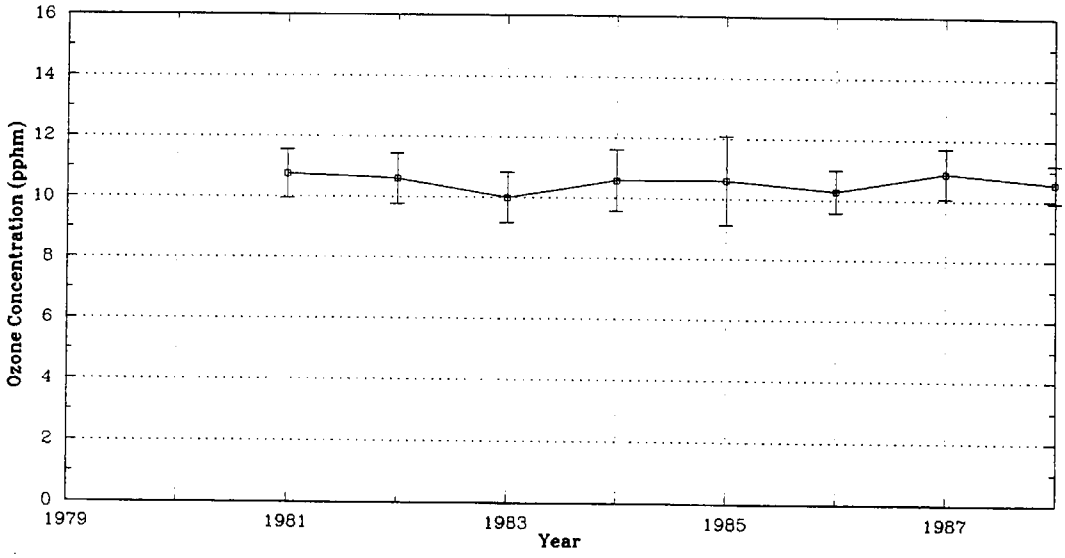

(a) Non-transport Days

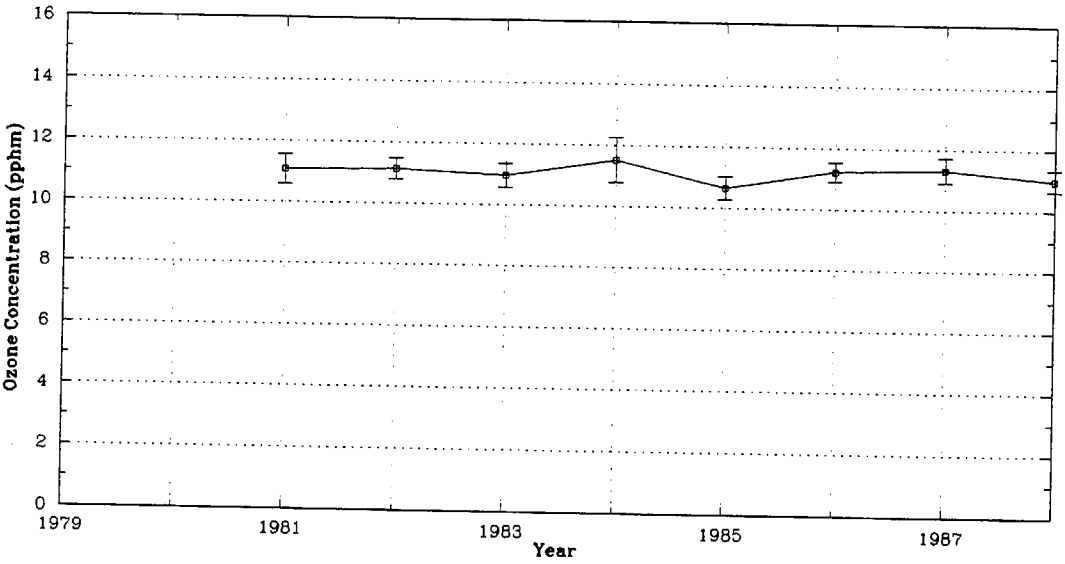

(b) Transport Days

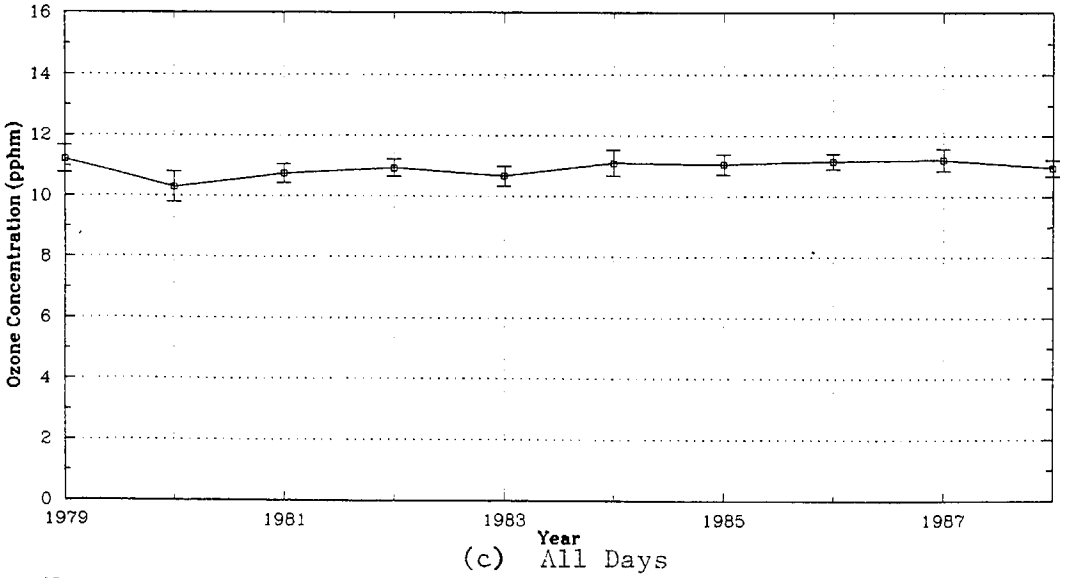

(c) All Days

Note: Error bars represent 95 percent confidence intervals.

FIGURE 3-9. Seasonal average basin peak daily maximum ozone trends for NSJV.

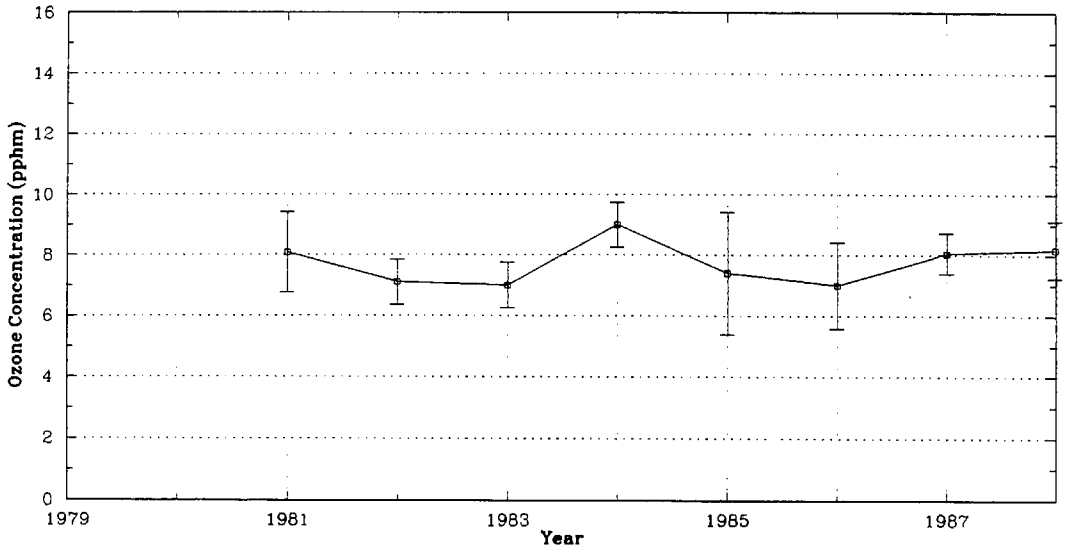

(a) Non-transport Days

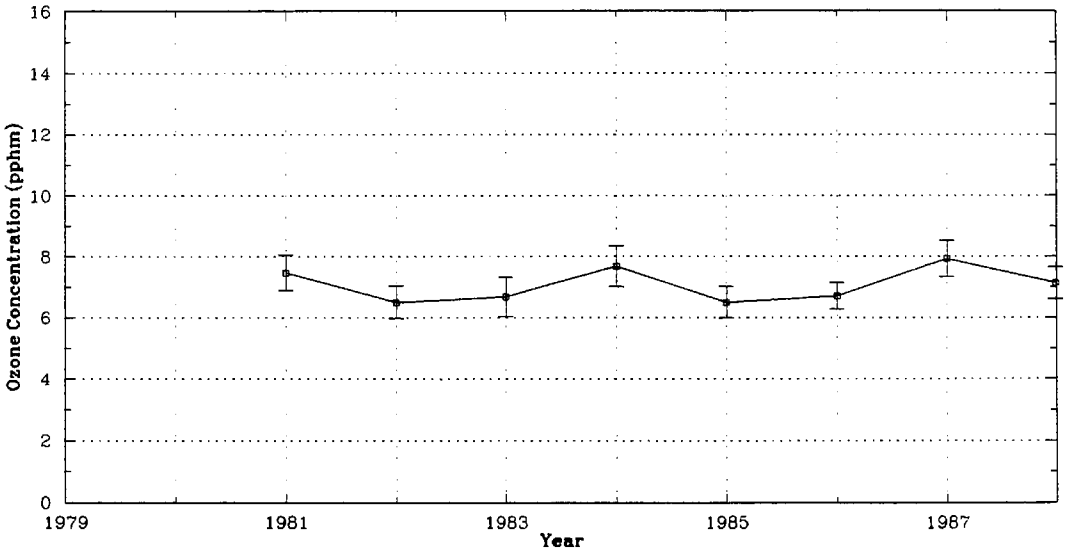

(b) Transport Days

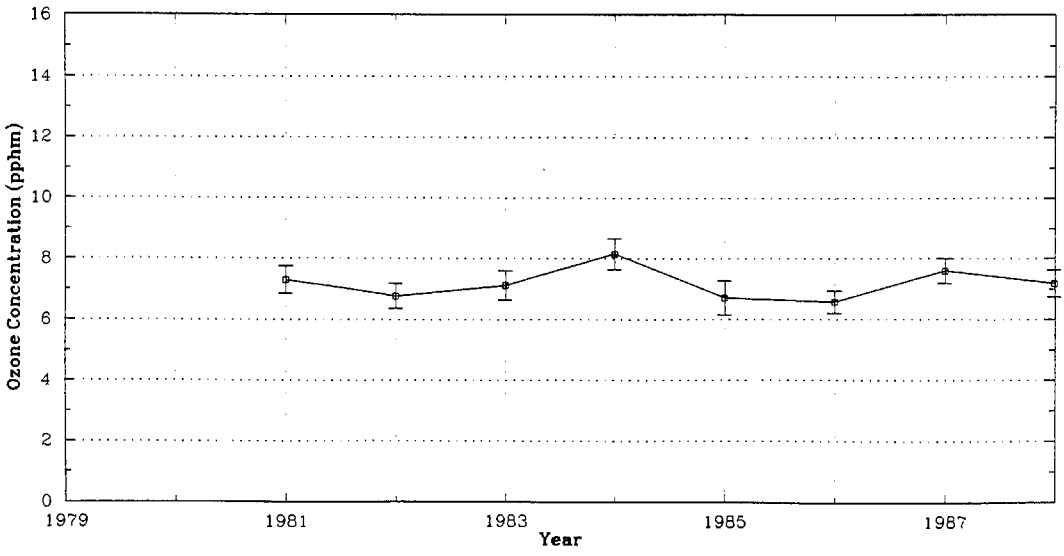

(c) All Days

Note: Error bars represent 95 percent confidence intervals.

FIGURE 3-10. Seasonal average daily maximum ozone trends for Bethel Island.

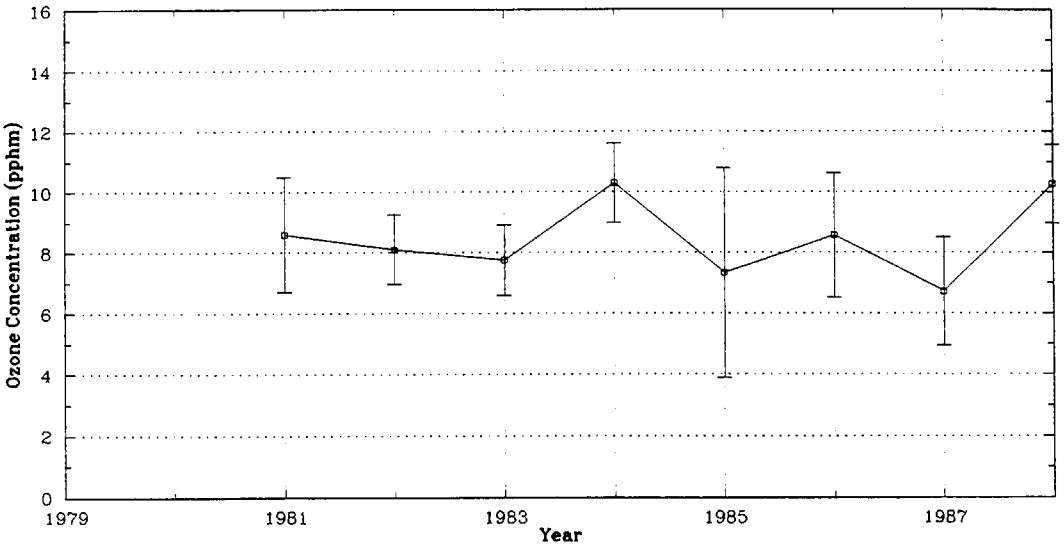

(a) Non-transport Days

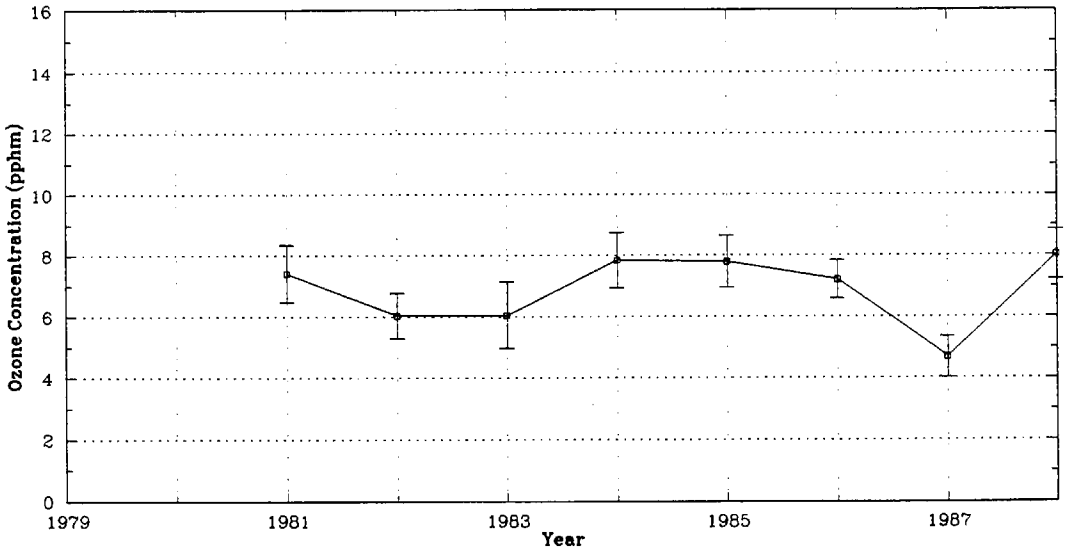

(b) Transport Days

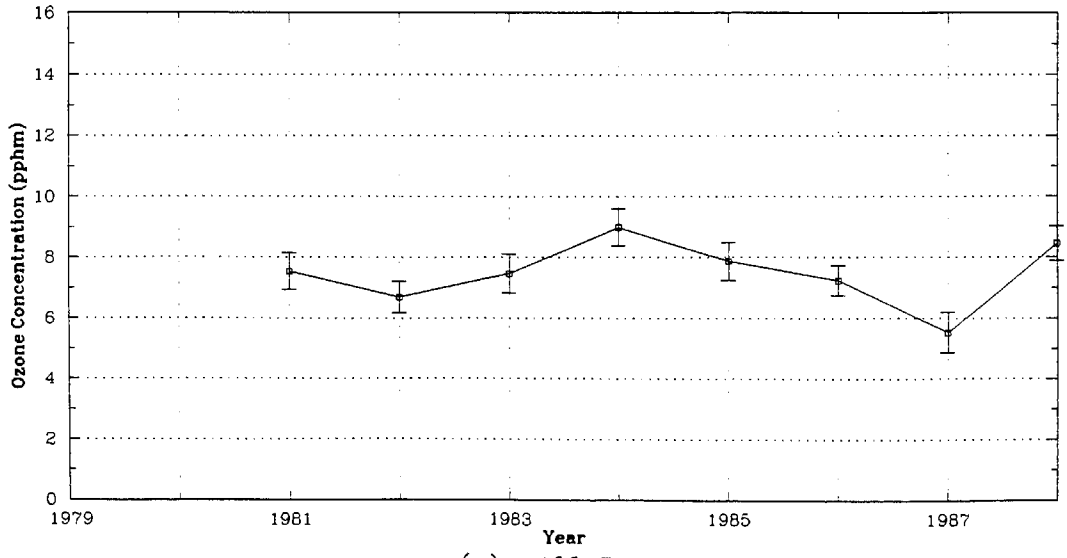

(c) All Days

Note: Error bars represent 95 percent confidence intervals.

FIGURE 3-11. Seasonal average daily maximum ozone trends for Livermore.

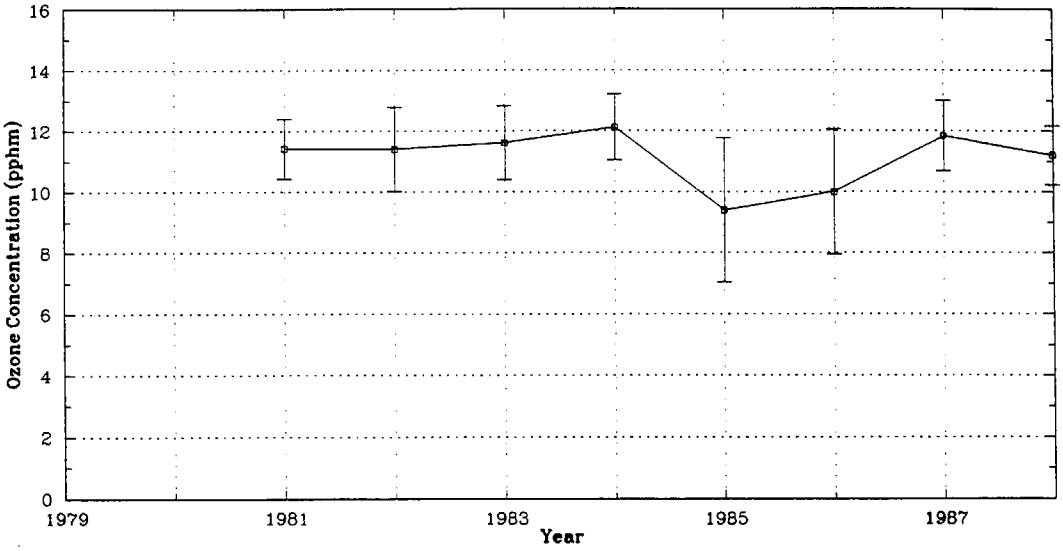

(a) Non-transport Days

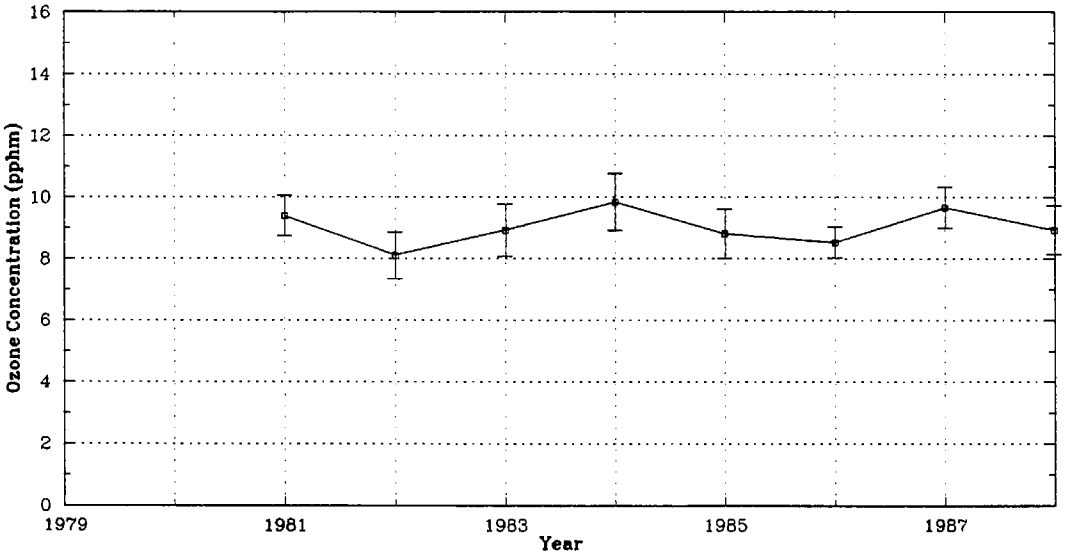

(b) Transport Days

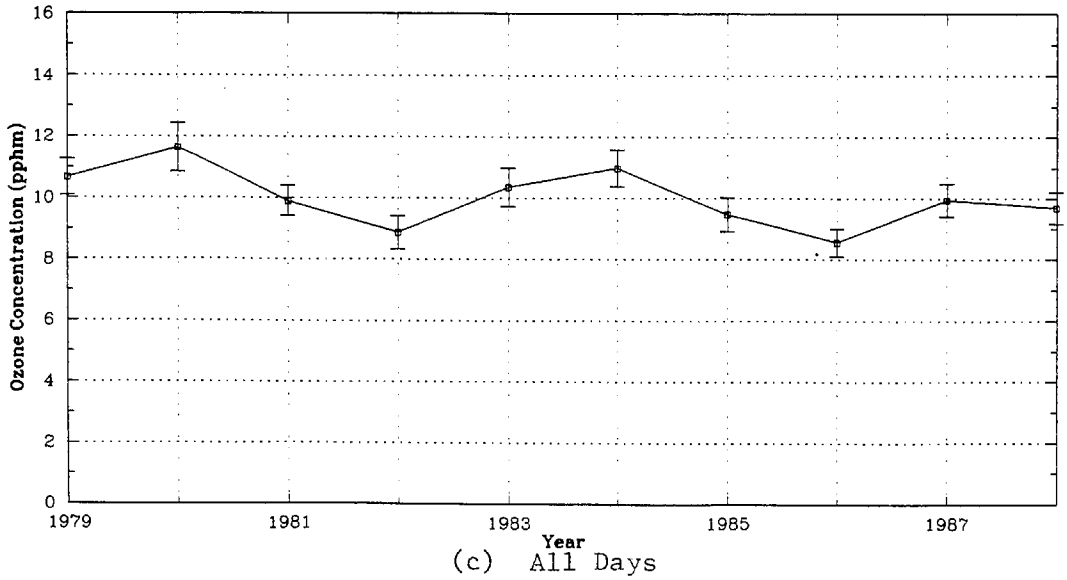

(c) All Days

Note: Error bars represent 95 percent confidence intervals.

FIGURE 3-12. Seasonal average basin peak daily maximum ozone trends for SFBA (NSJV data set).

TABLE 3-6. Results of linear regression analysis, NSJV data set.

Monitor(s)	Category	Trend (pphm/year)	Probability Trend ≠ 0	Trend Significant at 95 % Level
NSJV Basin Peak	All days	0.04	0.79	No
	Transport	0.004	0.08	No
	No-transport	0.01	0.20	No
Bethel Island	All days	0.002	0.02	No
	Transport	0.04	0.36	No
	No-transport	0.05	0.29	No
Livermore	All days	-0.02	0.07	No
	Transport	0.01	0.05	No
	No-transport	0.05	0.18	No
Stockton-Turlock-Modesto	All Days	0.03	0.42	No
	Transport	0.02	0.20	No
	No-transport	0.10	0.78	No
SFBA Basin Peak	All days	-0.15	0.85	No
	Transport	0.03	0.21	No
	No-transport	-0.08	0.39	No

Rosenbaum's trends are shown in Figure 3-13. Trends are shown for three daily summary statistics: the average over all hourly values in the day, the average over all daytime hours (defined as 0600 to 1800 LST), and the daily maximum hour. These daily summary statistics were computed at each SFBA monitoring station. Several seasonal summary statistics were then computed for each monitor: the 90th and 80th percentiles, the average of all concentrations above the 90th and 80th percentile, and the average over all days. Seasonal summary statistics were then averaged over all monitors to arrive at the values plotted in Figure 3-13. A weighted average was used in which the weighting factor for each monitor was based on the total population in the vicinity of the monitoring site. Since the trends in Figures 3-7 and 3-12 are based primarily on high ozone days in the SFBA, they are most closely related to the average of the concentrations above the 80th or 90th percentile calculated by Rosenbaum.

A comparison of Figures 3-7 and 3-12 with Figure 3-13 shows that the trends calculated for the present study are very similar to those calculated by Rosenbaum. The only major exception is the lack of a dip in concentrations during 1982 in Rosenbaum's results. However, Rosenbaum also calculated the magnitude of the largest concentration observed in the SFBA in each year as shown in Figure 3-14. This value does exhibit a sharp drop in 1982 suggesting that the decrease in seasonal mean concentrations at Gilroy in 1982, noted earlier may be a result of a lack of extremely high values at this location. One important aspect of Figure 3-13 is that the trends for the various seasonal summary statistics are all very similar. In fact, Rosenbaum also observed similar trends in various summary statistics based on the number of exceedances of 12 pphm. This result suggests that we would have obtained similar trends in the present study even if we had used a summary statistic other than the seasonal mean.

Summary

On the basis of ARB flow patterns and relative magnitudes of ozone concentrations, criteria were developed to identify incidences of ozone and precursor transport from the SFBA into the NCC and the NSJV. These criteria were used to classify days into transport and no-transport bins. An indeterminate bin was used for days that did not

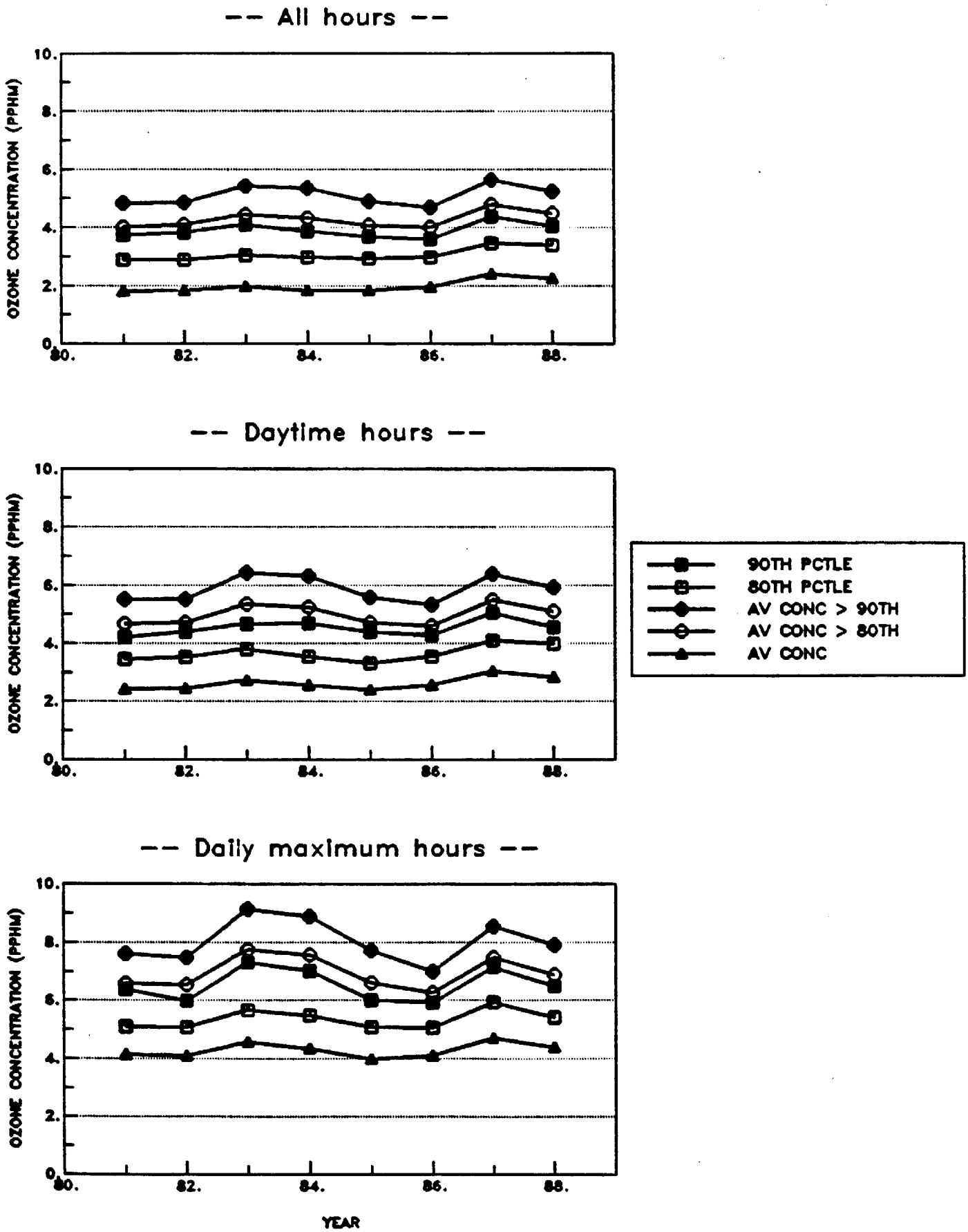

FIGURE 3-13. SFBA basin-wide average ozone trends for seasonal (April-October) summary statistics based on 24-hour average concentrations (top), daytime (0600-1800 LST) average concentrations (middle), and the daily maximum hourly average concentration (bottom).

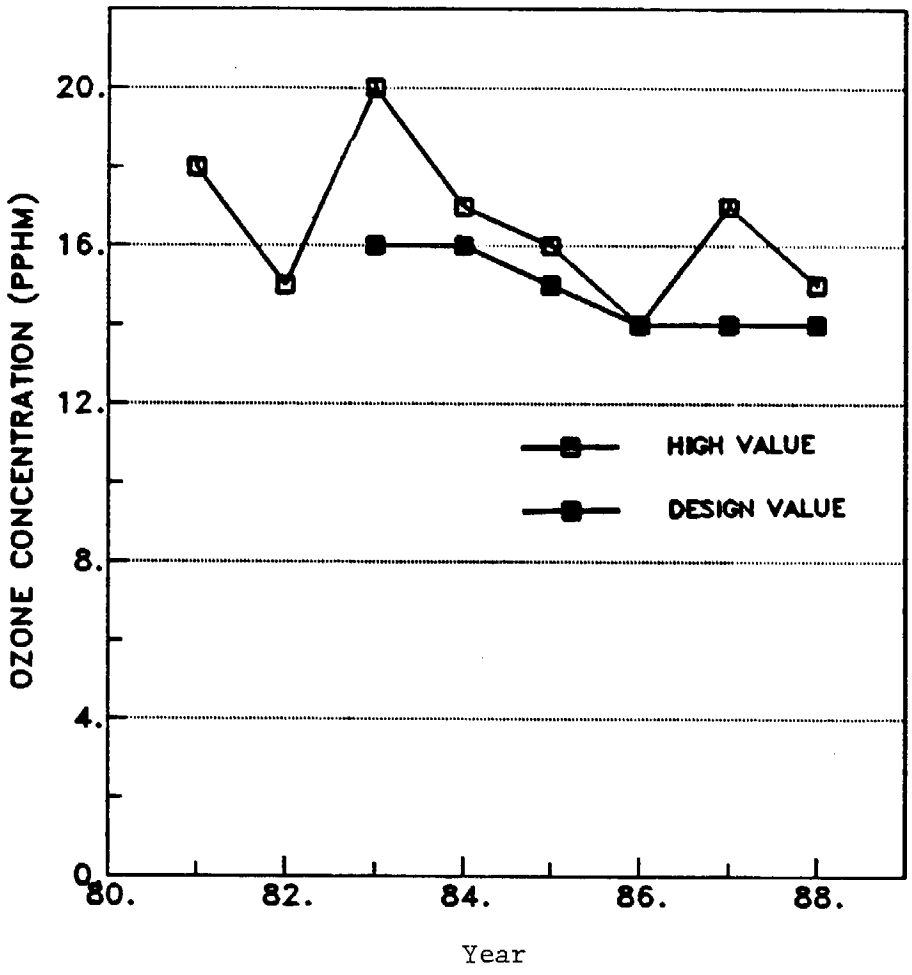

FIGURE 3-14. SFBA ozone trend for seasonal (April-October) basin-wide maximum concentration ("high value") and fourth highest concentration over preceding three years ("design value").

clearly satisfy either the transport or no-transport criteria. Classification was carried out separately for transport to the NCC and transport to the NSJV, thus resulting in two data sets with associated transport bins: one for the NCC and one for the NSJV. Because of a lack of meteorological and ozone data in the NCC, no clear-cut criteria for identifying transport days could be developed. Therefore, days not meeting the no-transport criteria were classified as indeterminate. Given prevaling wind directions, however, it is likely that transport actually occurs on many of these days.

Ozone concentration trends at selected monitoring sites were calculated for days falling in each transport category. No statistically significant linear trends over the 1979 - 1988 period were observed at the 95% confidence level. Furthermore, no systematic differences between trends on transport and no-transport or indeterminate days were observed, with the exception that concentrations at downwind monitors tend to be higher on transport days, as expected. Our results are consistent with those contained in an unpublished report on SFBA trends by Rosenbaum (1989). Since Rosenbaum obtained basically similar trends for a variety of summary statistics, we would not expect our results to be sensitive to the selection of summary statistic.

4 FLUX-PLANE CALCULATIONS

Flux-plane calculations were performed using the meteorological and air quality modeling results from the San Joaquin Valley Air Quality Study (SJVAQS) (Douglas, 1989; Morris et al., 1990; Morris and Kessler, 1990). These provide quantitative estimates of pollutant flux between the San Francisco Bay Area (SFBA) and the North Central Coast (NCC) and between the SFBA and the San Joaquin Valley (SJV) during the period 7-8 August 1984. High ozone concentrations were observed in the SFBA, NCC, and SJV during this period and the airflow patterns indicate possible transport from the SFBA to both the NCC and SJV. To examine the effect of emissions changes on the transport of ozone and precursor pollutants, fluxes were calculated for two different emissions scenarios.

SJVAQS MODELING STUDY OF 7-8 AUGUST 1984

Meteorological Modeling

The Colorado State University Mesoscale Model (CSUMM) (Pielke, 1974; Mahrer and Pielke, 1977,1978) was used to simulate the airflow within a modeling domain that includes the SFBA, the NCC, and the SJV. Wind fields were generated at nine levels between the surface and 2000 m above ground level (AGL). A terrain-following vertical coordinate was used. Simulation results are described by Kessler and Douglas (1989). The wind fields derived from the prognostic-model simulation did not adequately replicate the available meteorological observations. Specifically, certain features of the airflow, such as the Fresno eddy, were not resolved.

To improve the agreement between observed and simulated winds and to improve the resolution of certain air flow features, observations were incorporated into the simulated wind fields using an objective-combination procedure (Douglas, 1989). The

incorporated data consist of actual and "pseudo" data that represent the meteorological conditions in the modeling region on 7 and 8 August. The pseudo observations were derived from a subjective analysis of the airflow patterns.

The objective-combination wind fields are described by Douglas (1989). Features of the wind fields include (1) airflow from the SFBA to the NCC via inland and over-water routes, (2) airflow from the SFBA to the SJV through the Carquinez Strait and Pacheco Pass, and (3) predominantly up-valley flow in the SJV.

Particle paths were calculated using the SJVAQS objective-combination wind fields to estimate pollutant transport pathways during the 7-8 August period. The particle paths do not incorporate vertical transport or turbulent mixing. Particle paths were initiated at six-hour intervals beginning at 0000 PST 7 August from Sacramento, Pittsburg, San Jose, and Stockton. The calculations were discontinued either at 1800 PST 8 August or when the particle was advected out of the domain. The particle path analysis is described by Douglas (1989).

Based on this analysis, transport from San Jose to the NCC (Hollister area) is indicated throughout the period. This is followed by transport into the SJV through Pacheco Pass. Particles released from Pittsburg are advected directly into the SJV. Surface layer particle paths initiated at 1200 PST 7 August from Pittsburg, San Jose, and Stockton are shown in Figure 4-1. Similar patterns are indicated aloft.

Air Quality Modeling

Air quality modeling of 7-8 August 1984 was performed as part of the SJVAQS (Morris et al., 1990; Morris and Kessler, 1990). The air quality modeling domain for 7-8 August also includes the SFBA, the NCC, and the SJV. Simulations were performed using a variable-grid regional oxidant model (RTM-III).

The RTM-III was configured with six vertical layers and a horizontal grid spacing that ranged from 5 km in the southern SJV (Fresno and Bakersfield area), 10 km in the northern SJV and the SFBA, 20 km over the remaining coastal and mountainous areas, and 40 km over the ocean. Analysis of the base-case simulation indicates

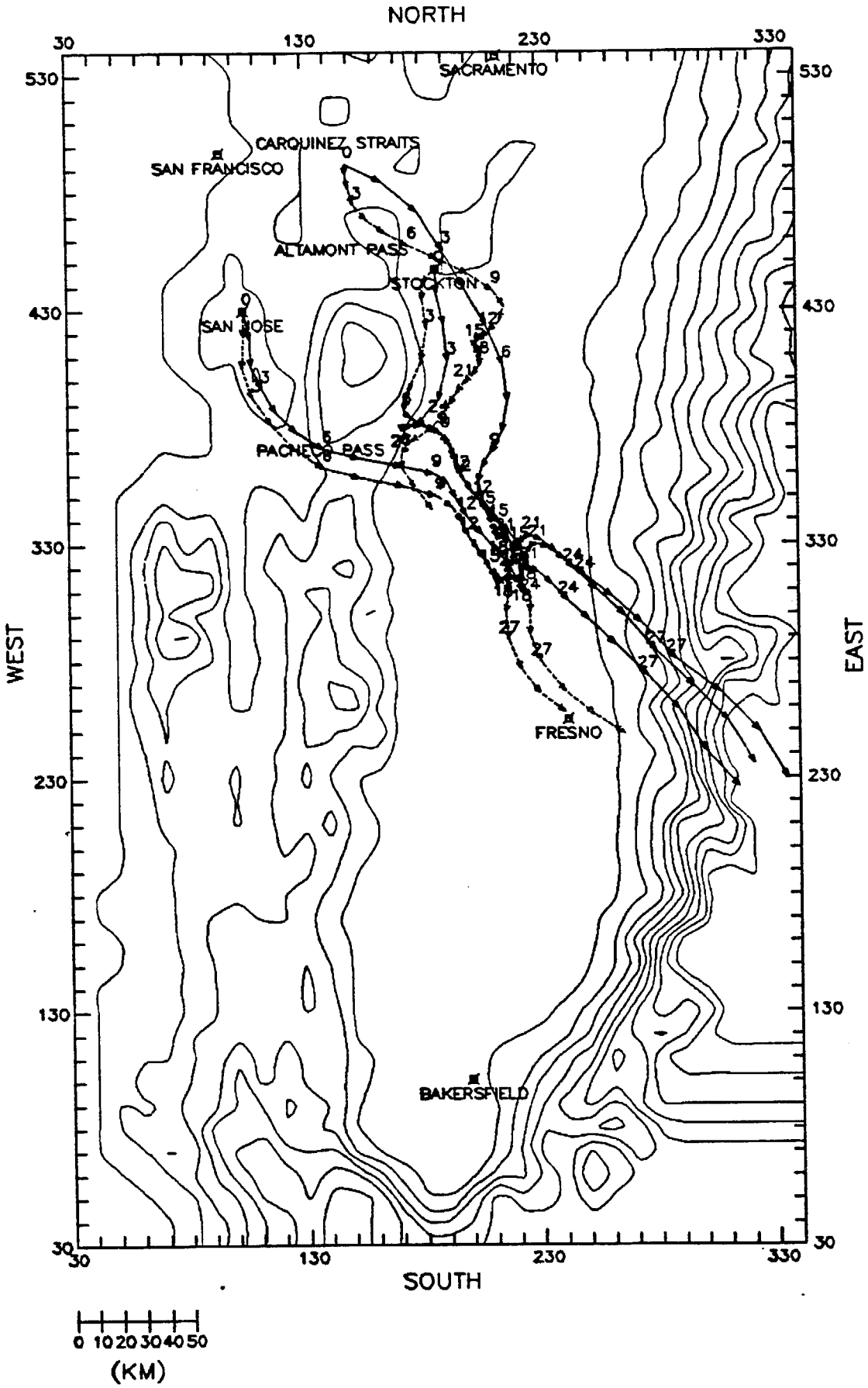

FIGURE 4-1. Surface-layer particle paths initiated at Pittsburg, San Jose, and Stockton at 1200 PST 7 August 1984. Each arrow represents one hour.

transport of pollutants between the SFBA and the NCC along the Santa Clara Valley, and transport between the SFBA and the SJV through the Carquinez Strait and Altamont and Pacheco passes. Ozone maxima occur just downwind from the Carquinez Strait and Pacheco Pass on both 7 and 8 August. Secondary maxima in the SJV near Fresno and Bakersfield suggest that local sources contribute as well. Peak ozone concentrations are not well simulated; simulated values are lower than observations on both days. Observed ozone concentrations in the SJV increase between 7 and 8 August, suggesting day-to-day carryover of pollutants. Simulated concentrations, however, indicate little day-to-day carryover.

To examine the extent of the influence of SFBA emissions on ozone formation in the downwind air basins, a sensitivity test was performed in which all anthropogenic emissions within the SFBA were eliminated. This simulation will be referred to the no-SFBA-emissions simulation. In general, differences in the daily maximum ozone concentrations between the base case and no-SFBA-emissions case are greater on the second day of the simulation (Figure 4-2). In the no-SFBA-emissions simulation the daily maximum ozone concentration near San Jose on 8 August is reduced from approximately 100 ppb to 60 ppb. Large reductions in the daily maximum ozone concentration also occur near Sacramento (110 ppb to 90 ppb), near Hollister (100 ppb to 70 ppb), and downwind of Pacheco Pass (150 ppb to 80 ppb). This last difference represents nearly a 50 percent reduction. The effect of the elimination of SFBA emissions is greatest in the northern SJV. However, the influence is noted almost as far south as Fresno on 7 August and south of Bakersfield on 8 August.

While discrepancies between the observed and simulated ozone concentrations render any conclusions drawn from this study inexact, the no-SFBA-emissions sensitivity test indicates that changes in the SFBA emissions can influence ozone concentrations in the downwind air basins.

FLUX-PLANE METHODOLOGY

The simulated wind and concentration fields were used to calculate the pollutant flux between the SFBA and the NCC and between the SFBA and the SJV during 7-8 August 1984. The pollutant flux was calculated using:

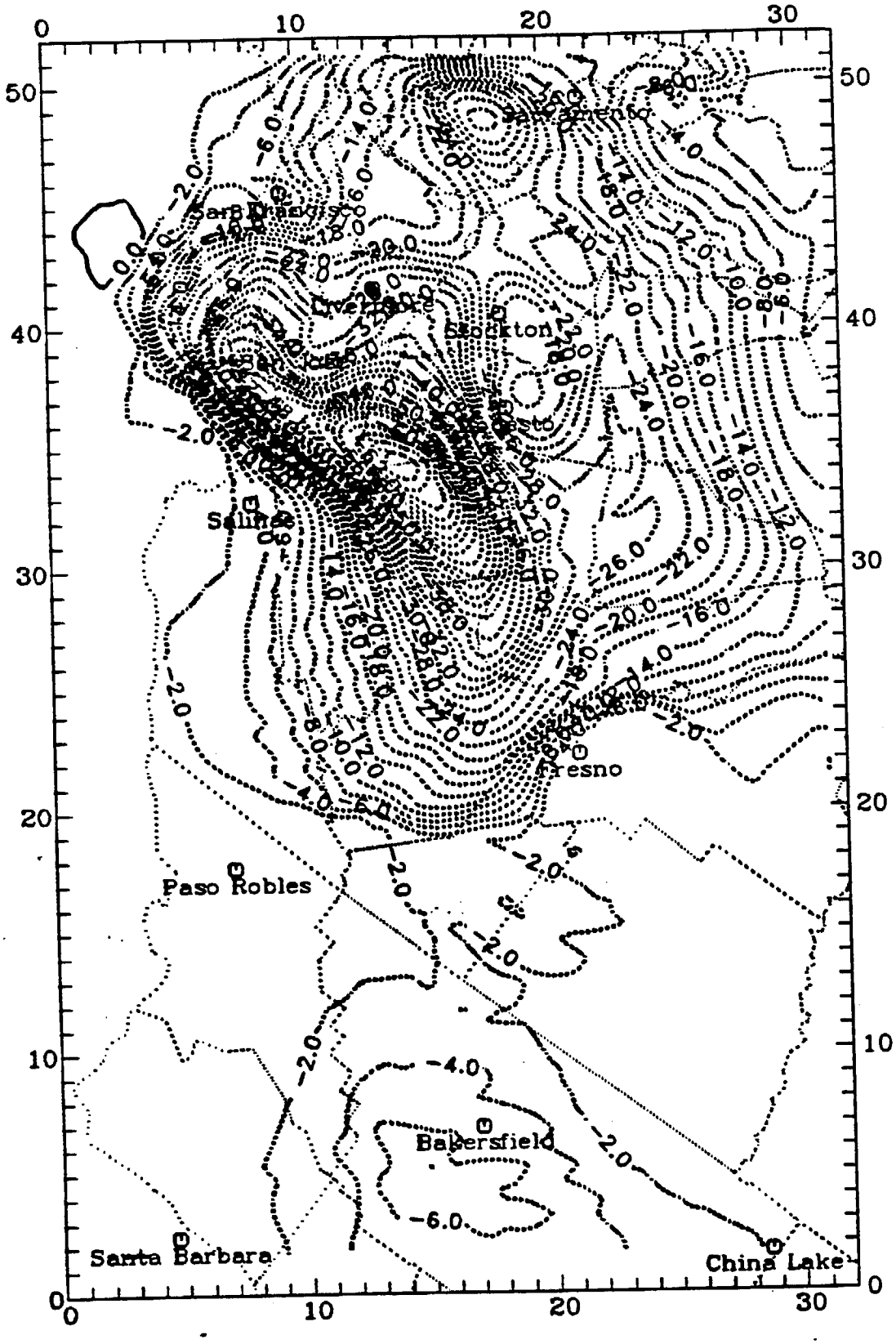

FIGURE 4-2. Differences in simulated maximum daily ozone concentrations (ppb) between the base-case and the no-SFBA-emissions simulations on 8 August 1984.
(Source: Morris et al., 1990.)

$$F = cvA \qquad (3\text{-}1)$$

where c is the simulated concentration, v is the wind component perpendicular to the flux plane, and A is the area of the flux plane. The locations of the flux planes are illustrated in Figure 4-3. Planes 1, 2, and 3 are positioned to examine transport between the SFBA and the SJV. Plane 1 extends across the Carquinez Strait, plane 2 across Altamont Pass, and plane 3 across Pacheco Pass. Planes 4 and 5 are positioned to examine transport between the SFBA and the NCC. Plane 4 extends across the Santa Clara Valley between Gilroy and Hollister. Plane 5 extends offshore and is perpendicular to the coast north of Santa Cruz. The sign of the flux depends upon the sign of the wind component perpendicular to the flux plane. For planes 1, 2, and 3 a positive value indicates a net mass flux from the SFBA to the SJV. Note that a coordinate transformation is used for plane 1. For planes 4 and 5 a negative value indicates a net mass flux from the SFBA to the NCC.

Pollutant fluxes were calculated for ozone, oxides of nitrogen (NO_x), paraffins (PAR), and peroxyacetyl nitrate (PAN). Ozone forms in the atmosphere through a series of photochemical reactions involving NO_x, ultraviolet (UV) radiation, and reactive organic gases (ROG). NO_x is the sum of nitrogen oxide (NO) and nitrogen dioxide (NO_2) and is needed for the formation of ozone in the atmosphere. NO can also react with ozone to form NO_2 and oxygen (O_2); a reaction in which ozone is destroyed. ROGs include a large number of classes of organic compounds that contain hydrogen and carbon atoms. ROGs are a precursor for ozone and are consumed in the process of generating ozone. The ratio of ROG to NO_x determines the rate of ozone formation. Because paraffins are the least reactive of the ROGs, they may play an important role in the transport of ROGs. PAN forms along with ozone and is a reservoir of NO_x. It can be transported long distances in cool nighttime air and can decompose during the daytime hours to yield NO_2 (Whitten, 1990), thus contributing to the next day's ozone cycle.

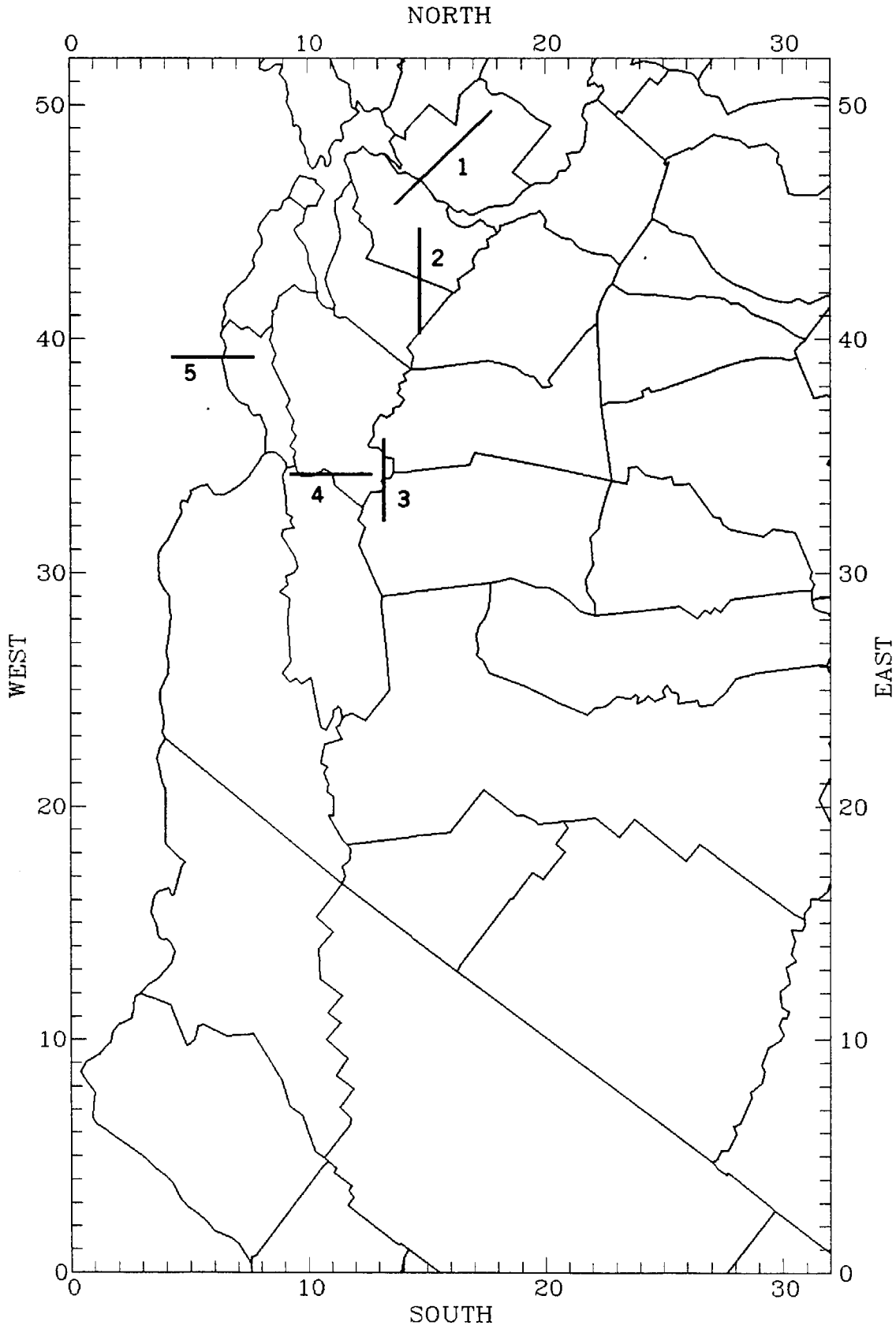

FIGURE 4-3. Flux plane locations.

RESULTS

The results of the flux-plane calculations are presented in this section. To illustrate the results, the following graphical displays are provided: (1) vertical cross sections of the net mass per unit area that is advected across the flux-plane during a specified period of time, and (2) time series plots of the net mass through the flux-plane. The net mass through each flux-plane on each simulated day is also tabulated. These results illustrate the vertical and temporal variability of pollutant transport and provide quantitative information regarding the amount and composition of pollutants transported across the flux-planes. Comparison of the fluxes for the base-case simulation and the no-SFBA-emissions simulation provides a quantitative estimate of the effect of changes in SFBA emissions on the transport of pollutants from the SFBA to the NCC and the SJV during meteorological conditions conducive to transport.

Pollutant Flux from the SFBA to the NCC

This discussion will focus on the flux calculations for planes 4 and 5, which address transport of pollutants from the SFBA to the NCC over land and water.

Simulation Day 1

The air quality simulations were initialized at 0200 PST on 7 August. The same initial concentrations were used for the base-case and no-SFBA-emissions simulations. Thus, we expect the differences between the two simulations to be smaller on the first day of the simulation than on the second day.

Vertical cross sections of the net mass per unit area advected across plane 4 on the first day of the simulation are shown in Figure 4-4. In the base-case simulation (Figure 4-4a) the flux is negative throughout the depth of the model atmosphere, indicating a net mass flux from the SFBA to the NCC. Maximum transport of NO_X, PAR, and PAN occurs near the surface, while the mass flux of ozone is greatest between 200 and 400 m agl. In the no-SFBA-emissions simulation (Figure 4-4b) there

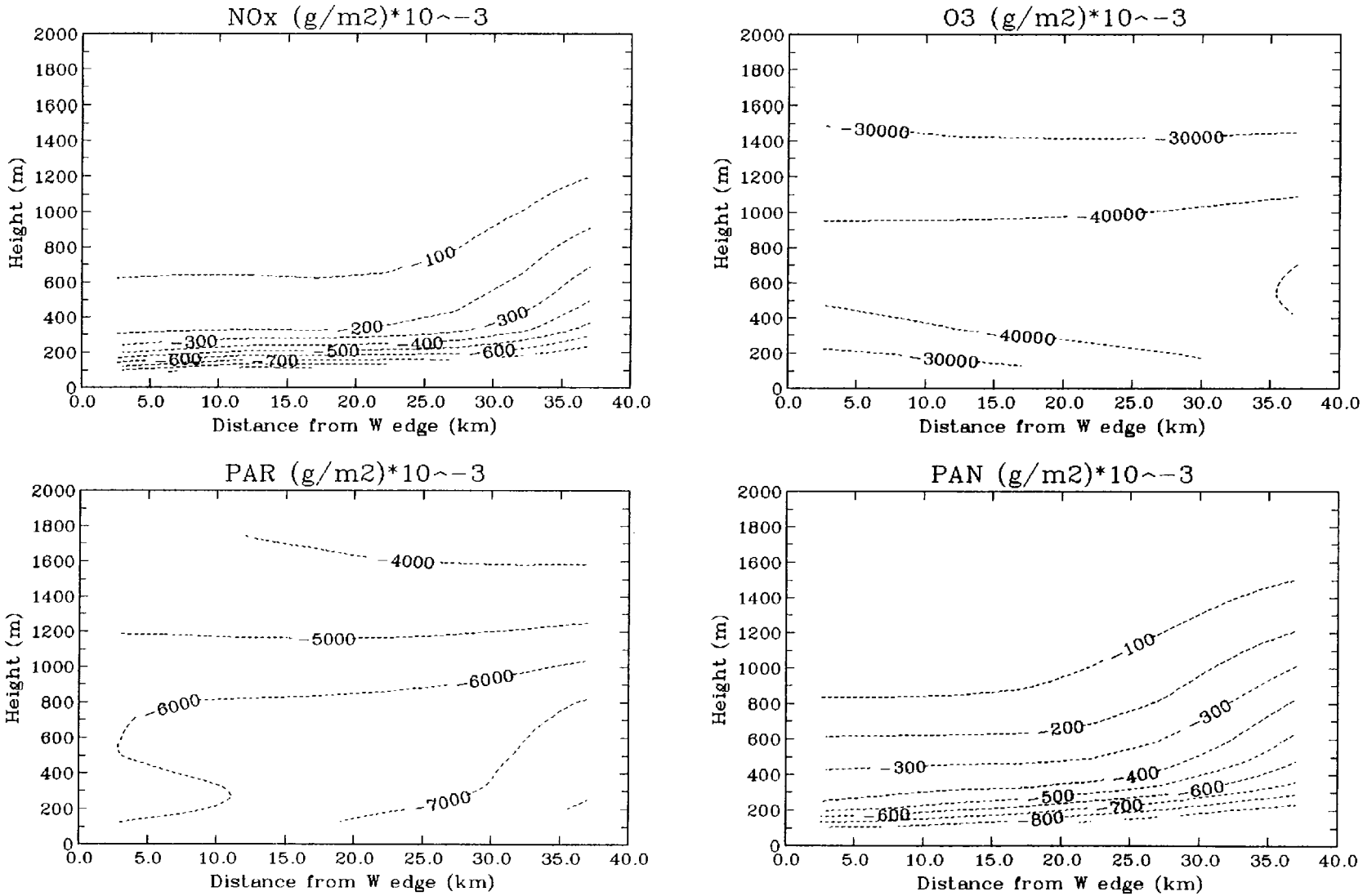

FIGURE 4-4a. Net mass per unit area advected across flux-plane 4 on simulation day 1 (0200-2400 PST): base case.

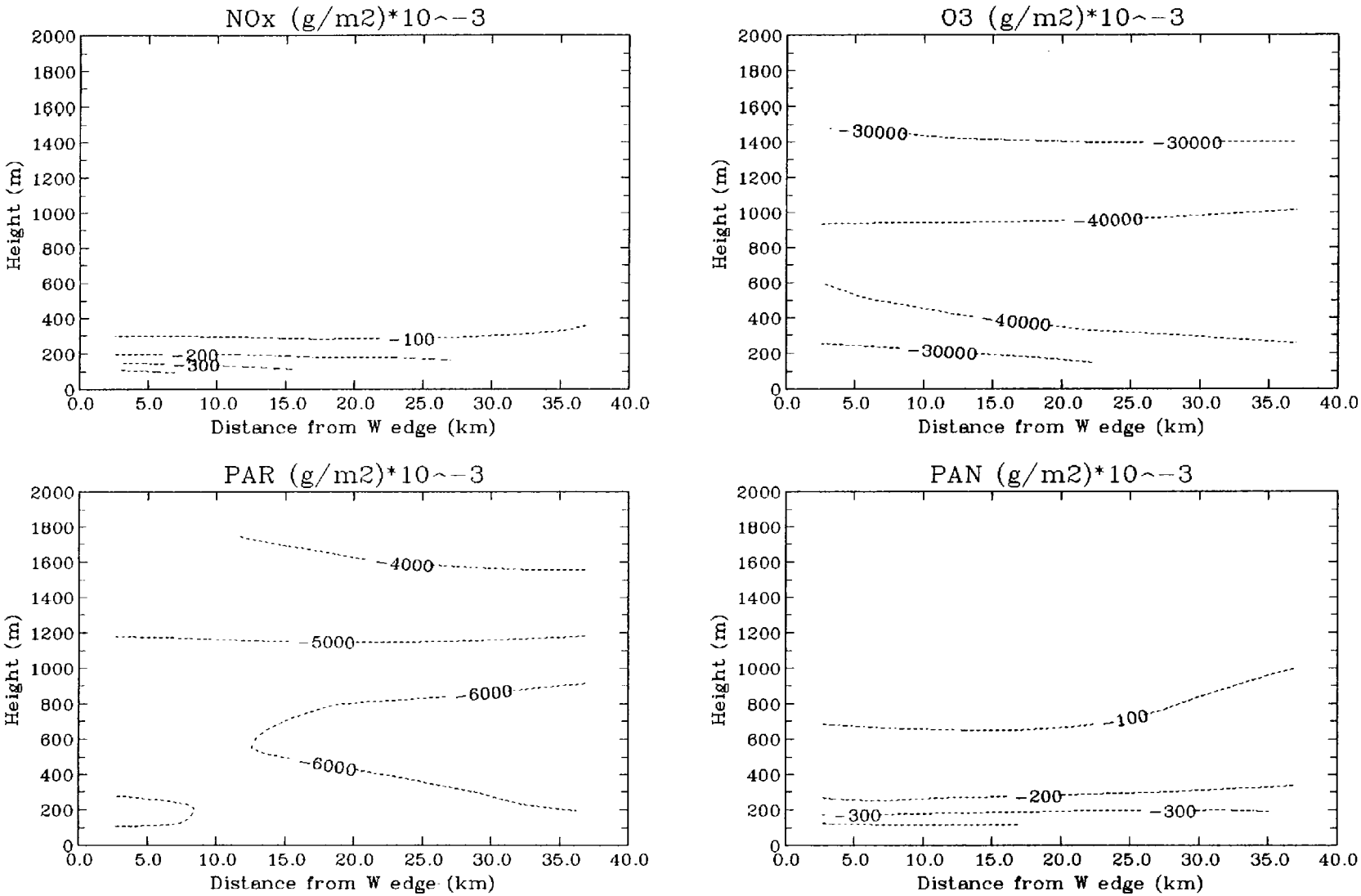

FIGURE 4-4b. No SFBA emissions.

is a substantial decrease in the amount of NO_x and PAN that is transported across the plane. PAR is reduced somewhat and ozone is reduced slightly.

Similar patterns are noted for plane 5 (Figure 4-5). An elevated maximum in the net mass flux of PAR (hydrocarbons) over the water portion of the cross section is present in both simulations. This may be due to boundary conditions.

The net amount of mass advected across planes 4 and 5 on simulation day 1 is given in Table 4-1. Elimination of the SFBA emissions results in substantial reductions in the amount of NO_x and PAN advected across the planes but little change in the amount of PAR and ozone. Somewhat larger differences for plane 4 indicate that the primary route for transport of pollutants from the SFBA to the NCC on this day was along the Santa Clara Valley.

Simulation Day 2

The mass flux through plane 4 on the second day of the simulation is negative at all levels throughout the day in both the base-case and no-SFBA-emissions simulations. Vertical cross sections of the 18-hour (0200 - 2000 PST) net mass advected through this plane are shown in Figure 4-6. An elevated NO_x plume is apparent in the base-case simulation and indicates transport aloft of NO_x. This feature is not present in the no-SFBA-emissions simulation. Elimination of the SFBA emissions also significantly reduces the amount of NO_x transported across the plane near the surface. A reduction in the net flux of PAN and smaller reductions for PAR and ozone are also noted. These differences are illustrated in Figure 4-7. The time series plots also show how pollutant flux varies throughout the day in both the base-case and no-SFBA-emissions simulations. The net mass advected through plane 4 during the 18-hour period is given in Table 4-2. Elimination of SFBA emissions results in a 82 percent reduction in the amount of NO_x and a 74 percent reduction in the amount of PAN advected across the plane. PAR is reduced by 7 percent and ozone is reduced by 10 percent.

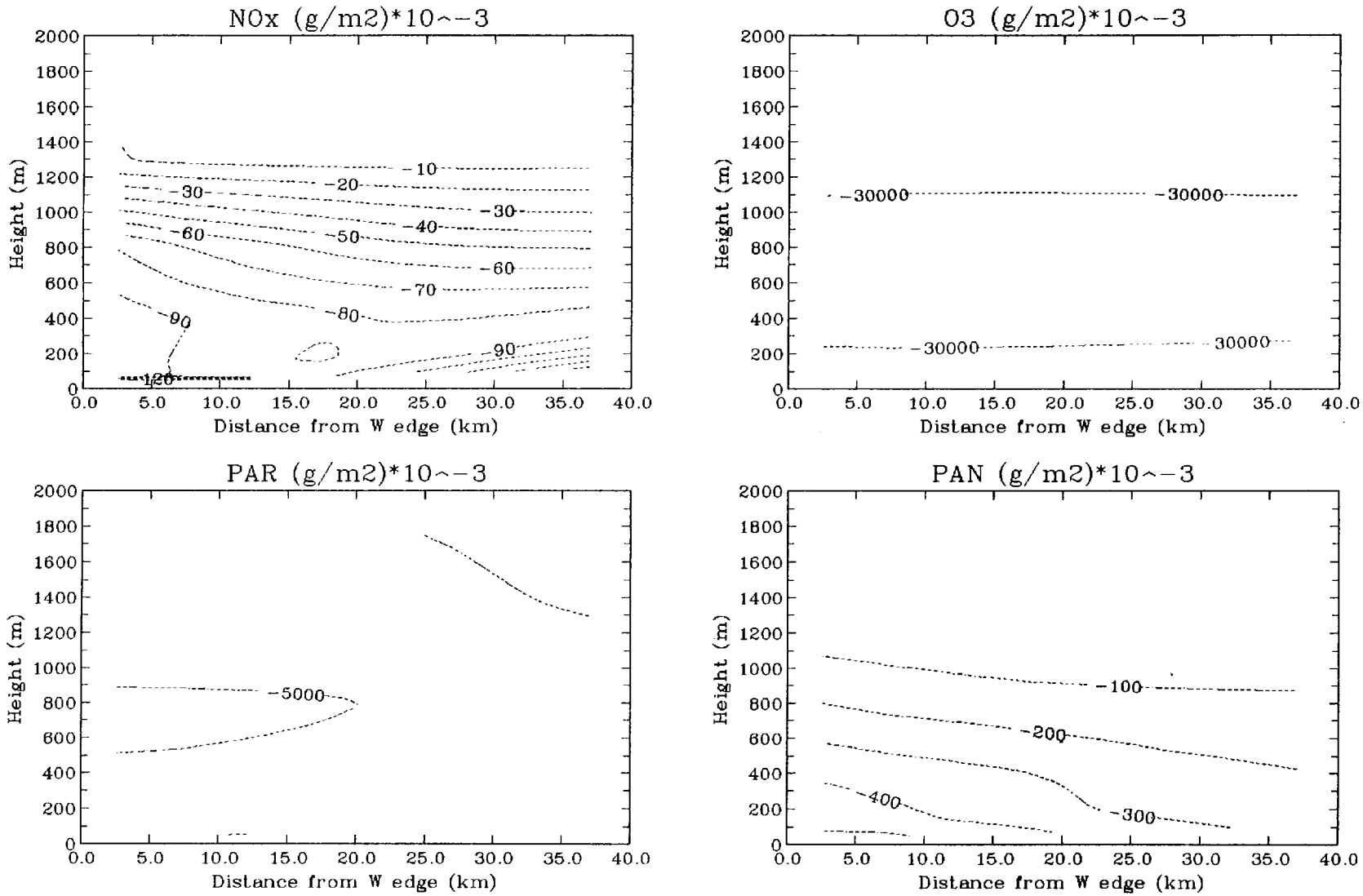

FIGURE 4-5a. Net mass per unit area advected across flux-plane 5 on simulation day 1 (0200-2400 PST): base case.

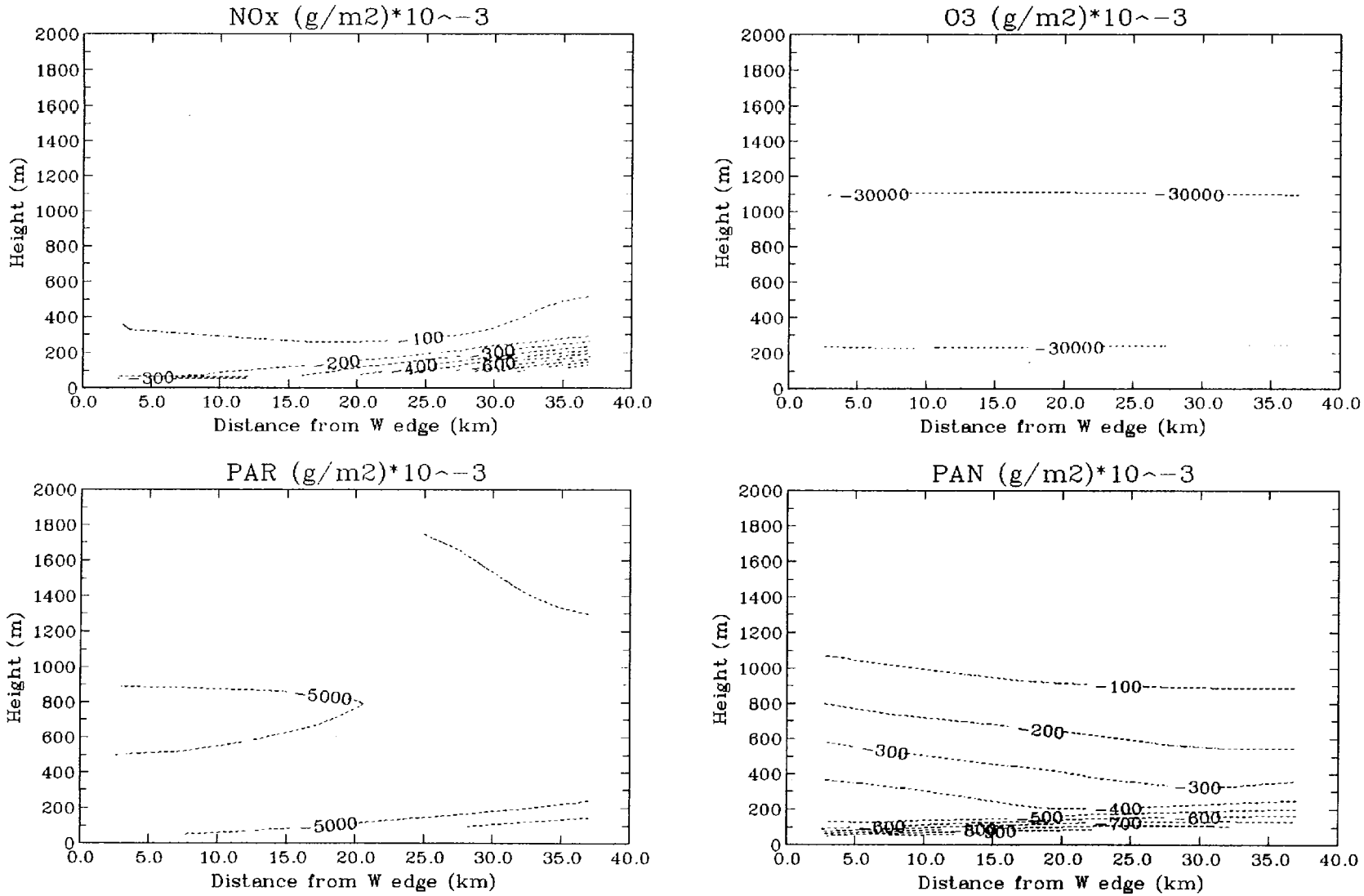

FIGURE 4-5b. No SFBA emissions.

TABLE 4-1. Net mass of NO_x, PAR, ozone, and PAN advected across the flux planes on simulation day 1 (0200-2400 PST).

	Base Case (g)	No SFBA Emissions (g)	Percent Change (%)
Plane 1:			
NOx	6.36×10^7	2.18×10^7	-65.7
PAR	6.01×10^8	5.36×10^8	-10.8
O3	3.64×10^9	3.61×10^9	-0.8
PAN	2.92×10^7	2.41×10^7	-17.5
Plane 2:			
NOx	6.76×10^7	5.19×10^6	-92.3
PAR	7.77×10^7	1.00×10^7	-87.1
O3	1.28×10^8	1.32×10^8	+3.1
PAN	5.14×10^6	3.04×10^6	-40.9
Plane 3:			
NOx	1.28×10^7	3.00×10^6	-76.6
PAR	4.24×10^7	1.10×10^7	-74.1
O3	7.50×10^7	-1.73×10^7	-123.1
PAN	1.11×10^7	2.99×10^6	-73.1
Plane 4:			
NOx	-1.39×10^7	-4.52×10^6	-67.5
PAR	-4.40×10^8	-4.09×10^8	-7.0
O3	-2.86×10^9	-2.74×10^9	-4.2
PAN	-1.96×10^7	-8.61×10^6	-56.1
Plane 5:			
NOx	-7.20×10^6	-3.60×10^6	-50.0
PAR	-3.73×10^8	-3.62×10^8	-2.9
O3	-2.35×10^9	-2.32×10^9	-1.3
PAN	-1.45×10^7	-1.09×10^7	-24.8

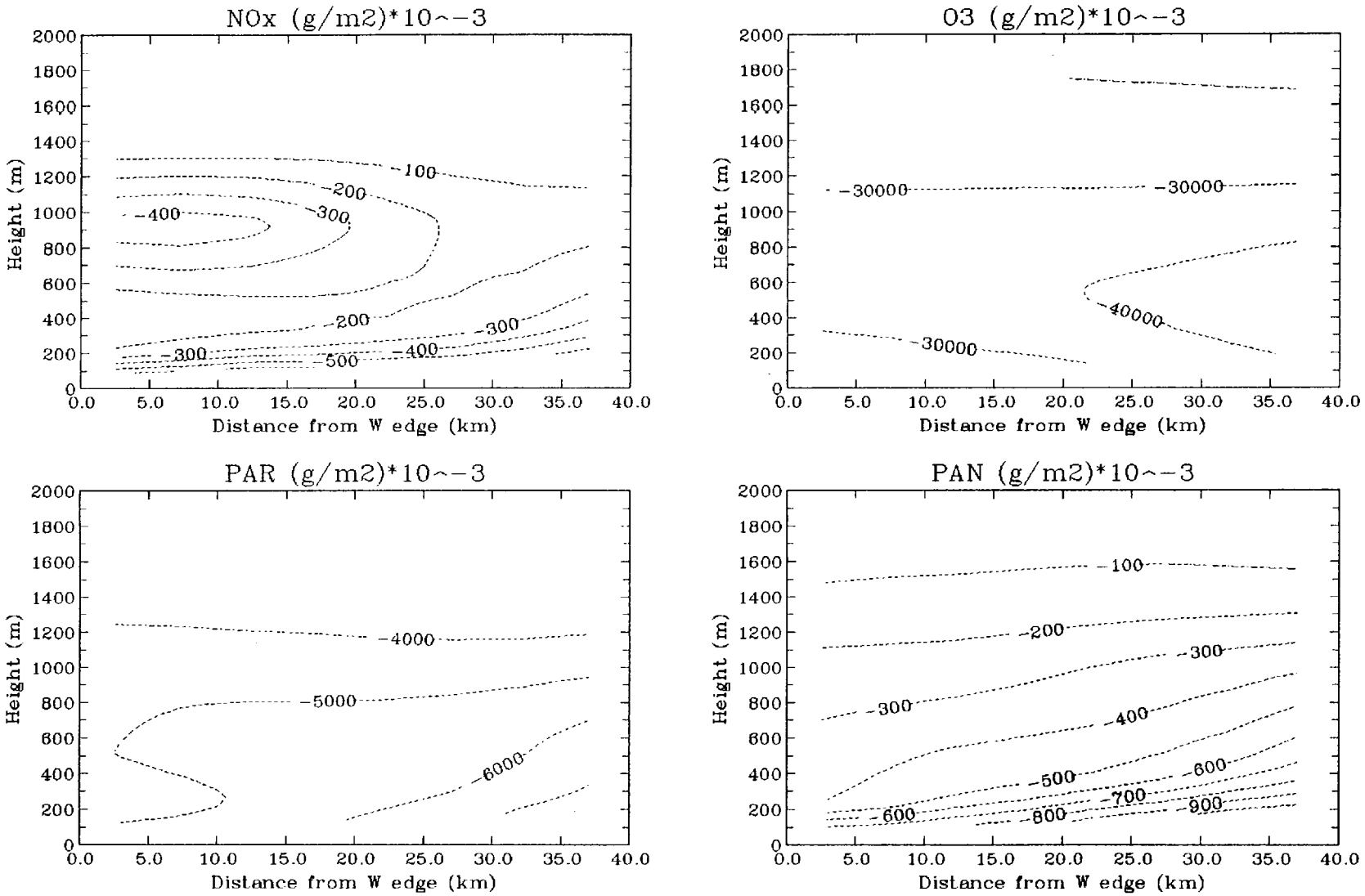

FIGURE 4-6a. Net mass per unit area advected across flux-plane 4 on simulation day 2 (0200-2000 PST): base case.

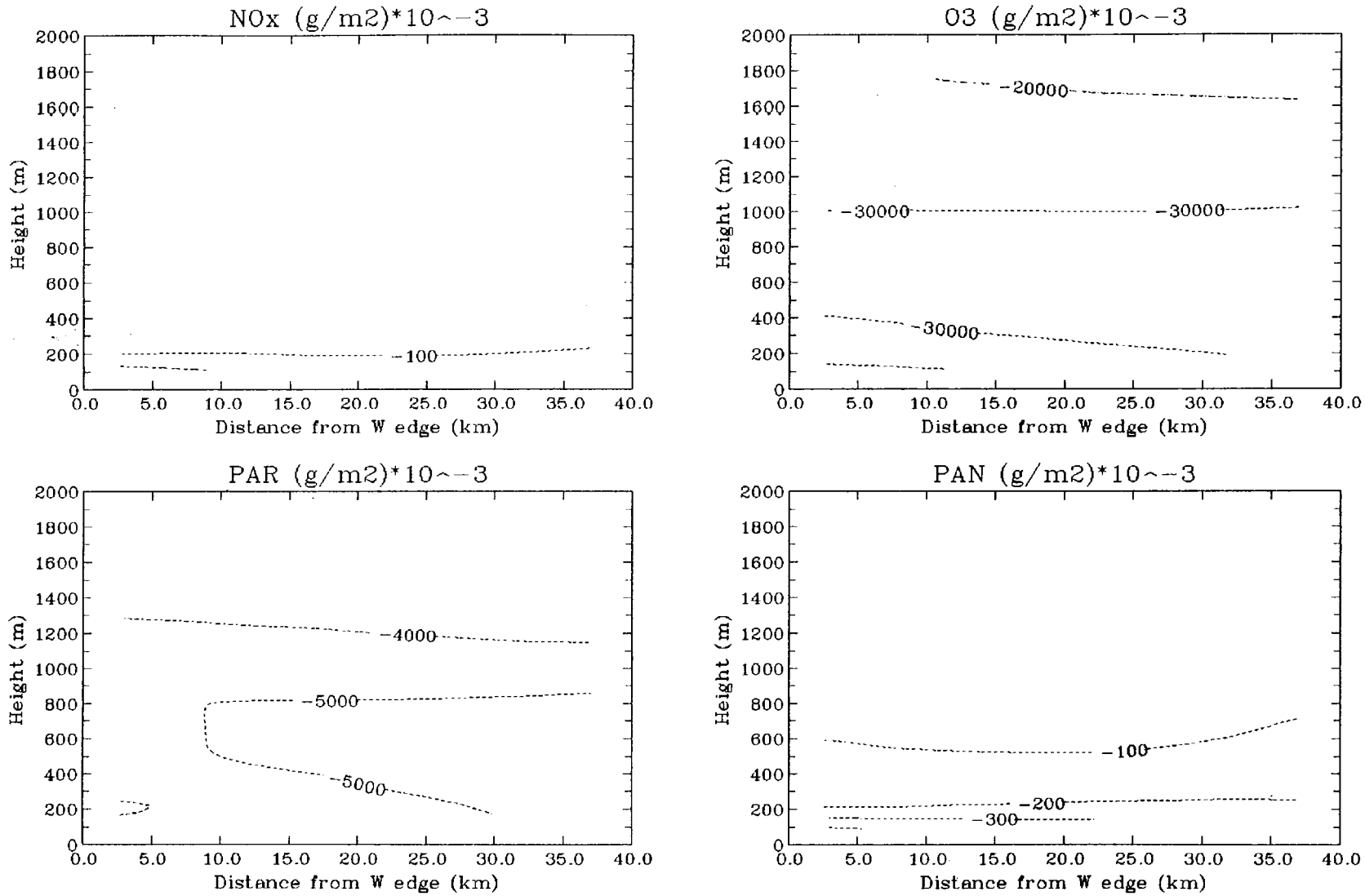

FIGURE 4-6b. No SFBA emissions.

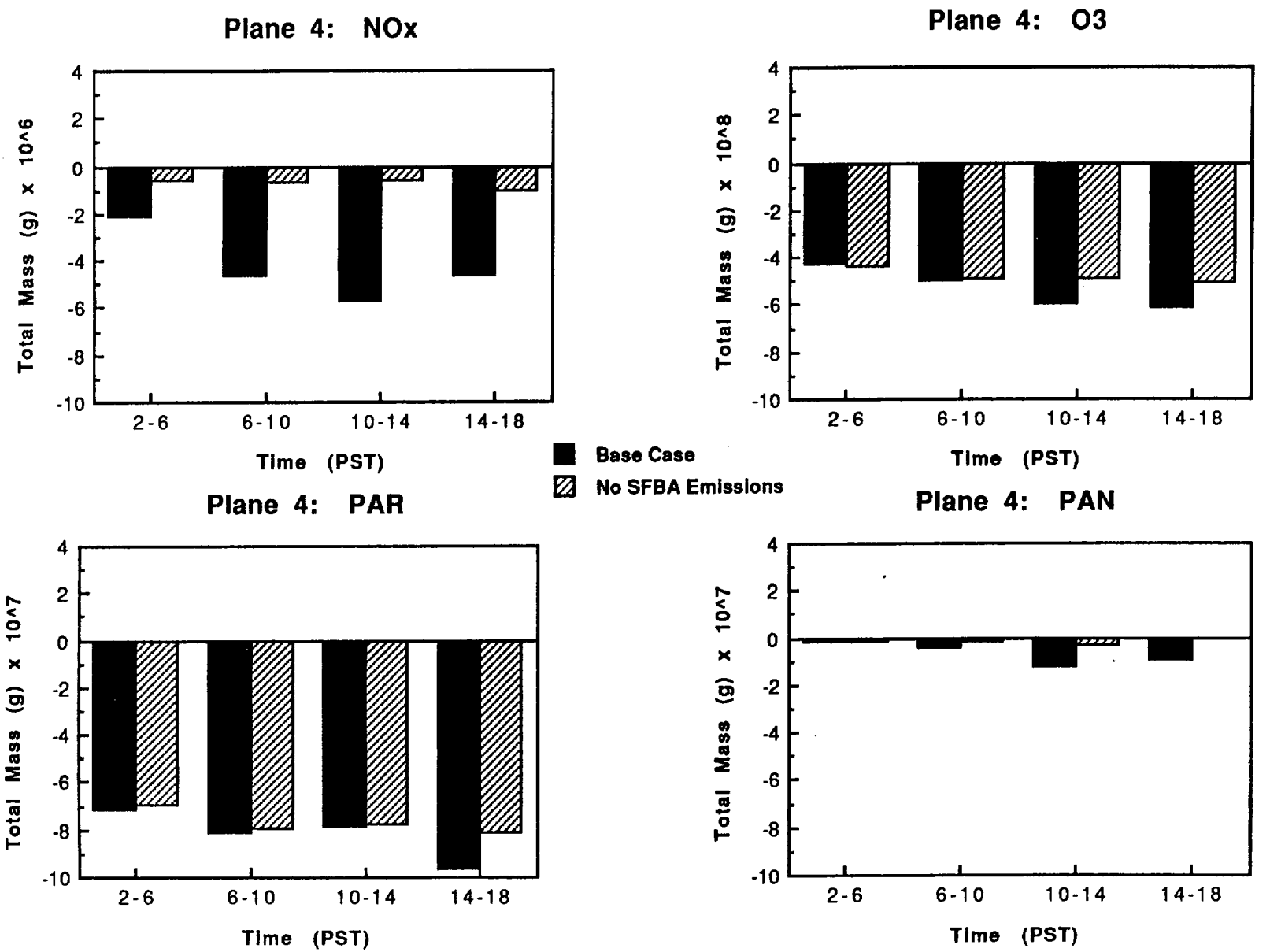

FIGURE 4-7. Time-series plots of the net mass of NO_X, PAR, ozone, and PAN advected across flux-plane 4 on simulation day 2.

TABLE 4-2. Net mass of NO_x, PAR, ozone, and PAN advected across the flux planes on simulation day 2 (0200-2000 PST).

	Base Case (g)	No SFBA Emissions (g)	Percent Change (%)
Plane 1:			
NOx	5.15×10^7	1.45×10^7	-71.8
PAR	5.13×10^8	4.46×10^8	-13.1
O3	3.05×10^9	3.04×10^9	-0.3
PAN	2.54×10^7	2.03×10^7	-20.0
Plane 2:			
NOx	5.00×10^7	1.90×10^6	-96.2
PAR	1.46×10^8	7.94×10^7	-45.6
O3	6.39×10^8	6.28×10^8	-1.7
PAN	5.79×10^6	2.88×10^6	-50.3
Plane 3:			
NOx	1.15×10^7	2.15×10^6	-81.3
PAR	9.08×10^7	5.55×10^7	-38.9
O3	4.67×10^8	3.09×10^8	-33.8
PAN	1.46×10^7	2.87×10^6	-80.3
Plane 4:			
NOx	-1.81×10^7	-3.16×10^6	-82.5
PAR	-3.73×10^8	-3.47×10^8	-7.0
O3	-2.41×10^9	-2.17×10^9	-10.0
PAN	-2.71×10^7	-6.93×10^6	-74.4
Plane 5:			
NOx	-1.05×10^7	-2.84×10^6	-73.0
PAR	-2.91×10^8	-2.82×10^8	-3.1
O3	-1.75×10^9	-1.73×10^9	-1.1
PAN	-1.34×10^7	-8.81×10^6	-34.3

The vertical cross sections of the net mass per unit area advected across plane 5 on day 2 of the simulation are shown in Figure 4-8. In the base-case simulation (Figure 4-8a) the mass flux at all levels is negative throughout the day and the elevated NO_x plume is apparent (this time along the eastern edge of the flux plane). Elimination of the SFBA emissions (Figure 4-8b) results in reductions in the amount of NO_x and PAN advected through the plane during day 2 of the simulation. Small reductions in PAR and ozone are noted. Time series plots illustrating the pollutant flux through plane 5 during day 2 of the simulation are given in Figure 4-9. Reductions due to the elimination of SFBA emissions are less than for plane 4, again indicating that the primary pathway for the transport of pollutants was along the Santa Clara Valley. The net mass through plane 5 during day 2 in both simulations is given in Table 4-2 for each of the four pollutants. Elimination of SFBA emissions results in a 73 percent reduction in the amount of NO_x and a 34 percent reduction in the amount of PAN advected across the plane. Reductions in the amount of PAR and ozone are quite small (3 and 1 percent, respectively).

Pollutant Flux from the SFBA to the SJV

Simulation Day 1

Vertical cross sections of the net mass advected across planes 1, 2, and 3 during day 1 of the simulation are given in Figures 4-10 to 4-12. Here a positive value indicates a net mass flux from the SFBA to the SJV. The base-case results for plane 1 (Carquinez Strait) show a positive net flux throughout the depth of the model domain for simulation day 1 (Figure 4-10a). Maximum values are near the surface. In the no-SFBA-emissions simulation, elimination of the SFBA emissions results in a decrease in the amount of NO_x, PAR, and PAN that is advected through the flux plane, but the amount of ozone remains relatively the same (Figure 4-10b). The reduction in the amount of precursor pollutants is greatest near the surface.

Vertical cross sections of the net mass advected across plane 2 (Altamont Pass) during simulation day 1 are shown in Figure 4-11. There is a negative net mass flux aloft across plane 2 during this day, but a positive net flux near the surface. Again,

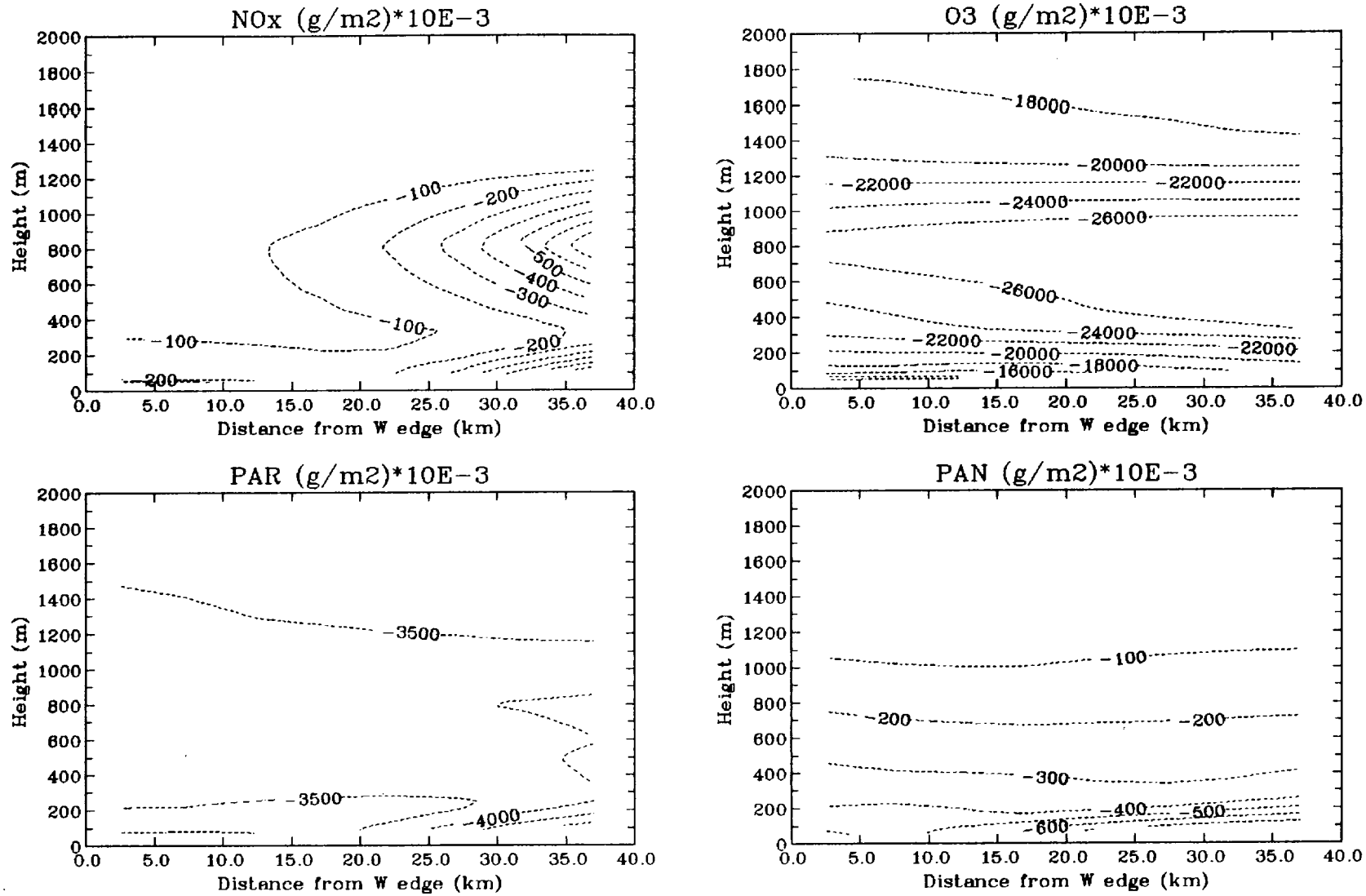

FIGURE 4-8a. Net mass per unit area advected across flux-plane 5 on simulation day 2 (0200-2000 PST): base case.

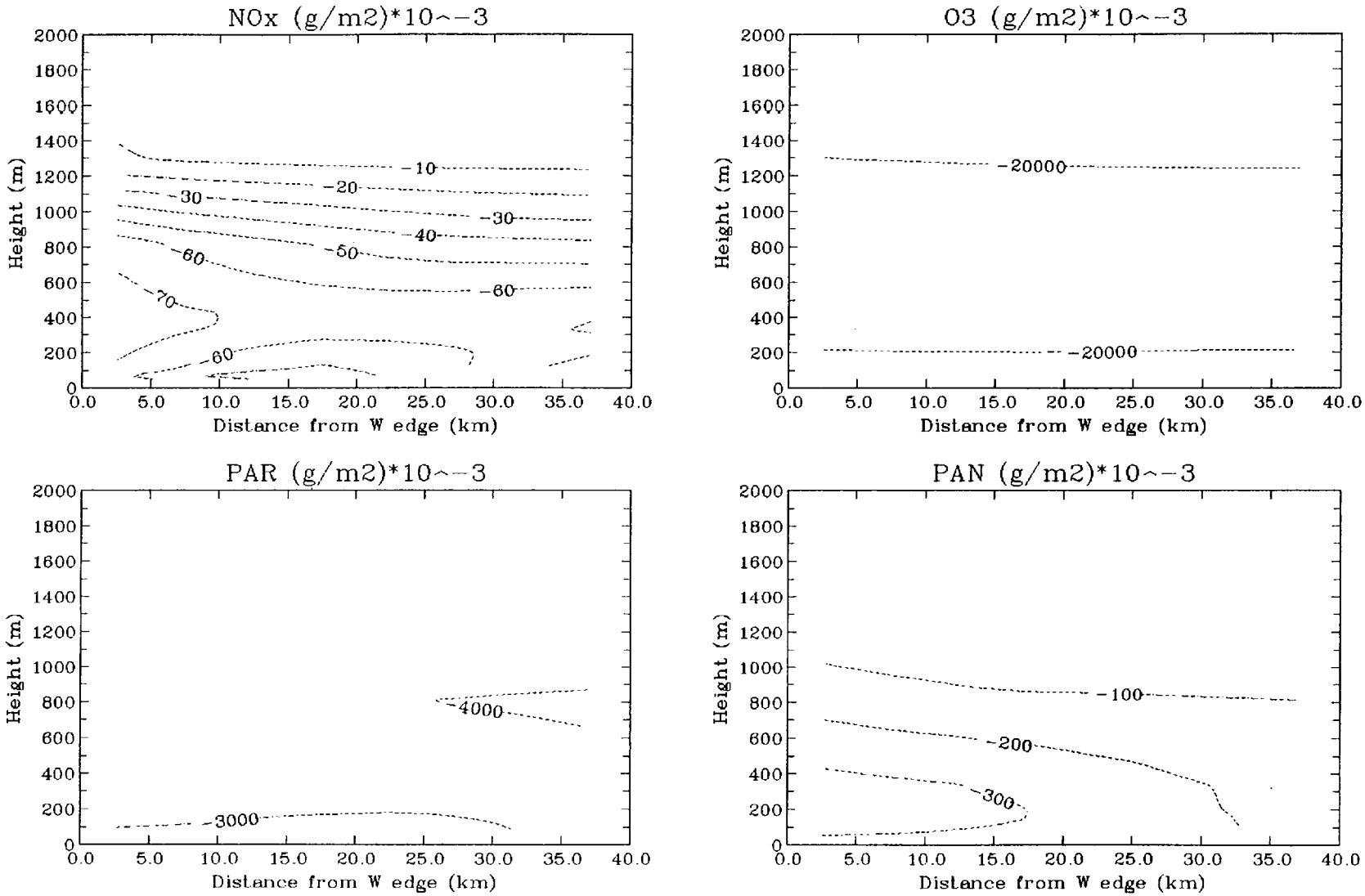

FIGURE 4-8b. No SFBA emissions.

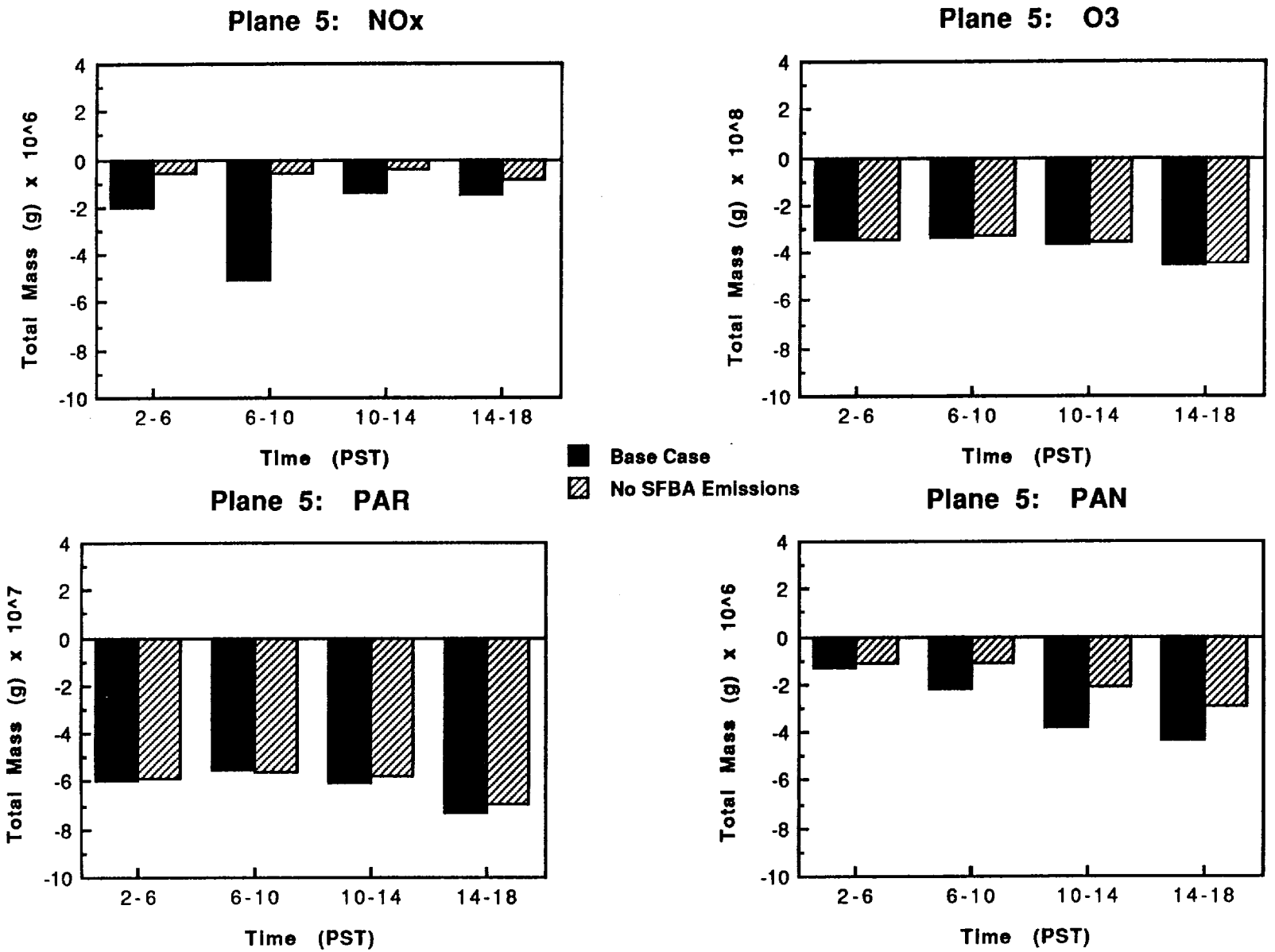

FIGURE 4-9. Time-series plots of the net mass of NO_x, PAR, ozone, and PAN advected across flux-plane 5 on simulation day 2.

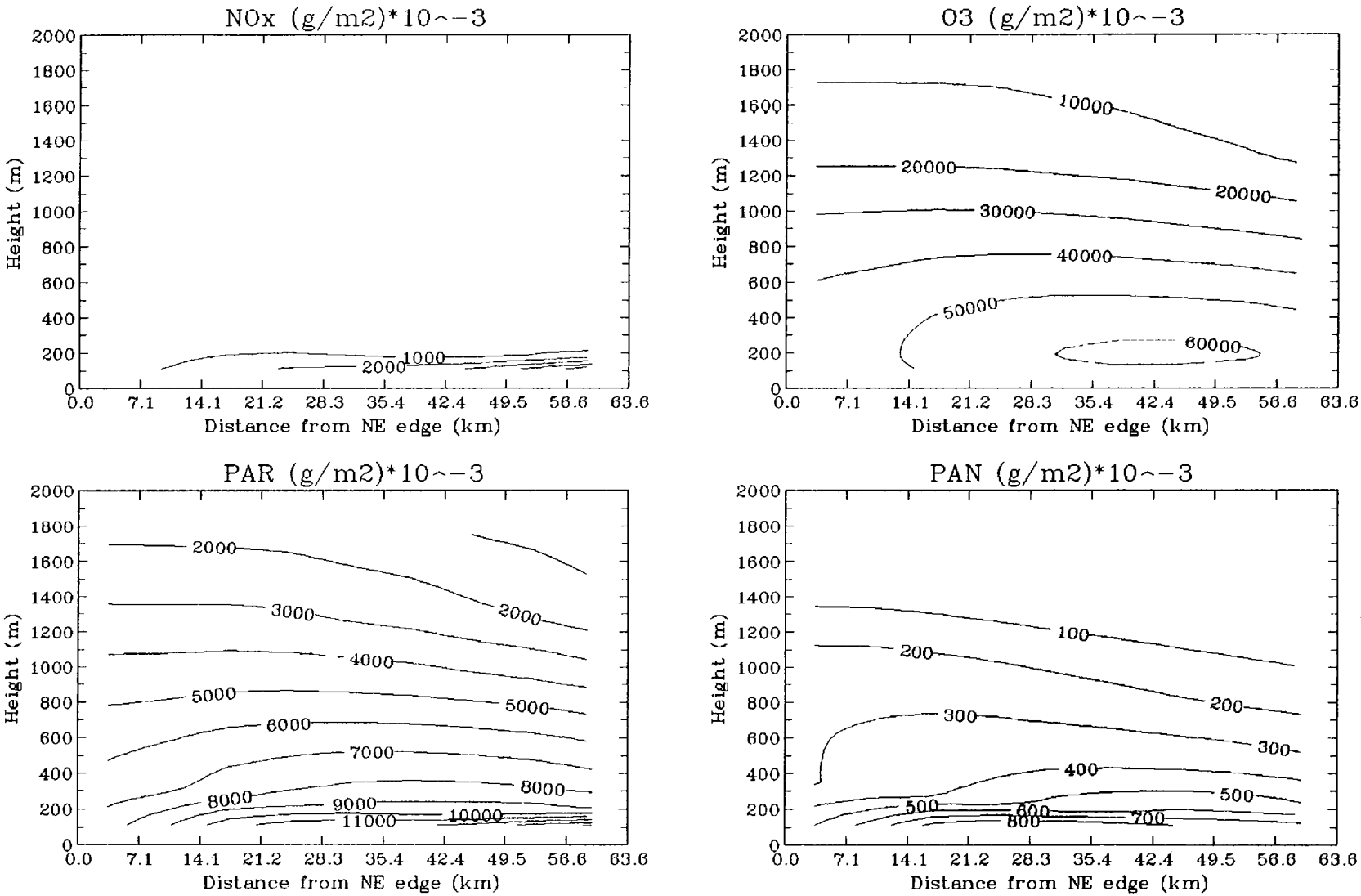

FIGURE 4-10a. Net mass per unit area advected across flux-plane 1 on simulation day 1 (0200-2400 PST): base case.

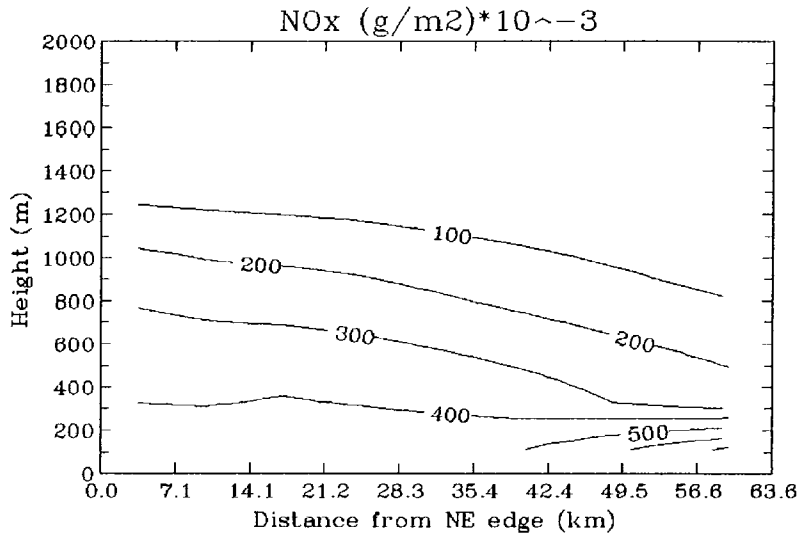

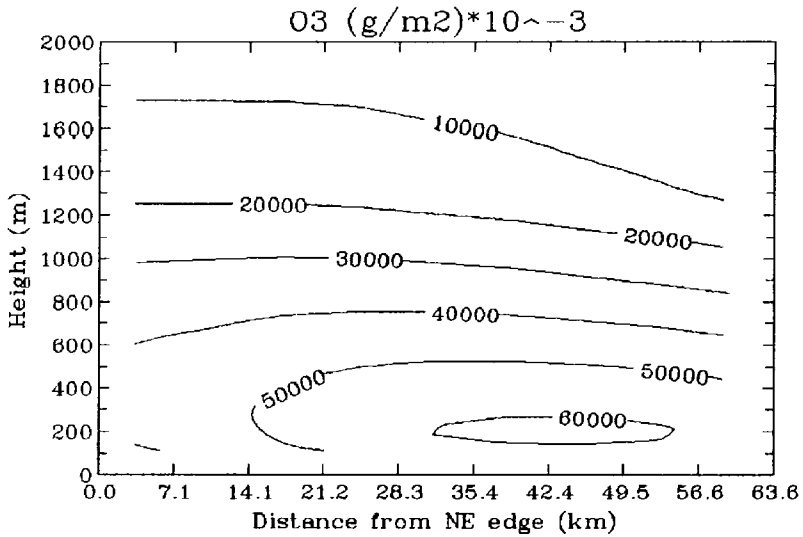

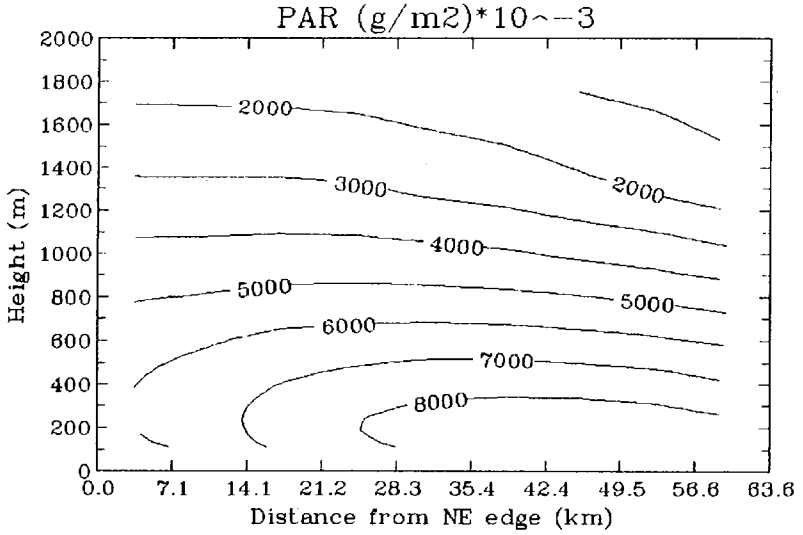

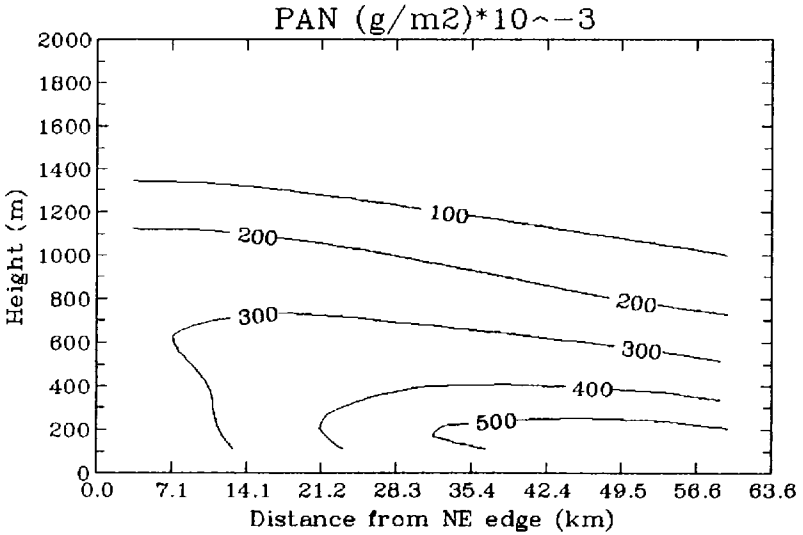

FIGURE 4-10b. No SFBA emissions.

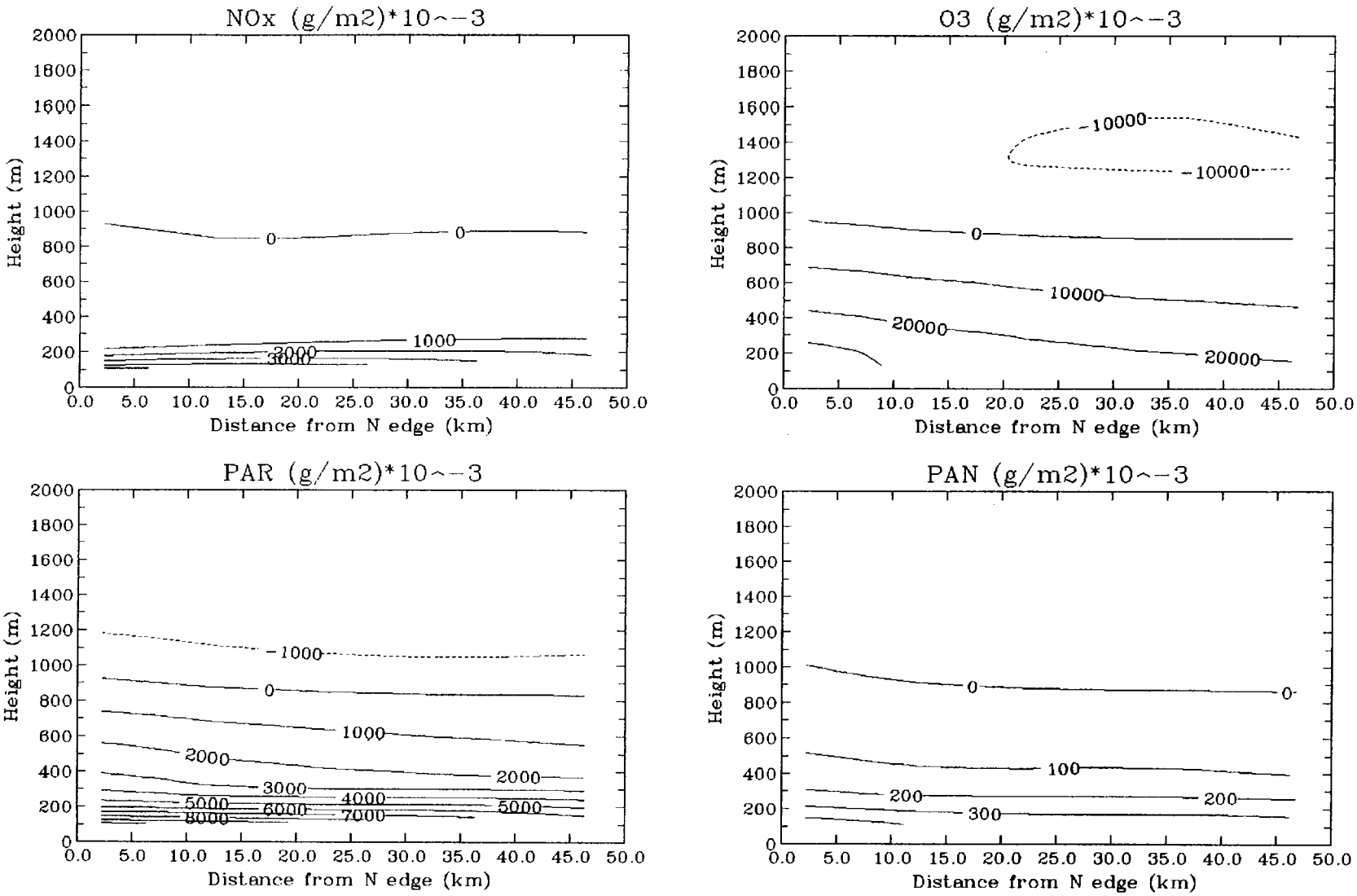

FIGURE 4-11a. Net mass per unit area advected across flux-plane 2 on simulation day 1 (0200-2400 PST): base case.

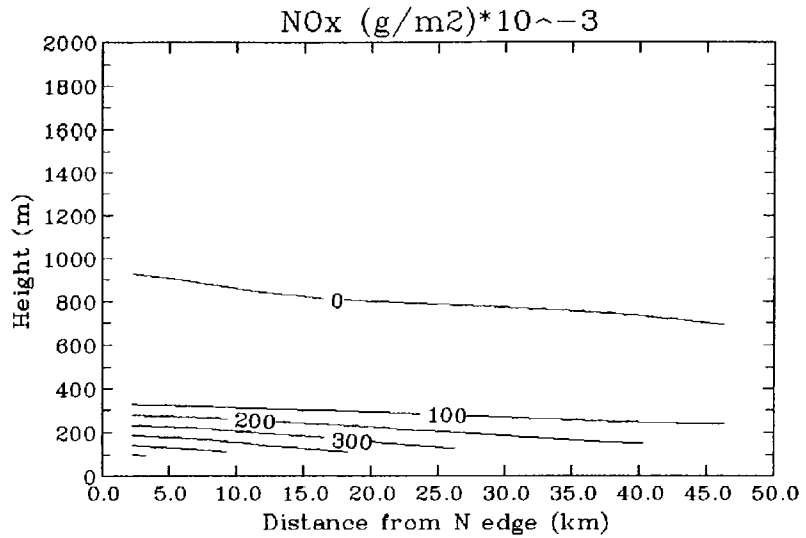

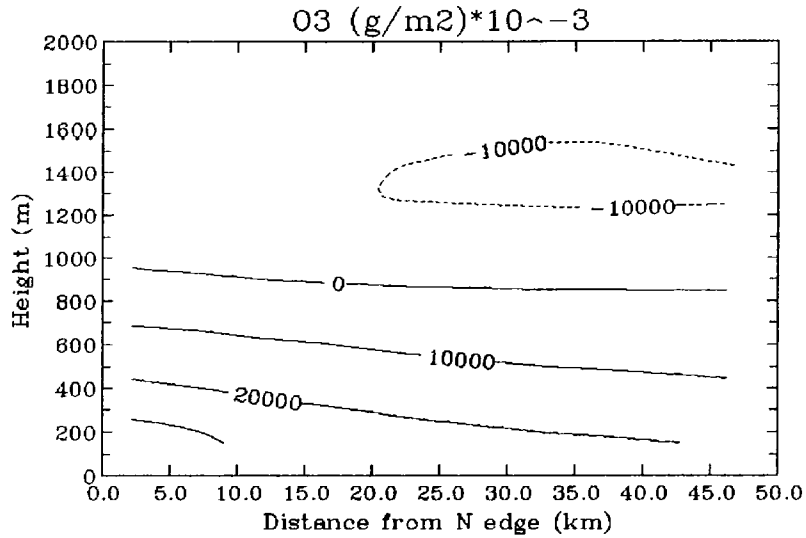

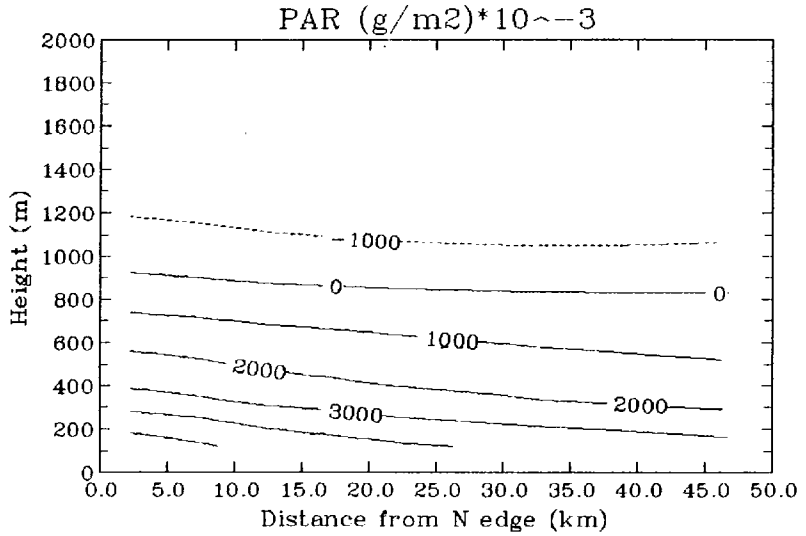

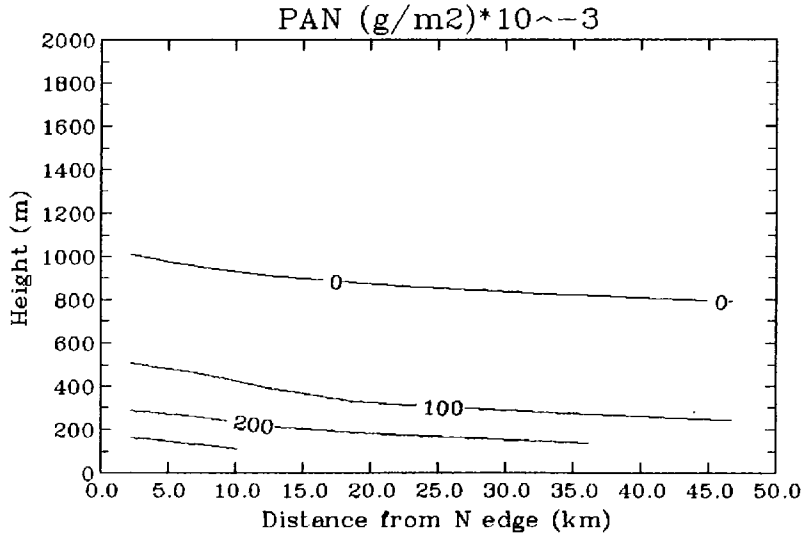

FIGURE 4-11b. No SFBA emissions.

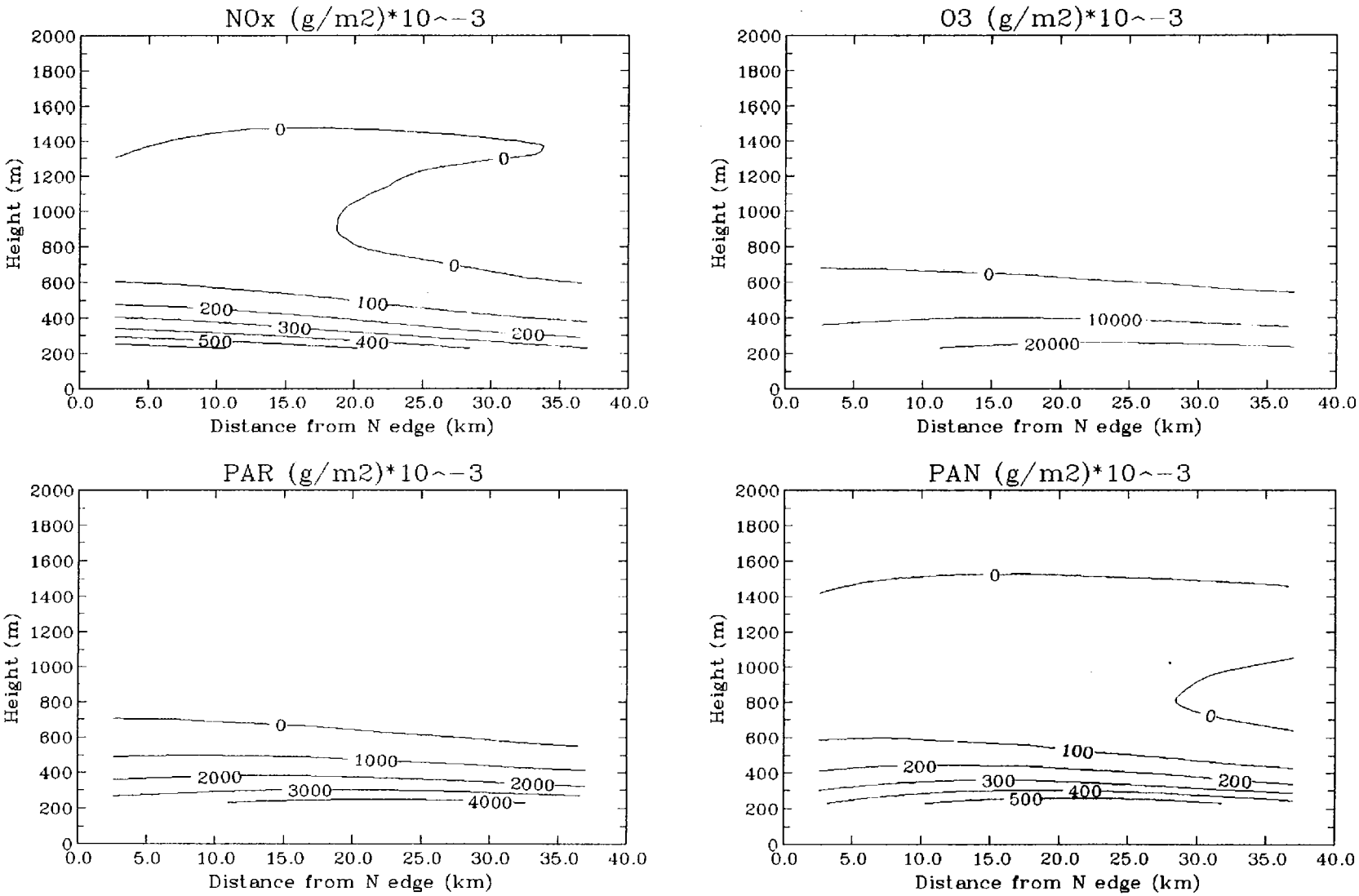

FIGURE 4-12a. Net mass per unit area advected across flux-plane 3 on simulation day 1 (0200-2400 PST): base case.

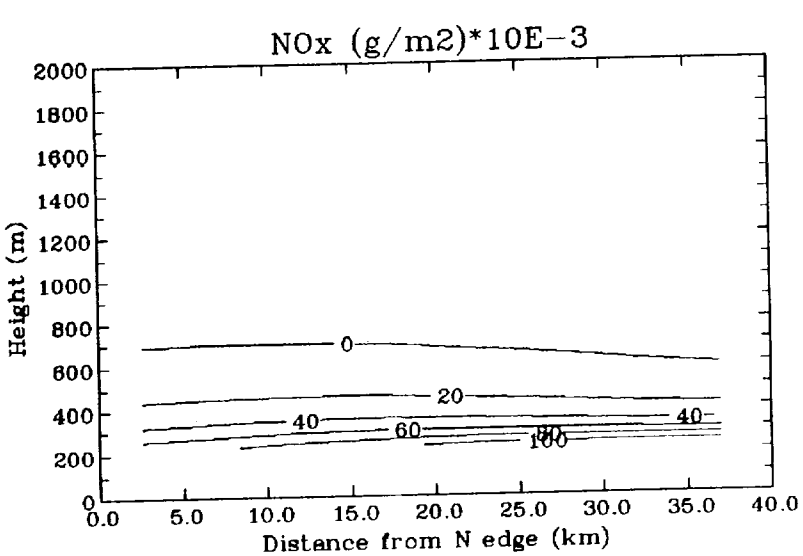

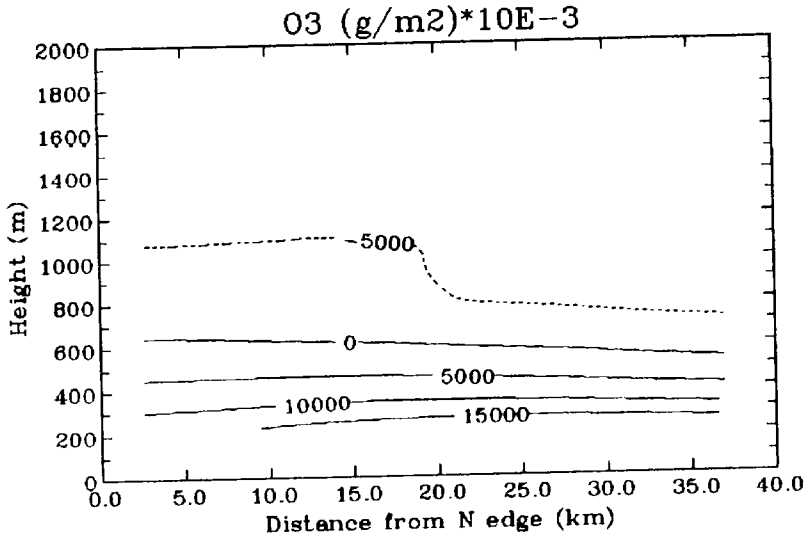

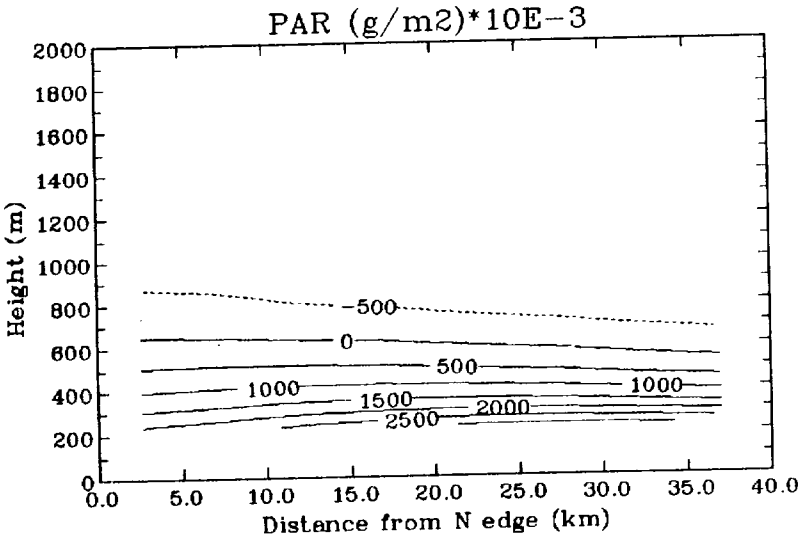

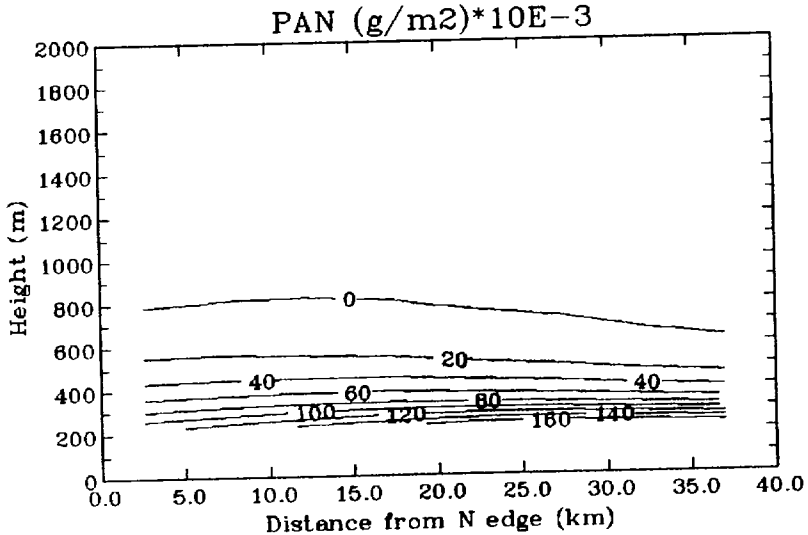

FIGURE 4-12b. No SFBA emissions.

elimination of SFBA emissions reduces the amount of NO_x, PAN and PAR carried across the plane during the first simulation day.

Vertical cross sections of the net flux advected across plane 3 (Pacheco Pass) during simulation day 1 are shown in Figure 4-12. Negative flux aloft and greater positive flux near the surface also characterizes the base-case results for plane 3. In the no-SFBA-emissions simulation the net flux of ozone is negative, indicating transport of ozone from the SJV to the SFBA (this occurs during the morning and nighttime hours). The net mass flux of NO_x, PAR, and PAN remains positive but the amount of precursor pollutants carried across the plane is significantly reduced.

The net mass advected across each of the three flux-planes during day 1 of the air quality simulation is given in Table 4-1. The amount of precursor pollutants advected across the three planes is significantly reduced in the no-SFBA-emissions simulation. The largest reduction is in NO_x. The total mass of ozone transported across plane 2 (from the SFBA to the NCC) on this day is actually greater in the no-SFBA-emissions simulation. This may be due to less NO and therefore less ozone depletion in the SFBA during the early morning hours. For plane 3, the reduction in the amount of ozone transported across the plane results in a net negative flux of ozone across this plane and is consistent with less ozone production in the Santa Clara Valley.

Simulation Day 2

Pollutant flux across plane 1 on simulation day 2 is characterized during the morning hours by negative flux aloft and positive flux near the surface. Later in the day the flux is positive throughout the depth of the modeling domain. Vertical cross sections of net mass per unit area advected across plane 1 during the 18-hour period from 0200 to 2000 PST are shown in Figure 4-13. A net positive flux indicates transport of pollutants from the SFBA to the SJV. Elimination of the SFBA emissions results in large reductions in the amount of NO_x, smaller reductions in the amount of PAR and PAN, and almost no reduction in the amount of ozone advected across the plane. Time-series plots (Figure 4-14) illustrate the temporal variation of mass flux as well as the differences between the base-case and no-SFBA-emissions simulations. The

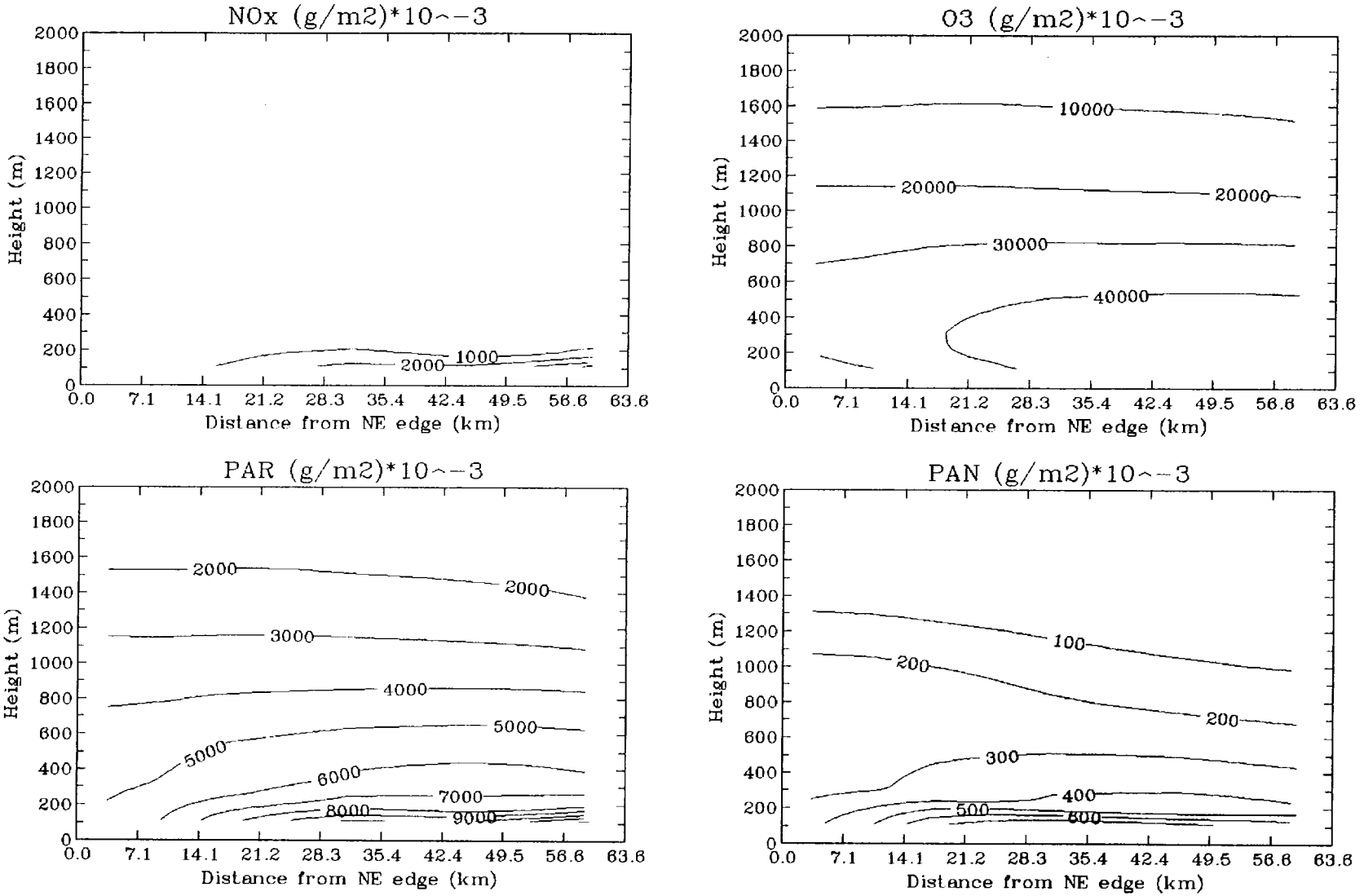

FIGURE 4-13a. Net mass per unit area advected across flux-plane 1 on simulation day 2 (0200-2000 PST): base case.

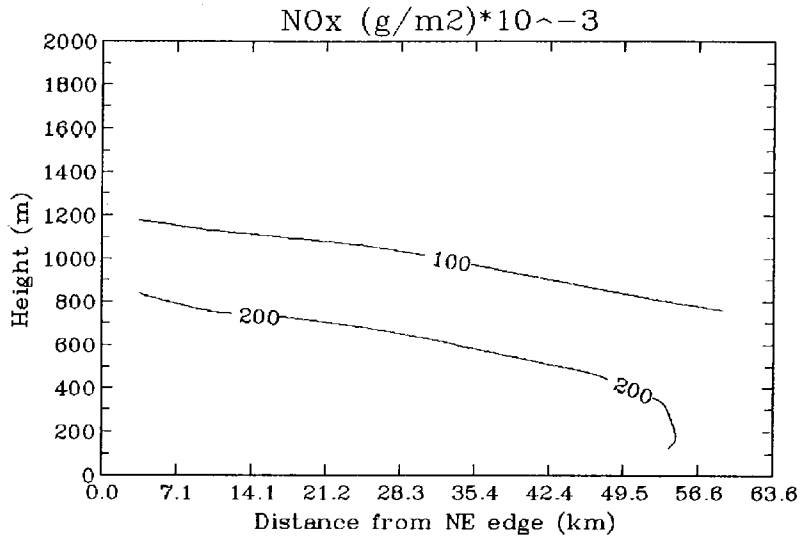

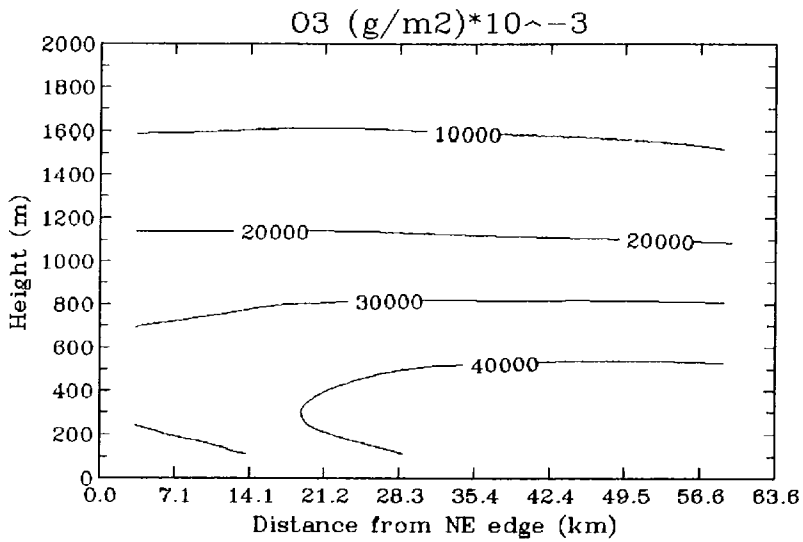

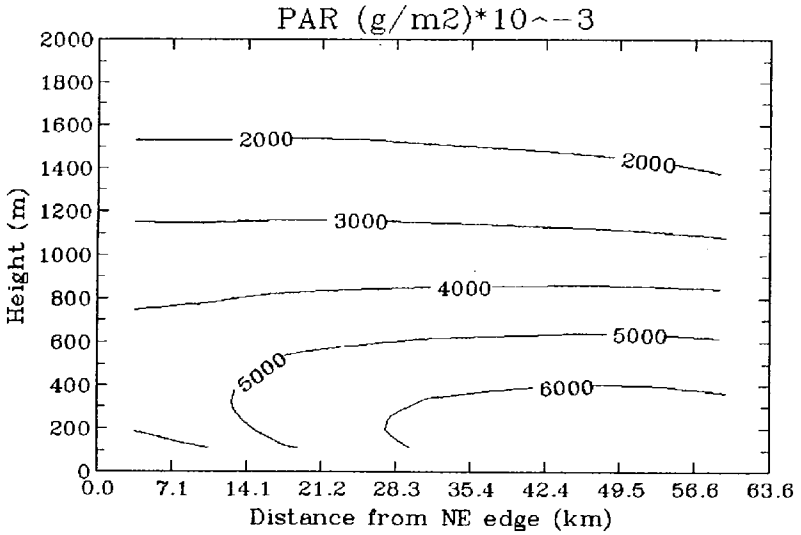

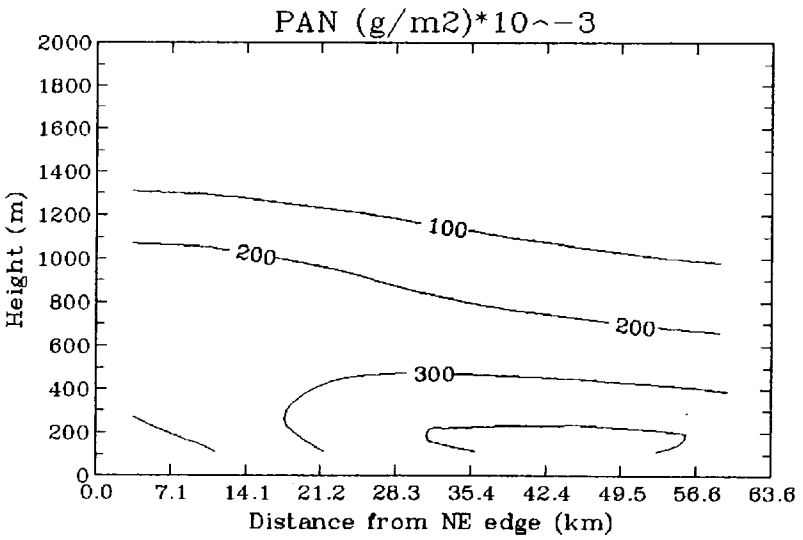

FIGURE 4-13b. No SFBA emissions.

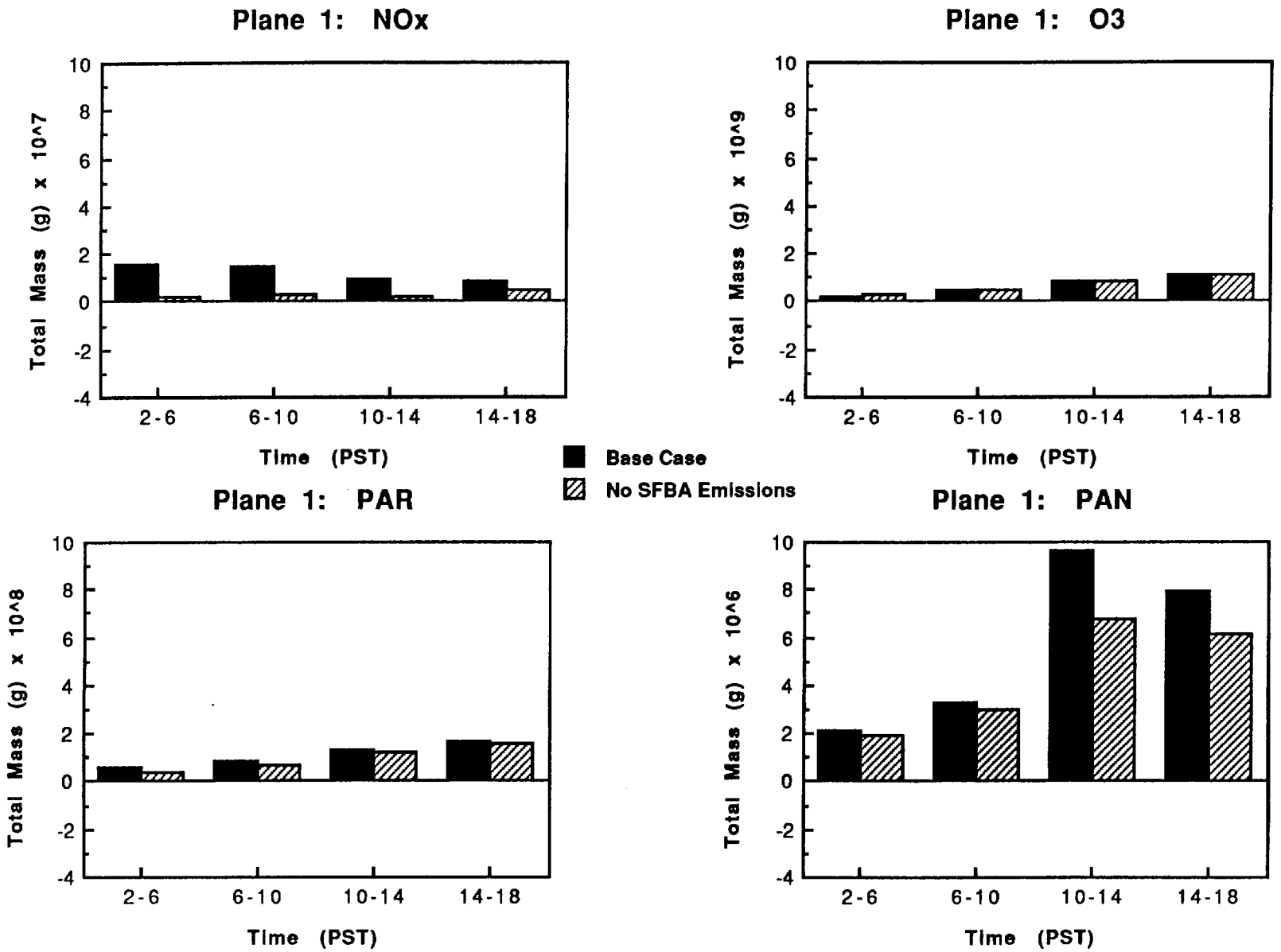

FIGURE 4-14. Time-series plots of the net mass of NO_x, PAR, ozone, and PAN advected across flux-plane 1 on simulation day 2.

net mass of each of the four pollutants advected through plane 1 during day 2 of the simulation is given in Table 4-2. Elimination of SFBA emissions results in a 71 percent reduction in the amount of NO_x, a 20 percent reduction in the amount of PAN, and a 13 percent reduction in the amount of PAR advected across the flux plane. The amount of ozone remains relatively unchanged.

Vertical cross sections of the net mass advected across plane 2 (Altamont Pass) during simulation day 2 are shown in Figure 4-15. A net positive flux indicates transport from the SFBA to the SJV. The elimination of SFBA emissions results in large decreases in the amount NO_x advected across the flux plane, smaller decreases in PAR and PAN, and almost no change in the net amount of ozone. The time series plots for plane 2 (Figure 4-16) show a negative flux of PAR and ozone (from the SJV to the SFBA) during the morning hours. This occurs at upper levels in both simulations. The net mass through plane 2 during day 2 of the simulation is given in Table 4-2. Elimination of SFBA emissions results in a 96 percent reduction in the amount of NO_x , a 50 percent reduction in the amount of PAN, and a 46 percent reduction in the amount of PAR advected across the flux plane. Ozone is reduced by only 2 percent.

Vertical cross sections of the net mass advected across plane 3 (Pacheco Pass) during simulation day 2 are shown in Figure 4-17. Again, a net positive flux indicates transport from the SFBA to the SJV. When the SFBA emissions are eliminated there is a decrease in the net flux of ozone across plane 3 as well as a reduction in the amount of precursor pollutants advected across the plane. The reductions are illustrated in time series plots in Figure 4-18. Again, a negative flux of PAR and ozone occurs aloft during the early morning hours. The net mass of NO_x, PAR, ozone, and PAN advected through plane 3 during day 2 of the simulation is given in Table 4-2. Elimination of SFBA emissions results in a 81 percent reduction in the amount of NO_x, a 80 percent reduction in the amount of PAN, a 39 percent reduction in the amount of PAR, and a 34 percent reduction in the amount of ozone advected across the flux plane.

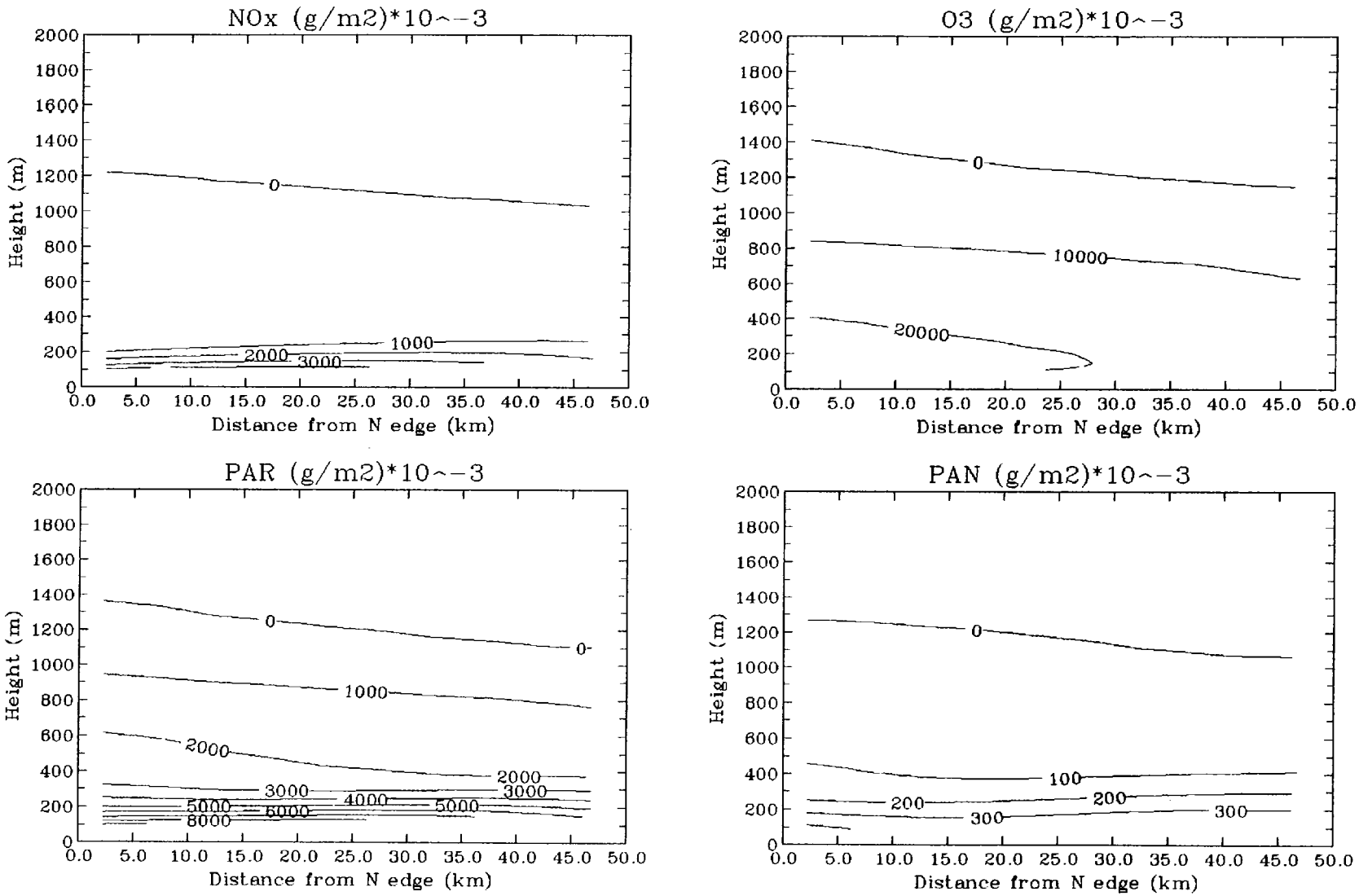

FIGURE 4-15a. Net mass per unit area advected across flux-plane 2 on simulation day 2 (0200-2000 PST): base case.

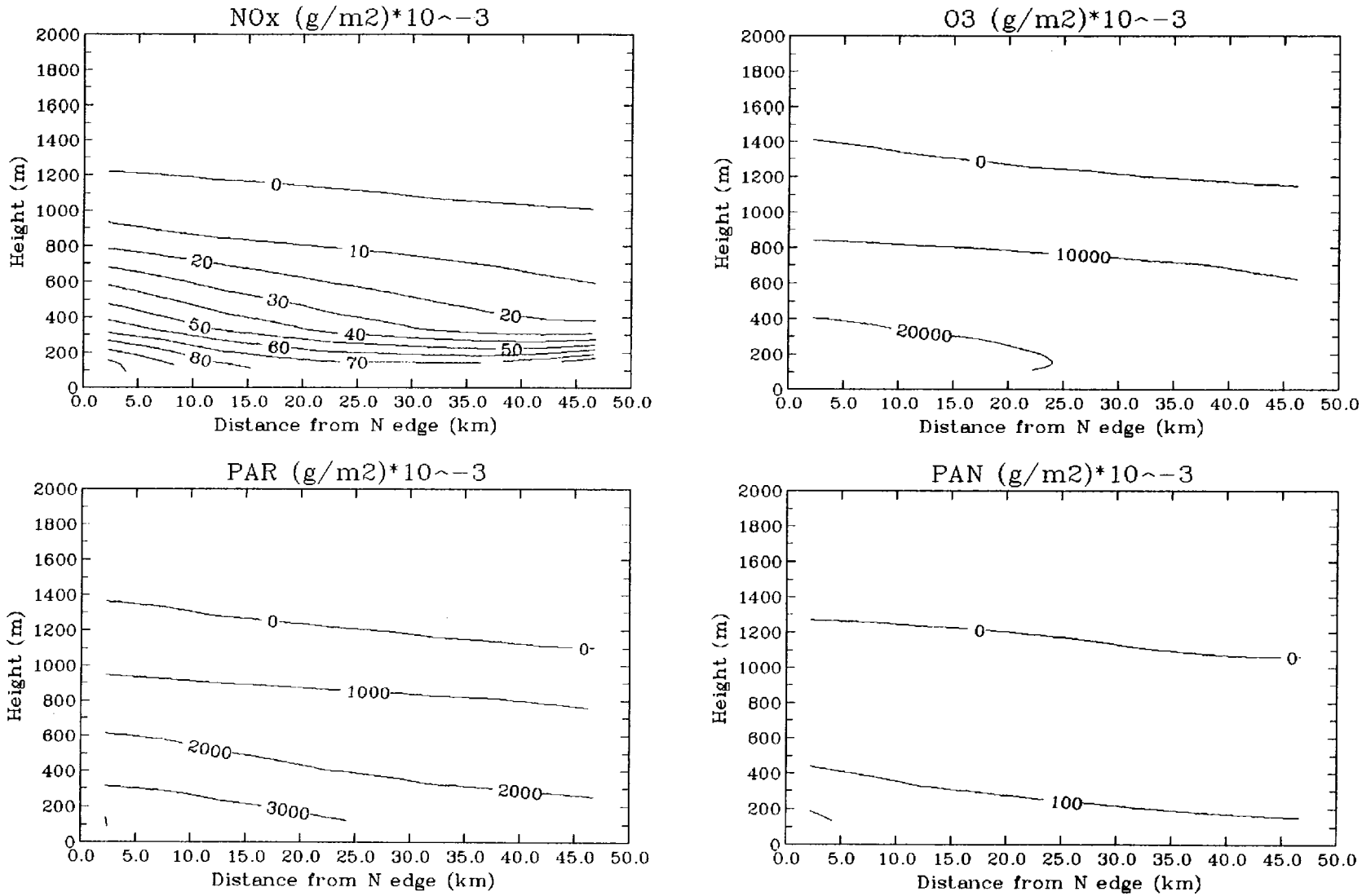

FIGURE 4-15b. No SFBA emissions.

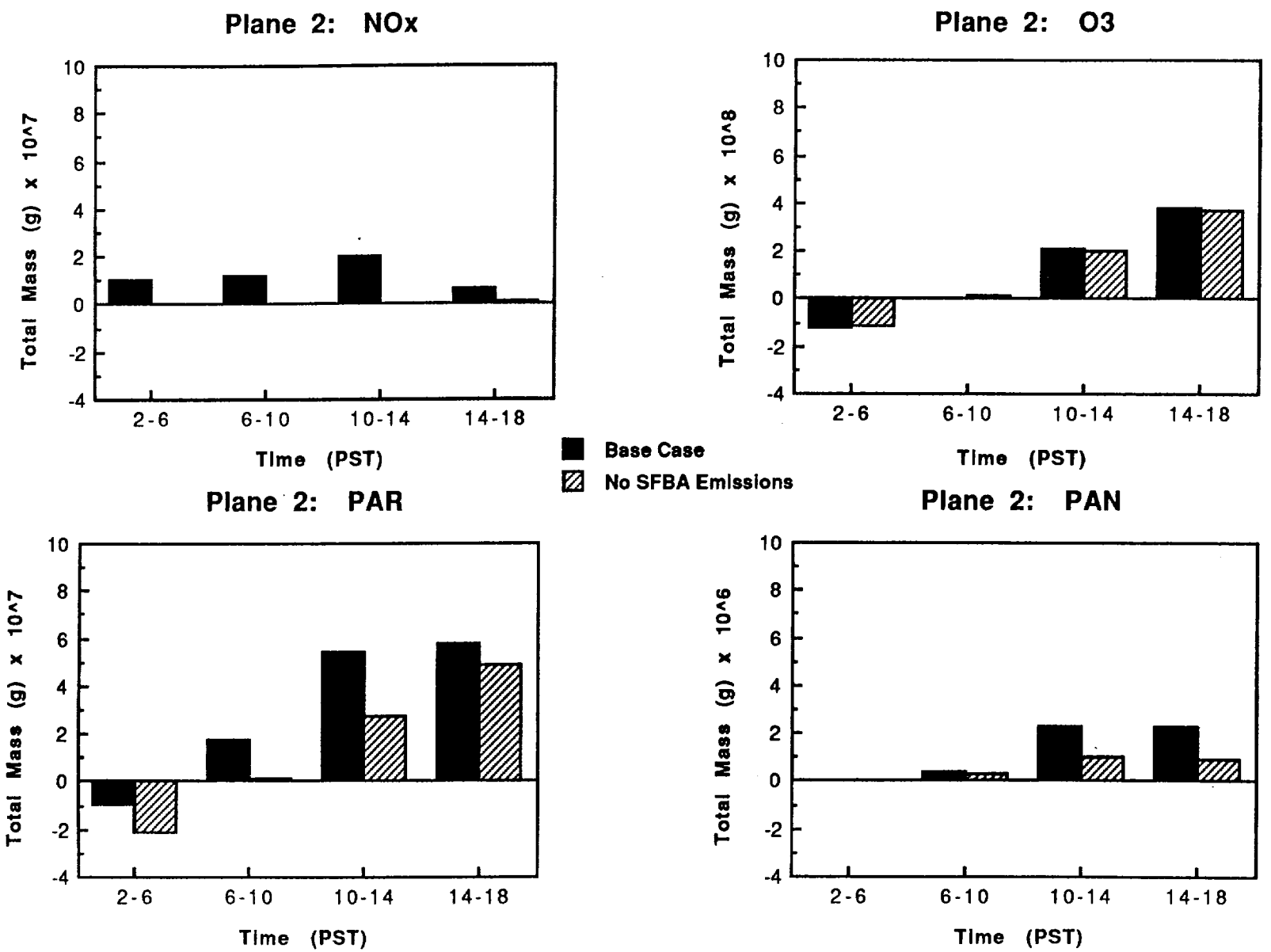

FIGURE 4-16. Time-series plots of the net mass of NO_X, PAR, ozone, and PAN advected across flux-plane 2 on simulation day 2.

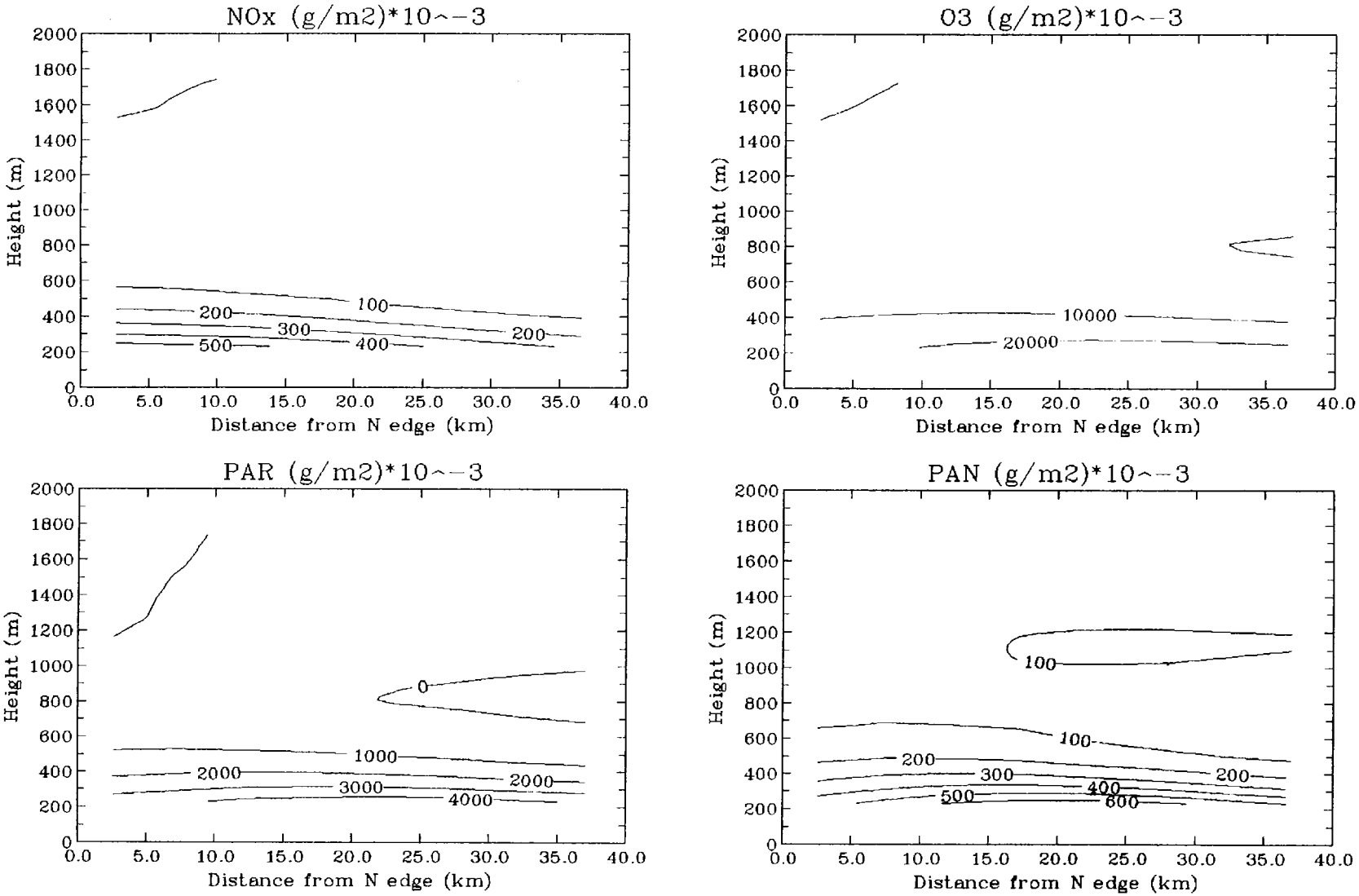

FIGURE 4-17a. Net mass per unit area advected across flux-plane 3 on simulation day 2 (0200-2000 PST): base case.

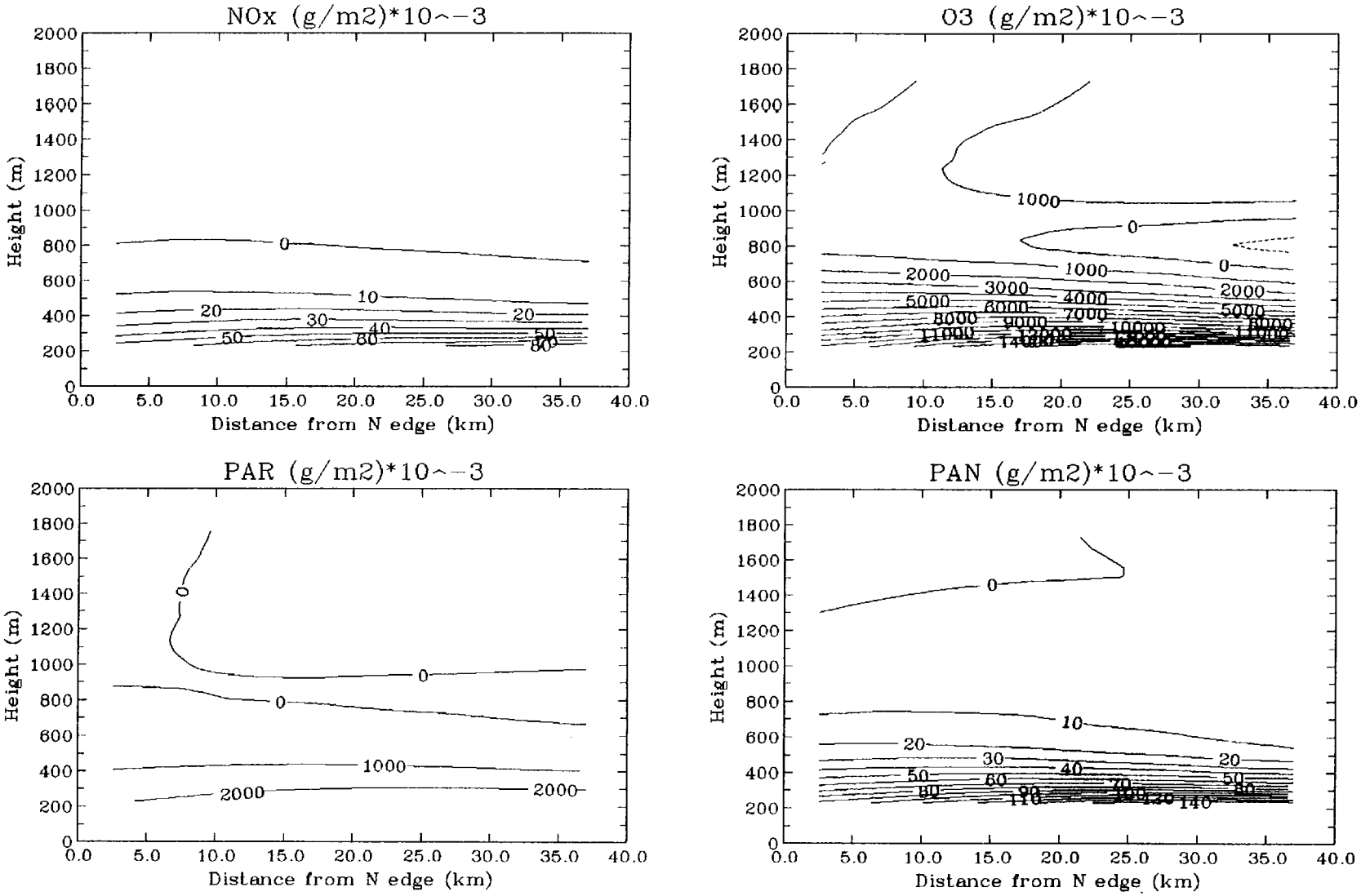

FIGURE 4-17b. No SFBA emissions.

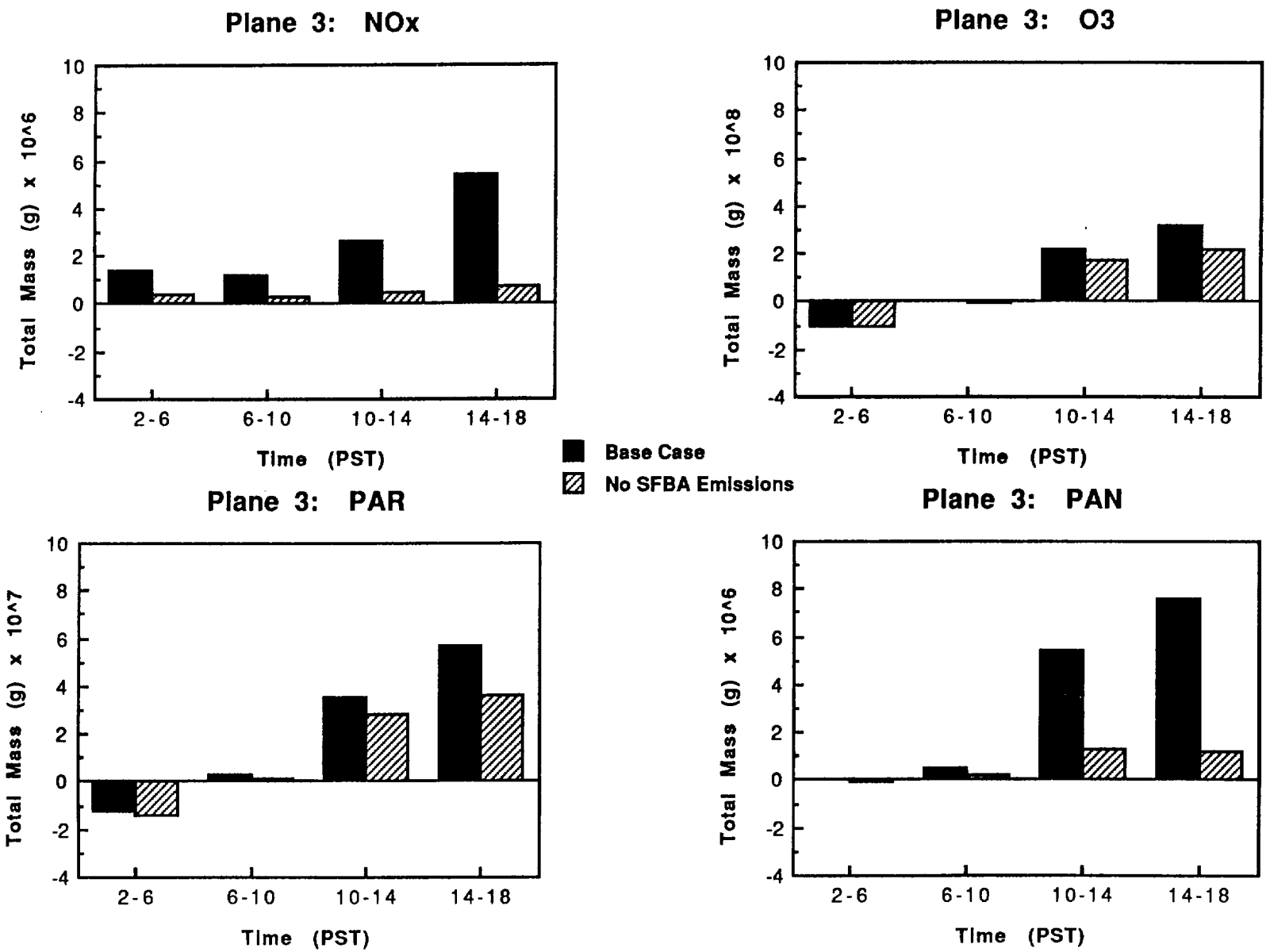

FIGURE 4-18. Time-series plots of the net mass of NO_x, PAR, ozone, and PAN advected across flux-plane 3 on simulation day 2.

SUMMARY AND CONCLUSIONS

Meteorological and air quality modeling results indicate that ozone and ozone precursor pollutants were transported from the SFBA to the NCC and SJV on 7-8 August. Flux-plane calculations for five flux planes separating the air basins have provided quantitative estimates of pollutant flux during this period under two different emissions scenarios (with and without SFBA emissions). A comparison of the flux estimates for the base-case and no-SFBA-emissions simulations indicates that elimination of the SFBA emissions can significantly reduce the flux of pollutants from the SFBA to the NCC and SJV when meteorological conditions are conducive to transport. Most of this reduction occurred in the amount of precursor material (NO_x, PAR, and PAN) transported to the downwind air basins. Significant reductions in the flux of ozone occurred only for plane 3 (Pacheco Pass).

The flux-plane calculations indicate that transport from the SFBA to the NCC occurred over land and water pathways during 7-8 August. Greater differences in mass flux across plane 4 than plane 5 when the SFBA emissions were eliminated indicate that the primary pathway for pollutant transport during this episode was along the Santa Clara Valley. Elimination of SFBA emissions reduces the flux of NO_x and PAN significantly and the flux of PAR and ozone only slightly on both days of the simulation.

Transport of pollutants from the SFBA to the SJV is also indicated during these two days. Although the 18-hour net flux is positive throughout the depth of the modeling domain, a negative flux aloft during the morning hours is indicated. Elimination of SFBA emissions results in a decrease in the amount of precursor pollutants advected across planes 1, 2, and 3 (Carquinez Strait, Altamont Pass, and Pacheco Pass). The flux of ozone is reduced only across plane 3. This is consistent with significantly lower ozone concentrations in the Santa Clara Valley in the no-SFBA simulation.

In the no-SFBA-emissions simulation the elimination of SFBA emissions results in reduced ozone concentrations in the NCC and SJV on 7 and 8 August. The flux-plane calculations suggest that this reduction is due primarily to a decrease in the amount of precursor pollutants advected into the downwind air basins. Reduced ozone concentrations in the Santa Clara Valley and reduced ozone flux from this region into

the downwind air basins may contribute to the lower ozone concentrations near Hollister and areas downwind of Pacheco Pass. The largest reduction in ozone concentrations occurs in this area (refer to Figure 3-2). Differences further downwind are more likely due to reductions in the amount of precursor pollutants.

5 SUMMARY, CONCLUSIONS, AND RECOMMENDATIONS

The 1988 California Clean Air Act requires the Air Resources Board to assess the relative contribution of upwind emissions to downwind pollutant concentrations in areas where transported pollutants have been identified to cause or contribute to violations of the state ozone standard. In support of the requirement, our study was designed to examine the effect of emissions reductions in the San Francisco Bay Area (SFBA) on ozone levels in the North Central Coast (NCC), and San Joaquin Valley (SJV) air basins. It includes three tasks:

Emissions trends analysis for the SFBA, NCC, and SJV air basins;

Identification of possible transport days and analysis of ozone trends in both the source and receptor basins on transport and no-transport days; and

Application of flux-plane calculations using air quality modeling results from the San Joaquin Valley Air Quality Study to quantify the impact of emissions changes on interbasin transport.

In the emissions trends analysis we examined trends in emissions of reactive organic gasses (ROG), and oxides of nitrogen (NO_x) between 1979 and 1987 in the SFBA, NCC, and SJV air basins and selected counties within these air basins. To account for the fact that not all ROGs contribute equally to the formation of ozone, reactivity-weighted ROG trends were also examined. The analysis indicates that the SFBA has achieved large decreases in ROG (42 percent) and NOx (24 percent) emissions during the period 1979 - 1987. ROG decreases in the NCC and SJV air basins have also been significant (16 and 39 percent, respectively). NO_x emissions have decreased in the NCC (44 percent) but have remained virtually constant in the SJV.

Historical ozone concentration data for the SFBA, NCC, and SJV air basins were examined for the period 1979 - 1988. The objective was to determine how ozone levels within the air basins have changed during this period and to relate these changes to changes in emissions within the source and receptor basins. The first step in the analysis was the development of transport/no-transport criteria for each of the downwind air basins. High-ozone days in the NCC or SFBA and SJV or SFBA were identified and categorized as transport, no transport, or indeterminate. Due to a lack of meteorological and air-quality data in the NCC, no clear-cut criteria for identifying transport days could be developed. Therefore, days not meeting the no-transport criteria were classified as indeterminate. Ozone trends were then calculated for both the SFBA and the downwind air basins and for selected monitors within each basin. Separate trends were calculated for no-transport and transport days (indeterminate days for the NCC analysis). No statistically significant linear trends over the 1979 - 1988 period were observed at the 95% confidence level. Furthermore, no systematic differences between trends on transport and no-transport or indeterminate days were observed. However, ozone concentrations at the downwind monitors were higher on transport days.

Thus, despite large decreases in SFBA emissions inventories no statistically significant ozone trends were observed in the SFBA or the downwind air basins during the period 1979 - 1988. Possible reasons for this apparent inconsistency include: (1) uncertainties in the emission trends resulting from uncertainties in emission inventories and emission factors, (2) assumptions used to classify high-ozone days into the transport/no-transport categories, (3) possible influence of variable meteorological conditions on the ozone trends, and (4) an inability to detect a downward trend in the ozone concentrations due to the small number of days falling into each transport category. Good agreement with trends calculated by Rosenbaum (1989) using a variety of summary statistics indicates that the ozone trends are probably not sensitive to selection of the summary statistic.

Flux-plane calculations were performed using the meteorological and air quality modeling results from the San Joaquin Valley Air Quality Study (SJVAQS) to provide quantitative estimates of pollutant flux between the SFBA and the NCC and the SJV during the period 7 - 8 August 1984. High ozone concentrations were observed in the

SFBA, NCC, and SJV during this period and the airflow patterns indicate possible transport from the SFBA to both the NCC and SJV. To examine the effect of emissions changes on the transport of ozone and precursor pollutants, fluxes were calculated for two different emissions scenarios.

The air quality simulations consist of a base case and a sensitivity test in which anthropogenic emissions in the SFBA were eliminated. The results indicate that elimination of SFBA emissions can significantly reduce ozone concentrations in the NCC and SJV during meteorological conditions conducive to transport. The flux-plane calculations indicate that while reduced ozone concentrations in the SFBA under the no-SFBA-emissions scenario result in a reduction of the flux of ozone into the downwind air basins somewhat, lower ozone concentrations in the downwind air basins are primarily due to a reduction in the amount of precursor pollutants that are transported from the SFBA to the receptor basins. These results may differ for other meteorological conditions.

Thus, while the emissions trends and ozone trends analyses indicate that what may have been significant reductions in emissions in the SFBA between 1979 and 1988 have not resulted in a detectable trend in the seasonal average daily maximum ozone concentration in the SFBA nor the NCC and SJV air basins on either transport or no-transport days, the results from the flux-plane calculations suggest that elimination of anthropogenic SFBA emissions would significantly decrease ozone concentrations in the downwind air basins during transport-conducive meteorological conditions. Our categorization of high-ozone days showed that during the period 1979 - 1988 transport from the SFBA to the NCC was possible on more than 65 percent of the days and transport from the SFBA to the SJV was likely on more than 37 percent of the days. Together, these results suggest that continued reductions (beyond current levels) in SFBA emissions may eventually have a positive impact on ozone levels in the NCC and SJV air basins.

To test this hypothesis we recommend the following additional analyses:

Emissions Trends

Include biogenic emissions in the ROG emissions trends.

Improve the quality assurance of the emissions trends data.

Classification of Ozone Episodes

Improve the criteria for the classification of transport days. This may include analysis of surface and upper-level wind data at selected sites, air-parcel trajectories, surface pressure gradients, mixing heights, surface temperatures, ozone concentration patterns, and the timing of peak ozone concentrations.

Include a correction for temperature in the ozone trends or calculate ozone trends for meteorologically similar days only (to reduce the influence of meteorology on the trends).

Examine multi-day transport.

Extend the period over which trends are calculated. Difficulties may arise, however, from inconsistent monitoring methodologies and station locations over a longer period.

Flux-Plane Calculations

Perform additional air quality simulations for the 7-8 August simulation period, varying the emissions reductions in the SFBA. Use flux-plane calculations to examine the amount and composition of the pollutant flux.

Perform air quality simulations and flux-plane analyses for additional transport and no-transport days.

References

ARB. 1986. "Emission Inventory 1983." California Air Resources Board, Sacramento, California.

ARB. 1990a. "Emission Trends for the San Francisco Bay Area. Draft." California Air Resources Board, Sacramento, California.

ARB. 1990b. "Emission Trends for the North Central Coast. Draft." California Air Resources Board, Sacramento, California.

ARB. 1990c. "Emission Trends for the San Joaquin Valley. Draft." California Air Resources Board, Sacramento, California.

ARB. 1990d. "Assessment and Mitigation of the Impacts of Transported Pollutants on Ozone Concentrations within California." California Air Resources Board, Sacramento.

Dabberdt, W. F. 1983. "Ozone Transport in the North Central Coast Air Basin." SRI International (Contract A9-143-31).

Douglas, S. G. 1989. "Objective Combination of Prognostic Model Wind Fields and Observational Data for the San Joaquin Valley." Systems Applications International, San Rafael, California.

EPA. 1988. "Air Emissions Species Manual. Volume 1: Volatile Organic Compound Species Profiles." U.S. Environmental Protection Agency (EPA-450/2-88-003a).

Hayes, T. P., J.J.R. Kinney, and N.J.M. Wheeler. 1984. "California Surface Wind Climatology." Aerometric Data Division, California Air Resources Board.

Ingalls, M. N., L. R. Smith, and R. E. Kirksey. 1989. "Measurement of On-Road Vehicle Emission Factors in the California South Coast Air Basin. Volume I. Regulated Emissions." Southwest Research Institute, San Antonio, Texas.

Kessler, R. C., and S. G. Douglas. 1989. "Numerical Simulation of Summer Mesoscale Airflow in the Central Valley of California." Systems Applications International, San Rafael, California.

Lawson, D. R., P. J. Groblicki, Donald H. Stedman, G. A. Bishop, and P. L. Guenther. 1990. Emissions from in-use motor vehicles in Los Angeles: A pilot study of remote sensing and the inspection and maintenance program. J. Air Waste Manage. Assoc.

Mahrer, Y., and R. A. Pielke. 1977. A numerical study of the air flow over irregular terrain. Contr. Atmos. Phys., 50:98-113.

Mahrer, Y., and R. A. Pielke. 1978. A test of an upstream spline interpolation technique for the advective terms in a numerical mesoscale model. Mon. Wea. Rev., 106:818-830.

Morris, R. E., R. C. Kessler, S. G. Douglas, and L. R. Chinkin. 1990. "Preliminary Modeling for the San Joaquin Valley Air Quality Study." Systems Applications International, San Rafael, California (SYSAPP-90/106).

Morris, R. E.. and R. C. Kessler. 1990. "Development of a Variable Grid Regional Oxidant Model and Application to the San Joaquin Valley." AWMA Specialty Conference on Tropospheric Ozone and the Environment, 19-22 March, Industry Hills, California.

Pielke, R. A. 1974. A three-dimensional numerical model of the sea breezes over south Florida. Mon. Wea. Rev., 102:115-139.

Roberts, P. T., and H. H. Main. 1989. "The Measurement of Pollutant and Meteorological Boundary Conditions: Technical Support Study Number 10." Sonoma Technology, Inc., Santa Rosa, California (STI-98030-920FR).

Rosenbaum, A. S. 1989. Unpublished Study for Western States Petroleum Association. Systems Applications International, San Rafael, California.

Whitten, G. Z. 1990. "The Atmospheric Chemistry of Ozone Formation. A Brief Discussion of the Key Concepts Currently Accepted in the Scientific Community." Systems Applications International, San Rafael, California (SYSAPP-90/013).